Fall 1-1-2016

Impact of N-Acetyl-L-Cysteine on the Pathology of Experimental Parkinson's Disease in Vivo

Negin Nouraei

IMPACT OF *N*-ACETYL-L-CYSTEINE ON THE PATHOLOGY OF EXPERIMENTAL PARKINSON'S DISEASE *IN VIVO*

A Dissertation

Submitted to the Graduate School of Pharmaceutical Sciences

Mylan School of Pharmacy

Duquesne University

In partial fulfillment of the requirements for

the degree of Doctor of Philosophy

By

Negin Nouraei

December 2016

IMPACT OF *N*-ACETYL-L-CYSTEINE ON THE PATHOLOGY OF EXPERIMENTAL PARKINSON'S DISEASE *IN VIVO*

By

Negin Nouraei

Approved September 20th 2016

_____ David A. Johnson, Ph.D., Division Head of Pharmaceutical, Administrative & Social Sciences, Associate Professor of Pharmacology & Toxicology Graduate School Pharmaceutical Science (Committee Co-Chair)	_____ Rehana K. Leak, Ph.D. Associate Professor of Pharmacology Graduate School Pharmaceutical Sciences (Committee Co-Chair)
_____ Paula A. Witt-Enderby, Ph.D. Professor of Pharmacology Graduate School Pharmaceutical Sciences (Committee Co-Chair)	_____ Jane E. Cavanaugh, Ph.D. Associate Professor of Pharmacology Graduate School Pharmaceutical Sciences (Committee Co-Chair)
_____ Robert Gibbs, Ph.D. Professor of Pharmaceutical Sciences Director, Cell Imaging Core School of Pharmacy University of Pittsburgh, Pittsburgh, PA (Committee Co-Chair)	_____ James K. Drennen, III, Ph.D. Associate Dean, Research and Graduate Programs Graduate School Pharmaceutical Sciences
_____ J. Douglas Bricker, PhD, Dean Mylan School of Pharmacy and Graduate School Pharmaceutical Sciences	

ABSTRACT

IMPACT OF *N*-ACETYL-L-CYSTEINE ON THE PATHOLOGY OF EXPERIMENTAL PARKINSON'S DISEASE *IN VIVO*

By

Negin Nouraei

December 2015

Dissertation supervised by Dr. Rehana K. Leak and Dr. David Johnson

Parkinson's disease is a progressive neurodegenerative disorder associated with disruptions in motor as well as non-motor functions, such as cognitive and olfactory impairments. Postmortem tissue from Parkinson's patients shows evidence of oxidative stress in dopaminergic neurons and hallmark proteinaceous inclusions known as Lewy bodies in multiple brain regions spanning the medulla oblongata to the telencephalon. There are no therapies that decelerate the progression of this disease. Thus, the major goal of the present study was to test the therapeutic potential of two neuroprotective molecules, the antioxidant thiol *N*-acetyl-L-cysteine (NAC) and the steroid neuromodulator dehyroepiandrosterone sulfate (DHEAS), in experimental models of Parkinson's disease *in vivo*. To accomplish this goal, we first established multiple animal models of Parkinson's disease that mimicked oxidative and/or proteotoxic stress: the 6-hydroxydopamine (6-OHDA) model of dopaminergic neurodegeneration and the alpha-

synuclein model of Lewy-like pathology. NAC offered only transient protection in the 6-OHDA model, as demonstrated by multiple histological techniques that were validated in the present study. Indeed, NAC was mildly toxic at doses previously employed in the clinic, with implications for the long-term use of NAC in patients with chronic neurodegenerative conditions. We also developed a model of Lewy-like pathology in the hippocampus in which to examine the effects of DHEAS upon memory function. Although DHEAS failed to affect memory, we subsequently discovered that infusions of waterbath-sonicated alpha-synuclein fibrils into hippocampal CA2/CA3 led to robust Lewy-like pathology in some (but not all) of the brain regions that send first-order efferent projections to the hippocampus—the amygdala, entorhinal cortex, and contralateral CA3. Similar to the human condition, we collected evidence of selective vulnerability to alpha-synucleinopathy, as the septohippocampal projections were spared in our model. Notably, Lewy-like pathology in the hippocampus was statistically correlated with memory and olfactory deficits. Taken together, these studies reveal a novel model of proteinopathy in the hippocampus, which is known to develop Lewy pathology at mid-to-end stages of Parkinson's disease and may be partly responsible for cognitive deficits in this condition. This model can now be used to test neuroprotective drug candidates that have the potential to ameliorate proteinopathic stress and improve neurological outcomes.

DEDICATION

This dissertation is dedicated to my dear parents; Nasser Nouraei and Marzieh Behboudi; my wonderful brothers, Mehryar and Amirreza, and my loving husband, Arash Zandieh, who have provided endless love, support, and encouragement throughout my study.

ACKNOWLEDGEMENT

I would like to acknowledge and thank my advisors, Dr. Rehana Leak and Dr. David Johnson, for their inspirational and constant encouragement, and continuous support throughout my time as a Ph.D. student at Duquesne University. I would also like to thank my committee members, Dr. Paula A. Witt-Enderby, Dr. Jane Cavanaugh, Dr. Robert Gibbs for their scientific guidance and advice.

I thank Dr. Virginia Lee and Dr. Kelvin Luk from the University of Pennsylvania for generating the alpha-synuclein fibrils used in my project. I would also like to acknowledge the assistance of Denise Butler-Buccilli and Christine Close in maintaining the animal colonies.

I thank all of the graduate students, faculty, and administrative staff in the Graduate School of Pharmaceutical Sciences.

Finally, I thank my family and friends, especially my husband, Arash Zandieh, whose love and support made all of this possible.

TABLE OF CONTENTS

Page

LIST OF FIGURES

Page

Introduction

The impact of Parkinson's disease

Parkinson's disease is the second most common neurodegenerative disorder. It affects 1–3% of the global population over 50 years of age—about 1 million people in the United States and more than 5 million people worldwide (Dehay et al., 2015). A systematic review of Parkinson's incidence studies have shown that that aging plays a major role in the development of Parkinson's disease (Pringsheim et al., 2014). Parkinson's disease affects 1.5-fold more men than women (Wooten et al., 2004).

Parkinson's disease is characterized by motor deficits such as bradykinesia, rigidity, postural instability and resting tremor, which are generally attributed to the loss of dopaminergic neurons in the substantia nigra, pars compacta, and a subsequent decrease in dopamine levels in the striatum, the site of termination of the nigrostriatal pathway (Alexander, 2004). Parkinson's patients are also known to suffer from non-motor symptoms, such as psychosis, memory loss, and dementia, which do not respond well to conventional dopaminergic therapies and severely reduce quality of life.

Parkinson's disease imposes a significant economic burden on patients and the healthcare system. The economic burden of Parkinson's disease is estimated at a minimum of $14.4 billion per year in the United States, at a cost of approximately $22,800 per patient (Kowal et al., 2013). Nursing home care is a major contributor to the medical costs, rather than medical treatment

itself. The prevalence and economic burden of Parkinson's disease are projected to grow substantially over the next few decades with the projected explosion of the aging population (Kowal et al., 2013).

The hallmarks of Parkinson's disease are progressive neuronal degeneration and the presence of neuronal alpha-synuclein-bearing inclusions known as Lewy bodies and Lewy neurites (Dehay et al., 2015). Currently there is no effective neuroprotective or neurorestorative therapy to cure or slow down the progression of this disease, at least partly because the pathophysiological mechanisms underlying the disease are incompletely understood.

Patterns of neurodegeneration — Parkinson's disease staging

Heiko Braak and coworkers have proposed neuropathological staging criteria for postmortem tissue from Parkinson's victims (Braak et al., 2003a). These criteria are based upon the topographical extent of the alpha-synuclein inclusions. As mentioned above, Lewy bodies and Lewy neurites are predominantly composed of the misfolded alpha-synuclein protein (Baba et al., 1998, Duda et al., 2000). Lewy neurites are found in neuronal processes and globular Lewy bodies are housed within neuronal perikarya (Pollanen et al., 1993, Dickson, 2012).

Based on the presence of Lewy bodies and Lewy neurites, there are six Braak stages along a continuum (Braak et al., 2003a). The presymptomatic phase of Parkinson's disease consists of stages I, II, and III and the symptomatic phases consist of stages IV, V and VI. In stage I lesions are found in the dorsal IX/X motor nucleus and/or intermediate reticular formation (Braak et al.,

2003a). The anterior olfactory nucleus is also frequently affected with alpha-synucleinopathy in stage I, which probably underlies the loss of smell that almost all Parkinson's patients suffer from years before the onset of motor deficits. Gastrointestinal symptoms are also present in these pre-symptomatic phases and are strongly associated with Lewy pathology in the enteric nervous system (Palma and Kaufmann, 2014). The pathology in the anterior olfactory nucleus spreads more slowly into interconnected brain regions compared to that expanding from the brainstem. Stage II (medulla, pontine tegmentum) involves denser pathology in those areas first involved in stage I and additional new pathology in the caudal raphe nuclei, the gigantocellular reticular nucleus, and the coeruleus–subcoeruleus complex. Stage III (midbrain) consists of dopaminergic lesions in the pars compacta of the substantia nigra. Stage IV (basal prosencephalon and mesocortex) consists of pathology of earlier stages plus additional lesions in the prosencephalon. Cortical involvement begins at this late stage but is still confined to the temporal mesocortex (transentorhinal region) and allocortex (CA2 plexus). Stage V (neocortex) consists of pathology in all of the previously involved subcortical and mesocortical structures, plus additional pathology in higher order sensory association areas of the neocortex and prefrontal cortex. Stage VI (neocortex) affects the entire neocortex, including first-order sensory association areas of neocortex and premotor areas, with occasional mild changes in primary sensory areas and the primary motor fields.

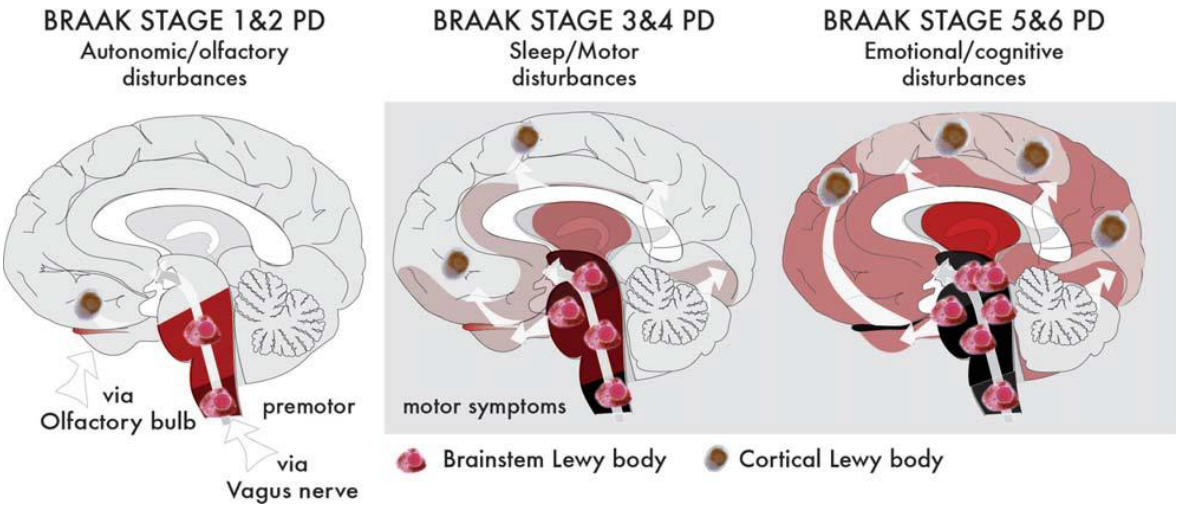

Fig. 1. Caudo-rostral progression of Lewy bodies in the brain in Parkinson's disease. Reprinted from "Milestones in Parkinson's disease—Clinical and pathologic features," by G. Halliday, A. Lees, and M. Stern, 2011, *Movement Disorders, 26,* p. 1015-1021. Copyright 2011, by John Wiley and Sons. Reprinted with permission.

Patterns of neurodegeneration — Alzheimer's disease staging

Similar to Parkinson's disease, Alzheimer's disease is associated with the spread of aggregated proteins across multiple brain regions. The major hallmarks of Alzheimer's disease are the appearance of neurofibrillary tangles and neuropil threads and senile plaques containing beta-amyloid (Ittner et al., 2010). Postmortem studies of Alzheimer's patients have mostly focused upon neurodegeneration in the cerebral cortex. The cerebral cortex is responsible for higher-order executive function, learning, and memory. In Alzheimer's disease, the temporal mesocortex and allocortex are affected with tau pathology before neocortex (Braak et al., 2006). Based on the spread of tau inclusions, Braak reported six stages in Alzheimer's disease. Alzheimer's disease stages I and II involve the transentorhinal region. Subsequently, the tau pathology extends into entorhinal regions, followed by involvement of the first and second CA fields of the hippocampal formation. In Alzheimer's disease stages III-IV (limbic system) there

is exacerbation of pathology in all previously involved regions, and initiation of pathology in neocortical higher order association areas. In end stages V-VI (neocortex), neocortical lesions become more severe and extend into primary sensorimotor areas of the frontal and parietal neocortex (Braak et al., 2006). Initial Alzheimer's disease pathology in limbic regions is associated with mild cognitive impairments in early stages of the disease (Weintraub et al., 2012). As neurodegeneration spreads to neocortical regions, more severe symptoms emerge and the full dementia syndrome becomes manifest (Braak and Braak, 1996). In Alzheimer's disease, both memory and executive function are strongly correlated with neuronal cell death in the entorhinal cortex (Albert, 1996, Gomez-Isla et al., 1996, Gomez-Isla et al., 1997).

In Alzheimer's disease, beta-amyloid formation begins in the neocortex. However, the total numbers of amyloid plaques do not correlate with the severity of the disease or with neuronal cell death (DaRocha-Souto et al., 2011). Furthermore, atrophy in the cerebral cortex follows the progression of tau pathology and not of amyloid formations (Arriagada et al., 1992, Josephs et al., 2008, Whitwell et al., 2008).

Cognitive impairments in Parkinson's disease dementia and dementia with Lewy bodies

The mechanisms underlying the cognitive deficits in Parkinson's disease and dementia with Lewy bodies are heterogeneous. Parkinson's disease dementia and dementia with Lewy bodies are both characterized by neuronal cell death and the formation of limbic and cortical Lewy pathology (Aarsland, 2016, Bellucci et al., 2016). Alzheimer's disease-related changes such as amyloid plaques and tau inclusions also contribute to the pathogenesis of both Parkinson's

disease dementia and dementia with Lewy bodies. However, the latter two pathologies are more common in dementia with Lewy bodies than in Parkinson's disease dementia. In Parkinson's disease dementia, parkinsonism typically occurs prior to the onset of cognitive impairments. In contrast, in dementia with Lewy bodies, cognitive deficits emerge after the onset of motor symptoms, or emerge almost simultaneously (Aarsland, 2016). The hippocampus develops Lewy pathology in Braak stages III and IV in Parkinson's disease. As mentioned above, stages V and VI are associated with the formation of alpha-synuclein inclusions in the expansive neocortex (Braak et al., 2003a). Alpha-synucleinopathy in the hippocampus and neocortex are strongly correlated with cognitive deficits in Parkinson's disease (Kalaitzakis and Pearce, 2009). To date, there are few models of Parkinson's disease dementia and of Lewy pathology in the hippocampus. Therefore, it has been difficult to establish whether Lewy pathology elicits or is merely correlated with impairments of cognitive function.

Pharmacological treatments for dementia in both Parkinson's disease dementia and dementia with Lewy bodies are largely limited to cholinesterase inhibitors and memantine, a partial NMDA-antagonist (Aisen et al., 2012). However, there is insufficient evidence to support the efficacy of available treatments. Thus, there is an urgent unmet need for agents to help control dementia and/or to decelerate the cognitive decline in Parkinson's disease dementia and dementia with Lewy bodies.

The transmission of Lewy pathology in Parkinson's disease

Alpha-synuclein is a 14kDa protein composed of 140 amino acids and is found in the nucleus, presynaptic terminals, cytosol, mitochondrial membrane, and endoplasmic reticulum (Maroteaux et al., 1988, Guardia-Laguarta et al., 2014). As mentioned above, alpha-synuclein is one of the main components of Lewy bodies and Lewy neurites. Although it has been studied for many years, the exact function of alpha-synuclein remains unknown. Some studies suggest that alpha-synuclein directly interacts with membrane phospholipids and plays a dynamic role in vesicle trafficking during neurotransmitter release (Recasens and Dehay, 2014). Mutations in six genes encoding for alpha-synuclein (p.A53T, p.A30P, p.E64K, p.H50Q, p.G51D, p.A53E) have been found to cause autosomal-dominant forms of Parkinson's disease (Polymeropoulos et al., 1997, Kruger et al., 1998, Athanassiadou et al., 1999, Spira et al., 2001, Zarranz et al., 2004, Ki et al., 2007, Choi et al., 2008, Puschmann et al., 2009, Appel-Cresswell et al., 2013, Lesage et al., 2013).

Alpha-synuclein is a natively unfolded protein with no defined structure in aqueous solutions (Stefanis, 2012). Under pathological conditions such as oxidative stress or following post-translational modifications, alpha-synuclein can adopt an oligomeric or fibrillar conformation, leading to the formation of Lewy bodies (Recasens and Dehay, 2014). The corresponding misfolded species expose beta sheet stretches that are prone to protein-protein interactions and subsequent formation of detergent-insoluble aggregations (Saxena and Caroni, 2011). Approximately 90% of alpha-synuclein found in Lewy bodies is phosphorylated at serine 129 (Sato et al., 2013). In contrast, only 4% or less of total alpha-synuclein is phosphorylated at this

residue under physiological conditions. However, it remains unclear whether the conformational changes and accumulation of alpha-synuclein promote disease through a toxic gain or loss of function.

Recent evidence suggests that misfolded alpha-synuclein can be transmitted from cell to cell across neuroanatomically linked brain regions (Luk et al., 2012a, Luk et al., 2012b, Jucker and Walker, 2013). The concept of cell-to-cell transmissibility is consistent with Braak staging, as the staging theory also describes the progressive involvement of additional brain regions with the passage of time (Braak et al., 2003a). In addition, Braak has observed that the areas sequentially corralled into exhibiting Lewy pathology are connected by neuroanatomical circuitry (Braak et al., 2003b).

Recent studies suggest that cell-to-cell transmission of alpha-synuclein is mediated by the release of fibrillar or oligomeric alpha-synuclein by exocytosis or necrosis into the extracellular milieu and subsequent uptake into neighboring neurons through endocytotic pathways (Luk et al., 2009, Volpicelli-Daley et al., 2011). Once inside the neighboring cell, misfolded □lpha-synuclein might continue to act as a seed or template, promoting the misfolding and aggregation of additional alpha-synuclein molecules, eventually resulting in further inclusion formation and Lewy pathology (Luk et al., 2009, Volpicelli-Daley et al., 2011).

Recent studies strongly suggest that alpha-synucleinopathy can be transmitted from the diseased host brain to healthy, young transplanted tissue. For example, Lewy bodies have been detected in fetal mesencephalic neurons that were transplanted into the striatum of Parkinson's patients 12-

16 years prior to death and postmortem analyses (Angot et al., 2010). Host-to-graft transfer of alpha-synuclein has also been confirmed in animal studies, as post-mitotic dopaminergic neurons grafted into the striatum of mice overexpressing human alpha-synuclein exhibit human alpha-synuclein immunoreactivity six months after transplantation (Hansen et al., 2011). The latter study further suggests that multiple forms of alpha-synuclein, including monomers, oligomers and fibrils, can be taken up by neurons (Hansen et al., 2011). Intracerebral injections of brain homogenates derived from old symptomatic alpha-synuclein transgenic mice into the neocortex and striatum of young asymptomatic transgenic mice accelerate the spread of alpha-synucleinopathy throughout the central nervous system (olfactory bulb to the spinal cord), and reduce lifespan (Luk et al., 2012a). Furthermore, injections of synthetic recombinant alpha-synuclein fibrils alone are sufficient to initiate and propagate alpha-synuclein pathology within interconnected brain regions in healthy wildtype mice in a time-dependent manner (Luk et al., 2012b). Exogenous alpha-synuclein fibrils induce the misfolding and aggregation of endogenous alpha-synuclein molecules and lead to cell loss in the substantia nigra and impairments in motor coordination. Finally, recent *in vitro* studies have demonstrated that alpha-synuclein fibrils can recruit endogenous alpha-synuclein to form pathologic, insoluble aggregates in cultured cells overexpressing alpha-synuclein (Luk et al., 2009, Hansen et al., 2011, Volpicelli-Daley et al., 2011). It is important to note that the development of Lewy-like pathology in these models is abolished in cells from alpha-synuclein knockout mice, strongly supporting the view that it is the misfolding of endogenous alpha-synuclein molecules that is responsible for the emergence of inclusion bodies (Bernis et al., 2015). In addition to the spread of the pathology through interconnected neural networks, selective regional vulnerabilities may also play a role in the determining the topography of Lewy body formations.

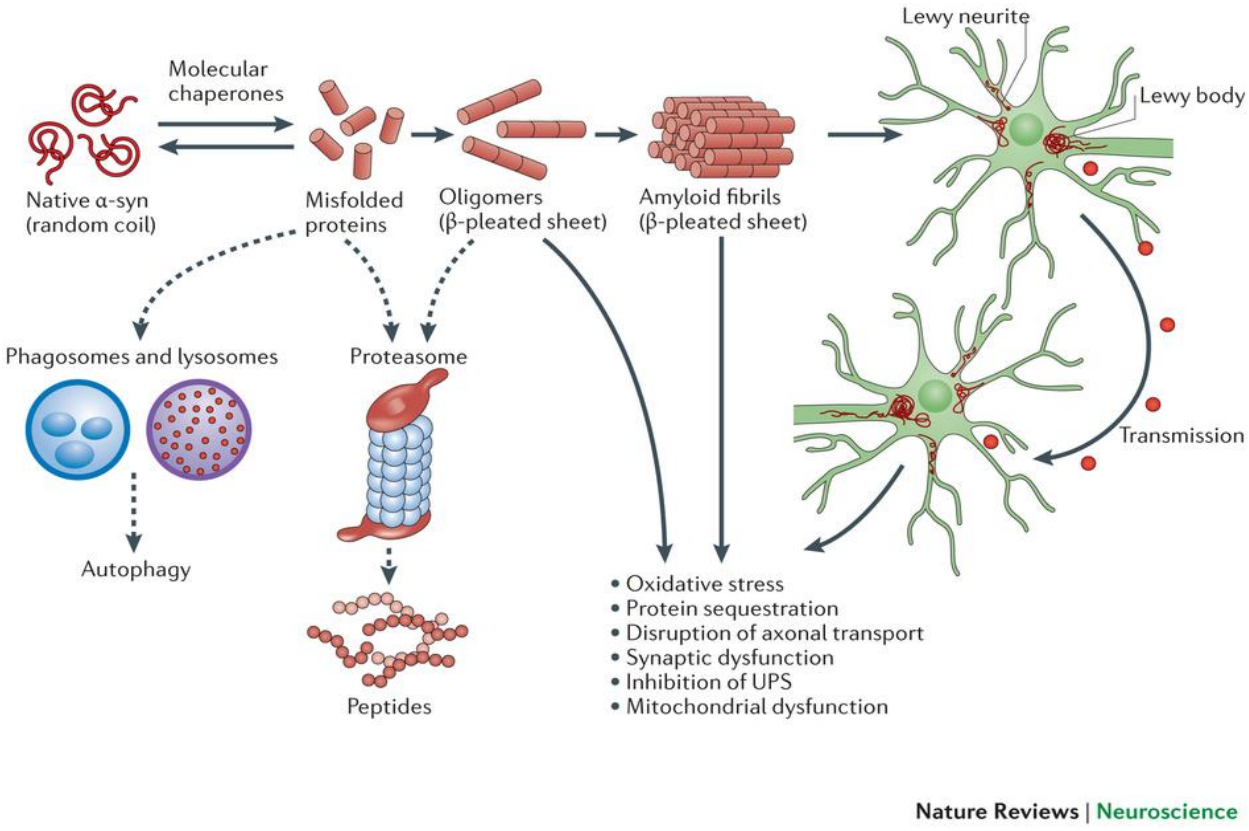

Fig. 2. Hypothetical model of alpha-synuclein toxicity and spread of pathology in Parkinson's disease and Parkinson's disease dementia. Reprinted by permission from Macmillan Publishers Ltd: *Nature Reviews Neuroscience* ("Parkinson's disease dementia: convergence of [alpha]-synuclein, tau and amyloid-[beta] pathologies," by David J. Irwin, Virginia M.-Y. Lee, John Q Trojanowski, 2013, *Nature Reviews Neuroscience*, 14, p. 626–636). Copyright (2013).

Neurodegenerative Mechanisms in Parkinson's disease —Accumulation of misfolded proteins

Similar to other neurodegenerative disorders, Parkinson's disease is characterized by the accumulation of protein aggregates and disruptions in the ubiquitin proteasome system and the autophagy-lysosomal pathway. Soluble alpha-synuclein is degraded by the proteasome. Mutant alpha-synuclein adopts a fibrillar structure that can directly interact with the 20S core of the proteasome and decrease its proteolytic activity (Lindersson et al., 2004). Loss of proteasome

function and 20S proteasomal subunits has been reported in the substantia nigra of Parkinson's patients (McNaught and Jenner, 2001, Fishman-Jacob et al., 2009).

Molecular chaperones such as the heat shock proteins Hsp70/Hsc70, Hsp40, and Hsp90 are critical for maintaining protein homeostasis (Ebrahimi-Fakhari et al., 2011b). Sequestration of chaperones in Lewy bodies might result in a general depletion of chaperones in experimental models of Parkinson's disease as well as in patients. Ubiquitin proteasomal dysfunction has been shown to elicit alpha-synuclein aggregation in primary mesencenphalic neurons, dopaminergic neuronal cell lines, as well as in animal models (McNaught et al., 2002a, McNaught et al., 2002b, Sun et al., 2006). Autosomal recessive loss-of-function mutations in the E3 ubiquitin ligase parkin are associated with familial Parkinson's disease (Imai et al., 2000, Shimura et al., 2000). Furthermore, mutations in ubiquitin carboxy-terminal hydrolase L1 are also associated with familial Parkinson's disease and lead to impairments in protein quality control (Leroy et al., 1998). The accumulation of ubiquitinated proteins, heat shock proteins, and components of the ubiquitin proteasome system within Lewy bodies and the inhibition of proteasome activity in the substantia nigra all suggest that loss of proteasome function plays an important role in the pathogenesis of Parkinson's disease (Lennox et al., 1989, Lowe et al., 1990, Ii et al., 1997, Auluck et al., 2002, McNaught et al., 2002d, Schlossmacher et al., 2002) .

Impairments in the ubiquitin-proteasome system have been modeled in the substantia nigra in order to investigate the mechanisms underlying neurodegeneration in Parkinson's disease and to test potential therapeutics (McNaught et al., 2002c, Petrucelli et al., 2002, Rideout et al., 2005, Sun et al., 2006). *In vitro* studies suggest that proteasome inhibitors elicit relatively selective degeneration of cultured dopamine neurons and the formation of ubiquitin and alpha-synuclein^{+}

inclusions. In addition, infusions of proteasome inhibitors into animals lead to Lewy-like inclusions in the basal ganglia (Fornai et al., 2003, McNaught et al., 2004, Xie et al., 2010). For example, the peptide aldehyde MG132 has been shown to induce degeneration in the substantia nigra, pars compacta, and to deplete dopamine levels in both cell culture and animal models of Parkinson's disease (Sun et al., 2006). Injections of the cyclic amide lactacystin into the medial forebrain bundle of C57BL/6 mice induces dopaminergic neurodegeneration in the substantia nigra, and this is accompanied by inhibition of proteasomal activity and the formation of alpha-synuclein positive inclusions, activated glia, and decreased motor activity (Xie et al., 2010). Thus, proteasome inhibition recapitulates many important biochemical and behavioral features of Parkinson's disease, making it suitable for testing potential neuroprotective therapies.

Impairments in the autophagic-lysosomal pathway can also contribute to loss of protein homeostasis and is associated with multiple neurodegenerative diseases. For example, neuron-specific autophagy gene knockout mice have been found to develop intraneuronal aggregates and neurodegeneration (Hara et al., 2006, Komatsu et al., 2006). Furthermore, overexpression of alpha-synuclein has been shown to impair autophagic clearance in mammalian cells and mice by inhibiting autophagosome formation (Winslow et al., 2010). Mutant alpha-synuclein may also disrupt chaperone-mediated autophagy by blocking the translocation of substrates into the lysosome through the LAMP2A lysosomal receptor (Cuervo et al., 2004, Martinez-Vicente et al., 2008).

Neurodegenerative mechanisms in Parkinson's disease — Oxidative stress

The molecular mechanisms underlying the loss of dopaminergic neurons in Parkinson's disease still remain unclear. However, oxidative stress is thought to play an important role in dopaminergic neurotoxicity (Blesa et al., 2015). Parkinson's disease has long been associated with excess production of reactive oxygen species and alterations in the metabolism of excitatory amino acids and neurotransmitters, all of which can lead to formation of toxic byproducts. Oxidative stress is thought to be the common underlying mechanism leading to cellular dysfunction and cell death in both familial and sporadic forms of Parkinson's disease (Ryan et al., 2015). Reactive oxygen species can directly cause protein and DNA damage in addition to lipid peroxidation. For example, oxidatively damaged proteins are present in the substantia nigra, pars compacta in Parkinson's disease (Yoritaka et al., 1996, Alam et al., 1997). Antioxidant enzymes serve to blunt the impact of reactive oxygen species and include superoxide dismutase, glutathione peroxidase, and catalase (Powers and Jackson, 2008). Deficiencies in complex I of the mitochondrial respiratory chain, protein folding, and the ubiquitin proteasome system also generate oxidative stress and exacerbate the toxicity of existing reactive oxygen species (Double et al., 2010).

Neurons are post-mitotic cells with an abundance of unsaturated lipids, which makes them particularly sensitive to peroxidation and oxidative modification (Uttara et al., 2009). In addition, the brain has lower levels of antioxidant defenses compared to other tissues such as the liver, which renders it especially susceptible to reactive oxygen species. Enzymes such as tyrosine hydroxylase and monoamine oxidase make dopaminergic neurons particularly sensitive to

oxidative stress because dopamine can be metabolized into toxic byproducts such as hydrogen peroxide and dopamine quinones if it is not sequestered into acidic vesicles (Halliwell, 1992). Furthermore, nigral dopaminergic neurons contain high levels of iron, which can catalyze the Fenton reaction and generate superoxide radicals and hydrogen peroxide, thereby resulting in further oxidative stress.

Reactive oxygen species may induce intracellular calcium influx through glutamate receptors and elicit excitotoxicity, which may culminate in cell death (Uttara et al., 2009). Chronic oxidative stress can also interfere with autophagic degradation system, causing incomplete degradation of lysosomal cargo and subsequent intralysosomal accumulation of cross-linked products such as lipofuscin, and further lysosomal dysfunction (Terman and Brunk, 2004, Cuervo et al., 2005, Kiffin et al., 2006).

A strong link between oxidative stress and neuronal death has been established in animal models. Paraquat, a structural analog of 1-methyl-4-phenylpyridinium (MPP^+), is a redox cycling compound and was previously widely used as an herbicide. This compound causes mitochondrial damage by inhibition of complex I of the electron transport chain and increases the levels of reactive oxygen species such as the superoxide free radical (Jenner, 2003, Castello et al., 2007). Chronic administration of paraquat in mice or rats decreases the number of dopaminergic neurons in the substantia nigra, pars compacta, and striatal levels of dopamine and impairs motor function (McCormack et al., 2002, Shimizu et al., 2003, Thiruchelvam et al., 2003).

Epidemiological studies suggest an association between chronic exposure to pesticides, particularly paraquat and rotenone, and an increased risk for developing Parkinson's disease (Hertzman et al., 1990, Semchuk et al., 1993, Liou et al., 1996, Gorell et al., 1998). Thus, neuroprotective therapies that target multiple pathological pathways such as mitochondrial and ubiquitin–proteasome dysfunction are urgently needed to prevent or slow the progression of neurodegeneration. It is likely that mitochondrial dysfunction leads to loss of protein quality control by an increase in oxidatively damaged proteins and reduced protein clearance whereas protein misfolding may lead to an increase in reactive oxygen species by impairing the normal function of the mitochondrion.

Traditional and novel animal models of Parkinson's disease

As mentioned above, there are no effective treatments to cure or slow down the progression of Parkinson's disease because the underlying pathophysiology is incompletely understood. In order to accelerate the identification of a cure, it is essential to understand the mechanisms underlying neurodegeneration in animal models and in the human condition. However, all currently available animal models fail to mimic every aspect of the human pathology and, perhaps as a result, the results obtained from these models have not always translated to the clinic. Here we will discuss the strengths and limitations of several commonly used *in vivo* models of Parkinson's disease including: 1) toxicant models, such as the 6-hydroxydopamine (6-OHDA) and the 1-methyl-4-phenyl-1,2,3,6-tetrahydropyridine (MPTP) models, which selectively and rapidly destroy catecholaminergic systems through oxidative stress and mitochondrial dysfunction; 2) agricultural chemicals such as rotenone and paraquat, which also

lead to neurodegeneration through mitochondrial dysfunction and increased reactive oxygen species; 3) proteasome inhibitor-induced neurodegeneration as a result of loss of protein degradation via the ubiquitin–proteasome system (UPS) and subsequent protein aggregations; 4) fibrillized alpha-synuclein protein and proteotoxic stress induced by protein misfolding and aggregation. However, the specific toxicity of proteasome inhibitors would be expected to be somewhat distinct from the toxicity of fibrillized alpha-synuclein, because many more proteins would be affected via general loss of protein degradation through the proteasome. In contrast, alpha-synuclein would be expected to act as a template for the seeding of neighboring alpha-synuclein molecules, and may or may not encompass the misfolding of other endogenous proteins. Below we discuss the strengths and weaknesses of each model and their contributions to our understanding of Parkinson's disease.

Toxicant models: 6-Hydroxydopamine

6-hydroxydopamine (6-OHDA) is an analog of dopamine with an additional hydroxyl group. It was first described 50 years ago (Tieu, 2011, Blesa et al., 2012) and was initially reported to induce depletion of noradrenaline in the mouse heart (Porter et al., 1963, Porter et al., 1965, Deumens et al., 2002, Tieu, 2011). 6-OHDA has been widely used to lesion the nigrostriatal dopaminergic pathway and thereby model Parkinson's disease. 6-OHDA is taken up by catecholamine transporters, including dopamine and norepinephrine transporters (Sachs and Jonsson, 1975a, b), and can induce cell death through increased production of reactive oxygen species such as H_2O_2 as well as dopamine quinones. 6-OHDA does not cross the blood-brain barrier. Therefore, in order to induce dopaminergic neuronal loss in Parkinson's disease models, it needs to be directly injected into the striatum, medial forebrain bundle, or substantia nigra

using stereotaxic brain surgery. The magnitude of the lesion depends on the dose of 6-OHDA, the site of injection, the manufacturer of the neurotoxin, and the species of the animal used (He et al., 2000, Smith et al., 2006, Rodriguez-Pallares et al., 2007). One major advantage of using 6-OHDA in Parkinson's disease models is the induction of motor deficits, and the ability to test experimental therapies that reverse or lessen the histological and behavioral insult.

Toxicant models: Methyl-4-phenyl-1, 2,3,6 tetrahydropyridine (MPTP)

MPTP was accidentally discovered in 1982 when drug addicts developed acute parkinsonian symptoms after intravenous injections of this neurotoxin. L-DOPA treatments were successful in controlling behavioral abnormalities in these patients, suggesting similar underlying neuropathological features as those seen in Parkinson's patients (Sachs and Jonsson, 1975a, Bezard et al., 1999, Tieu, 2011, Blesa et al., 2012). These findings led to the development of rodent and nonhuman primates models of Parkinson's disease. MPTP is highly lipophilic and can readily pass the blood brain barrier upon systemic administration. In astrocytes, MPTP is metabolized and converted to MPP^+—the active metabolite—, which is transported into catecholaminergic neurons through the dopamine and norepinephrine transporters. MPP^+ induces dopaminergic neurodegeneration mainly by inhibiting complex I of the electron transport chain in mitochondria, resulting in ATP depletion, formation of reactive oxygen species, and increased oxidative stress (Nicklas et al., 1987, Nicklas et al., 1992, Tieu, 2011, Blesa et al., 2012), (Mizuno et al., 1987). Rats are relatively insensitive to MPTP neurotoxicity due to the lack of monoamine oxidase-B in their brains, and currently this model is mostly employed in murine and primate species.

Toxin models: Lipopolysaccharide (LPS)

LPS is an endotoxin isolated from Gram-negative bacteria. It serves as a glial activator and induces neuroinflammation as well as selective and progressive dopaminergic neuronal loss following injections in the nigrostriatal pathway (Dutta et al., 2008, Liu and Bing, 2011). LPS induces neuronal damage by inducing the release of the proinflammatory factors interleukin 1 and 6 (IL-1 and IL-6), tumor necrosis factors (TNF), and nitric oxide (NO), all of which activate the immune response (Czlonkowska et al., 2002, Mosley et al., 2006, Laurie et al., 2007, Qin et al., 2007, Liu and Bing, 2011). LPS-based models of Parkinson's disease can be used to model inflammation-associated dopaminergic neurodegeneration, in addition to being useful for neuroprotective drug discovery.

Proteasome inhibitors: Lactacystin, MG132, PSI (Z-lle-Glu (OtBu)-Ala-Leu-al)

Impairment of the ubiquitin proteasome system has been reported to play an important role in the pathogenesis of Parkinson's disease. Systemic exposure to proteasome inhibitors causes levodopa-responsive motor dysfunction in mice and rats (Xie et al., 2010). Naturally derived proteasome inhibitors, as well as synthetic proteasome inhibitors (PSI), (Z-lle-Glu (OtBu)-Ala-Leu-al) have been recently used to induce neurodegeneration in the substantia nigra, locus coeruleus, dorsal motor nucleus of vagus, and the nucleus basalis of Meynert (Braak et al., 2003a, Zarow et al., 2003, McNaught et al., 2004, McNaught and Olanow, 2006). In addition to neuronal loss, intracytoplasmic Lewy-body-like inclusions that stained positively for alpha-synuclein, ubiquitin, and other proteins have been reported in proteasome inhibitor-induced models of Parkinson's disease. Inhibition of proteasomal function can induce progressive

neurodegeneration with similarities to Parkinson's disease and may be useful in developing and testing neuroprotective therapies (McNaught et al., 2004, McNaught and Olanow, 2006). Unfortunately, the systemically delivered approach exhibits poor reproducibility and failed to cause any noticeable behavioral or neuropathological abnormality in rodents in most other labs (Bove et al., 2006). On the other hand, other labs have shown that intrastriatal infusions of proteasome inhibitors elicit dopaminergic neurodegeneration (Fornai et al., 2004, Sun et al., 2006).

Pesticide/Herbicide/ Fungicide models: Rotenone

Rotenone is a highly lipophilic insecticide and pesticide (Blesa et al., 2012) that can easily cross the blood brain barrier. This neurotoxin is a strong inhibitor of mitochondrial complex I (Li et al., 2003). Chronic exposure to rotenone has been reported to cause important features of Parkinson's disease, including nigrostriatal dopaminergic degeneration (Betarbet et al., 2000, Hisahara and Shimohama, 2010) and intracellular Lewy body-like inclusions immunoreactive for ubiquitin and alpha-synuclein (Betarbet et al., 2000, Sherer et al., 2003, Blesa et al., 2012) Similar to Parkinson's disease, neurodegeneration induced with rotenone expands beyond the dopaminergic system, and is associated with toxicity in serotonin, noradrenergic, and cholinergic neurons (Heikkila et al., 1985, Fornai et al., 2005, Hoglinger et al., 2005, Blesa et al., 2012). Attempts to lesion animal species other than rats have not always been successful. In addition, there are no convincing reports of human Parkinson's disease symptoms due to rotenone exposure (Blesa et al., 2012).

Pesticide/Herbicide/ Fungicide models: Paraquat (N, N'-dimethyl-4,4'-bipyridinium dichloride)

Paraquat is an herbicide with structural similarities to MPP^+, the active metabolite of MPTP. A few cases of paraquat-induced Parkinson's disease symptoms have been reported among humans (Hoglinger et al., 2003, Hoglinger et al., 2005, Blesa et al., 2012). Paraquat exhibits its toxicity mainly due to oxidative stress and generation of superoxide, hydroxyl, and hydrogen peroxide radicals. Some researchers have reported that animals exhibit dose-dependent loss of striatal TH-positive striatal fibers and midbrain substantia nigra neurons following systemic paraquat exposure (Brooks et al., 1999, McCormack et al., 2005, Blesa et al., 2012). However, others demonstrated that high doses of paraquat interfere with the function of dopamine transporters and organic cationic transporter-3. Paraquat is therefore toxic to dopaminergic neurons in the substantia nigra only when used in high doses (Blesa et al., 2012). Recent studies suggest that combined exposure to paraquat and the fungicides Maneb and Ziram lead to greater risk of developing Parkinson's disease in humans (Zhang et al., 2010, Tanner et al., 2011, Blesa et al., 2012). However, further investigations are needed to determine the involvement of environmental exposures in the etiology of Parkinson's disease.

Pathological alpha-synuclein fibril models

Lewy bodies and Lewy neurites are the neuropathological hallmark of Parkinson's disease and are composed of aggregated proteins such as alpha-synuclein (Spillantini et al., 1998a, Malek et al., 2014). Virginia Lee's lab has shown that intracellular alpha-synuclein aggregation can be triggered by the introduction of exogenous recombinant alpha-synuclein fibrils into cultured cells engineered to overexpress alpha-synuclein. Unlike unassembled alpha-synuclein, these alpha-

synuclein fibrils convert endogenous soluble alpha-synuclein protein into insoluble, hyperphosphorylated, and ubiquitinated pathological forms (Luk et al., 2012a, Luk et al., 2012b). The same authors also reported that intrastriatal inoculation of synthetic alpha-synuclein fibrils in wild-type nontransgenic mice led to the development of motor deficits, nigral cell loss, and Parkinson's-like Lewy pathology in anatomically interconnected regions, although the extent of the neuroanatomical transmission of Lewy pathology was not thoroughly investigated. Lewy pathology accumulation following intrastriatal fibril infusions resulted in progressive loss of neurons in the substantia nigra, pars compacta, but not in the adjacent ventral tegmental area. This novel approach recapitulates key features of Lewy bodies in human Parkinson's disease brains and establishes a mechanistic link between transmission of pathologic alpha-synuclein, inclusion formation, and cell death (Luk et al., 2012a, Luk et al., 2012b). Thus, alpha-synuclein pathology is sufficient to induce some of the behavioral and pathological features of sporadic Parkinson's disease.

Table 1: Animal models of Parkinson's disease

Model	Nigrostriatal neurodegeneration	Extranigral pathology	Motor symptoms	Non-Motor Symptoms	Animal Species	Disadvantages	Citation
Toxin/Toxicant-Induced Models							
6-hydroxydopamine (6-OHDA)	Yes (dopaminergic cell bodies in SN-and dopaminergic terminal in STR)	No	Yes	Yes (Dementia, psychiatric, GI disorder)	Rat, Mouse	Acute, intracerebral	(Hisahara and Shimohama, 2010, Tieu, 2011, Blesa et al., 2012)
Methyl-4-phenyl-1, 2,3,6 tetrahydropyridine (MPTP)	Yes (dopaminergic cell bodies in SN-and dopaminergic terminal in STR)	Yes (Locus coeruleus)	Yes	Cognitive deficit	Rat, Mouse, nonhuman primates	Acute, hazardous	(Hisahara and Shimohama, 2010, Tieu, 2011, Blesa et al., 2012)
Lipopolysaccharide (LPS)	Yes (dopaminergic cell bodies in SN)	Yes (VTA)	Yes	Cognitive deficit	Rat, Mouse	Flu-like symptoms	(Qin et al., 2007)
Proteasome inhibitors							
Carbobenzoxy-l-isoleucyl-γ-t-butyl-l-glutamyl-l-alanyl-l-leucinal (PSI)	Yes (dopaminergic cell bodies in SN-and dopaminergic terminal in STR)	Yes (VTA)		No	Rat, Mouse	Acute, intracerebral	(Bukhatwa et al., 2009, Xie et al., 2010)
MG132	Yes (dopaminergic cell bodies in SN-and dopaminergic terminal in STR)	Yes (VTA)	Yes	Cocaine Reward Memory Retrieval	Rat, Mouse	Acute, intracerebral	(Xie et al., 2010, Ren et al., 2013)
Pesticide/Herbicide							
Paraquat	Yes (dopaminergic cell bodies in SN-and dopaminergic terminal in STR)	Yes (Locus coeruleus)	Not determined	GI disorder	Rat, Mouse	Acute, hazardous	(Hisahara and Shimohama, 2010, Tieu, 2011, Blesa et al., 2012)
Rotenone	Yes (dopaminergic cell bodies in SN-and dopaminergic terminal in STR)	Not determined	Not determined	Decrease in GI motility	Rat, Mouse	Acute, hazardous	(Hisahara and Shimohama, 2010, Tieu, 2011, Blesa et al., 2012)
Pathological alpha-synuclein fibrils	Yes (dopaminergic cell bodies in SN-and dopaminergic terminal in STR)	Yes (neocortex, amygdala, frontal cortex, Hippocampus.)	Yes	NO	Mouse, Rat	Time dependent.	(Luk et al., 2009, Luk et al., 2012a, Luk et al., 2012b)

Animal models have led us to a deeper understanding of the pathogenesis of Parkinson's disease. The animal models of Parkinson's disease have accelerated the discovery of novel treatments for the motor symptoms of Parkinson's disease. The majority of Parkinson's disease cases are known to be sporadic. Here, we have discussed the weaknesses and strengths of the most common *in vivo* non-transgenic models of Parkinson's disease. These models include neurotoxins, pesticides/herbicides, as well as the recent use of alpha-synuclein fibrils to induce Parkinson's-like Lewy pathology and/or dopaminergic neurodegeneration. However, none of these models can fully recapitulate the complexity of human Parkinson's disease. It is likely that Parkinson's disease has both genetic and environmental roots. Therefore, future models may involve a combination of neurotoxin-induced and genetically induced Parkinson's disease. It is also important to consider using aged animals to increase their predictive validity.

Protective molecules implicated in protection against Parkinson's disease: Glutathione and its precursor N-acetyl-$_L$-cysteine

As mentioned earlier, neurodegenerative disorders such as Parkinson's disease are characterized by oxidative stress. Under physiological conditions, oxidative stress is effectively handled by endogenous antioxidant defenses within the cell. Glutathione is the most abundant antioxidant in the brain and is found in millimolar concentrations is most cells (Pocernich and Butterfield, 2012). Glutathione is synthesized in both neurons and glia and detoxifies oxidants and electrophiles (Griffith, 1999, Dringen, 2000, Dickinson and Forman, 2002). Under pathological conditions, excessive production of reactive oxygen species and depletion of glutathione elicits oxidative damage (Dias et al., 2013).

The glutathione precursor *N*-acetyl-$_{L}$-cysteine (NAC) was recently tested on Parkinson's patients as a neuroprotective compound (Monti et al., 2016). In this study, NAC increased dopamine transporter binding and improved UPDRS motor deficit scores, but the sizes of the effects were relatively small (~10%) and the sample size was small. NAC can also elicit protection in glutathione-independent manners in cellular models (Jiang et al., 2013; Posimo et al., 2013; Unnithan et al., 2012; Unnithan et al., 2014). Recently, the Leak lab has shown that NAC may also facilitate a stress-induced increase in heat shock protein 70 (Hsp70) in cellular models of neurodegeneration (Jiang et al., 2013). Thus, in the present project, we hypothesize that treatment with NAC may reduce proteotoxic and oxidative stress in experimental Parkinson's disease. This subject will be discussed further in the chapter 2 of this dissertation.

Protective molecules implicated in protection against neurodegeneration: dehydroepiandrosterone sulfate

Neurosteroids play a crucial role in the proper functioning of the central and peripheral nervous systems, and help regulate neurotransmitter systems, promote neuronal viability, improve myelination, and control cognitive processes (Paul and Purdy, 1992, Mathis et al., 1994, Meziane et al., 1996, Maurice et al., 1998, Akwa et al., 2001). The term neurosteroid refers to steroid hormones that can be synthesized both in brain and/or endocrine glands, either *de novo* from cholesterol or by *in situ* metabolism of circulating hormones that accumulate in the nervous system independent from steroidogenic gland secretion rates (Baulieu, 1997, Wojtal et al., 2006).

Dehydroepiandrosterone sulfate (DHEAS) is the sulfated ester of the neurosteroid dehydroepiandrosterone (DHEA). DHEAS and DHEA are two of the most abundant

neurosteroids synthesized within the nervous system (Flood et al., 1988, Migues et al., 2002). Physiological concentrations of DHEA and DHEAS are maintained by the enzymes steroid sulfates and sulfuryl transferase in the peripheral tissues, as well as in the brain (Babalola et al., 2012). The levels of these two abundant adrenal steroids decrease with age in both men and women (Schumacher et al., 2003). The link between reduced levels of DHEAS and neurodegenerative diseases is still a controversial issue. However, some studies suggested that the levels of DHEAS are significantly reduced in the brains of patients with Alzheimer's disease compared with healthy individuals (Nasman et al., 1991, Leblhuber et al., 1993, Solerte et al., 1999, Murialdo et al., 2000). *In vivo* studies in rats using microdialysis suggest that intraperitoneal injections of DHEAS induce hippocampal acetylcholine release, which is an important neurotransmitter in cognitive function (Rhodes et al., 1996). Furthermore, inhibition of steroid sulfatase increases DHEAS levels by preventing its conversion back to DHEA, and facilitates the memory-enhancing effects of DHEAS (Johnson et al., 1997, Li et al., 1997, Johnson et al., 2000). Other studies have also demonstrated that DHEAS protects hippocampal neurons against glutamate-induced neurotoxicity in the hippocampus while little protection is obtained from the equivalent doses of DHEA (Mao and Barger, 1998). These results suggest that DHEAS is a neuroprotective agent with the potential to alleviate dementia associated with Lewy body disorders. This subject will be discussed further in the chapter 3 of this dissertation.

Materials and Methods

Animals and surgeries

All animal housing, treatments, and procedures were in accordance with the *NIH Guide* and approved by the Duquesne University Institutional Animal Care and Use Committee. Male Sprague Dawley rats were purchased from Hilltop Lab Animals (Scottdale, Pennsylvania). Male CD1 mice from Charles River (Horsham, PA) were bred in the Duquesne animal care facility and housed in a 12:12 photoperiod with *ad libitum* access to food and UV-disinfected water. On the day of surgery, animals were anesthetized with 2–3% vaporized isoflurane in 3% oxygen and stabilized in a stereotaxic frame.

Proteasome inhibitors: Male mice (3 months old) were infused with proteasome inhibitors MG132 (0.25 μg in 0.5 μl, 0.5 μg in 1 μl , 1 μg in 2 μl, 3.75 μg in 3 μl) or lactacystin (0.25 μg in 0.25 μl, 0.5 μg in 0.5 μl, 1 μg in 1 μl, 2 μg in 2 μl) or 1 μl vehicle into the hippocampus (ML −2.0 mm, AP −2.5 mm, and DV −2.7 mm from skull) with a Hamilton syringe (80085, Hamilton, Reno, NV) over the course of 4 min, followed by a 4 min rest period prior to removal, to minimize diffusion into dorsal structures during withdrawal. Animals were perfused 7 days post-injection.

Alpha-synuclein: Male mice (3 months old) were infused with preformed alpha-synuclein fibrils of wild-type mouse origin, as described previously (Luk et al., 2012a) (5 μg in 1 μl, 6.25 μg in 1.25 μl, 12.5 μg in 2.5 μl, 25 μg in 5 μl) or 1 μl vehicle into the hippocampus (ML −2.0 mm, AP

−2.5 mm, and DV −2.7 mm from skull) and perfused 30 or 90 days post-injection. For this experiment, the fibrils were sonicated with the probe sonicator (Misonix model XL2020, Misonix incorporated, Farmingdale NY), 60 pulses each for 0.2 sec.

Male rats (3 months old) were infused with 2 μg in 0.4 μl fibrils or 0.4 μl vehicle into the striatum (ML ±3.0 mm, AP +0.20 mm, and DV −4.0 mm from skull) and/or hippocampus (ML ±2.7 mm, AP −4.5 mm, and DV −3.2 mm from skull) bilaterally over the course of 4 min followed by a 4 min rest period. For this experiment, the fibrils were sonicated in the waterbath-sonicator (FS15 ultrasonic cleaner, Thermo Fisher Scientific incorporated, Waltham, MA) for 60 sec.

FluoroGold and 6-OHDA: Male CD1 mice (3 months old) were injected with FluoroGold (6 μg in 0.4 μL), 6-OHDA (4 μg in 1.6 μL) or an equal volume of vehicle into the caudoputamen (ML −2.0 mm, AP +0.5 mm, and DV −3.2 mm from bregma). For the studies using FluoroGold, the tracer was delivered one week before 6-OHDA infusions in the same striatal location to retrogradely label the nigrostriatal pathway. The doses chosen for 6-OHDA and FluoroGold are consistent with other reports (Liang et al., 2008, Cohen et al., 2011, Lazzarini et al., 2013, Bagga et al., 2015) and did not lead to any overt tissue necrosis at the injection site.

Animals were placed on a heating pad until resumption of spontaneous locomotor activity and then returned to their cages until sacrifice. All animals received 0.015 mg/kg buprenorphine subcutaneously during recovery from surgery and lidocaine and antibiotic treatment of the scalp wounds.

NAC: In the NAC experiments, mice received 100 mg/kg NAC in PBS or an equal volume of vehicle (4.44 mL/kg body weight or 0.176 mL per 40 g mouse) as a daily intraperitoneal injection using an insulin syringe (309311, Becton Dickinson, Franklin Lakes, NJ). These daily injections were initiated on the day of the 6-OHDA surgeries, immediately after the surgeries were completed. At the end of the experiment, animals were reanesthetized with isoflurane and perfused through the left ventricle with 50 mL of saline followed by 100 mL of 4% paraformaldehyde (9990244, Thermo Scientific, Kalama- zoo, MI) in 0.1 M phosphate buffer.

DHEAS: In the DHEAS experiments, animals received 10 mg/kg DHEAS in PBS or an equal volume of vehicle (1 mL/kg body weight or 0.4 mL per 400 g rat) intraperitoneally using an insulin syringe immediately before the novel object/place recognition tests. At the end of the experiment, animals were reanesthetized with isoflurane and perfused through the left ventricle with 100 mL of saline followed by 200 mL of 4% paraformaldehyde in 0.1 M phosphate buffer.

Chemicals and antibodies

Primary and secondary antibodies and their dilutions are listed in supplementary **Tables 3 and 4** in the Appendix**.** Omission of primary antibodies from the assays always resulted in loss of signal. Proteasome inhibitors MG132 (474790, EMD Millipore, Billerica MA) and lactacystin (AdipoGen Corporation, San Diego, CA) were stored at – 20 and – 80 ^{o}C, respectively, as 10 mM stock solutions in dimethyl sulfoxide (DMSO).

6-OHDA was purchased from Sigma-Aldrich (H116-5MG, Sigma-Aldrich, St. Louis, MO) and

stored at a concentration of 2.5 mg/mL at −20 °C until use. FluoroGold was purchased from FluoroChrome (Fluorochrome LLC, Denver, CO) and stored at a concentration of 1.5% in PBS at 4 °C until use.

NAC was purchased from Acros Organics (160280250, Acros Organics, Morris, NJ), dissolved in phosphate-buffered saline (PBS), sterile-filtered, and stored at a concentration of 22.5 mg/mL at −20 °C until use.

DHEAS was purchased from Sigma-Aldrich (D5297-1G, Sigma-Aldrich, St. Louis, MO) and prepared at a concentration of 10 mg/mL on the day of the experiment by dissolving in phosphate-buffered saline (PBS) and sterile-filtered before injections.

Histology

Perfused brains were immersed in 30% sucrose in 10 mM PBS for 48 h and cut on a freezing microtome in the coronal or sagittal plane. Free-floating sections (50 μm) were stored in cryoprotectant at − 20 °C until immunostaining was performed. Cryoprotectant was rinsed off with three exchanges of PBS and sections were then incubated in a 1:1 solution of Odyssey Block (LI-COR Bioscience, Lincoln, NE) in PBS for 1 h at room temperature on a shaker. Sections were subsequently incubated in primary antibodies at the concentrations listed in **Table 3** for 24–48 h on a shaker at 4 °C. Secondary antibodies were applied to tissue for 1h at room temperature with gentle agitation. Primary and secondary antibodies were both added to a 1:1 solution of Odyssey Block in PBS with 0.3% Triton X-100. Animals injected with 6-OHDA were perfused 7 or 10 days post-injection and brains were immunostained for tyrosine hydroxylase $(TH)^+$ dopaminergic terminals in the striatum. Animals injected with alpha-

synuclein were perfused 30 or 90d post-injection and brains were immunostained for the neuronal marker NeuN, the astrocyte marker glial fibrillary acidic protein (GFAP), pathologically phosphorylated alpha-synuclein (pSer129), and K48-linked ubiquitin. Unbound primary antibodies were rinsed off with three exchanges of PBS and sections were then incubated in the appropriate fluorescent secondary antibodies as indicated in **Table 4**, for 1 h on a shaker at room temperature. Hoechst 33258 (bisBenzimide) was added during the secondary incubation at a concentration of 0.005 μM to label nuclei, except in animals that received FluoroGold (which also fluoresces under UV illumination). Nuclei were also labeled with the infrared marker DRAQ5 (1:10,000 or 0.5 μM, Biostatus, Leicestershire, UK). Following six washes in PBS, sections were mounted onto glass slides (Superfrost Plus, Fisher Scientific, Pittsburgh, PA) and coverslipped with FluoroMount G (Southern Biotech, Birmingham, AL). Sections were scanned on an infrared Odyssey Imager for lower resolution analyses (21 μm resolution) or under epifluorescent microscopy (Olympus IX73, B&B Microscopes, Pittsburgh, PA) for higher resolution microscopy in the visible wavelengths, using objectives with magnification ranging from 4× to 100×.

For the (3,3'-diaminobenzidine (DAB) immunohistochemistry, sections were pretreated with 1% hydrogen peroxide for 15 minutes, followed by three exchanges of PBS. Non-specific antibody binding was minimized by incubating for one hour in 5% bovine serum albumin (A30075-100G, Research Products International Corp, Mt Prospect, IL) and 0.3% Triton-X 100 (Sigma) on a rotator at room temperature. This was followed by overnight mouse anti-TH primary antibody incubation on a rotator at room temperature. The next day, biotinylated anti-mouse secondary antibodies (PK6102, Vector Labs, Burlingame, CA) were applied (120 minutes on rotator at 24°

C) and followed by application of the Vectastain Elite ABC horseradish peroxidase reagents (PK6102, Vector Labs, Burlingame, CA). Following a 5 minute preincubation in diaminobenzidene (0.05% solution in Tris Buffer, pH 7.2) (D5905-50TAB, Sigma-Aldrich, St. Louis, MO), hydrogen peroxide was added to begin the peroxidase reaction (final dilution 3%) and terminated by buffer washes within 20 minutes. Sections were then washed, mounted, dehydrated in a graded series of ethanols, cleared in xylenes, and coverslipped with Permount (Fisher Scientific, Pittsburgh, PA). Immunolabeling was studied using a light microscope (Olympus BX41, B&B Microscopes, Pittsburgh, PA).

Thioflavin staining

Thioflavin S staining was used to measure insoluble and aggregated Lewy-like pathology, as previously published (Paumier et al., 2015, Mason et al., 2016). Briefly, sections were mounted onto glass slides and dried. Slides were then immersed in 10 mM PBS (5 min), followed by 0.05% KMnO4 / PBS (20 min). Following two rinses in PBS (2 min each), sections were immersed in 0.2% K2S2O5 / 0.2% oxalic acid / PBS for 1 min. After five PBS rinses (2 min each), slides were immersed in freshly filtered 0.0125% Thioflavin S / 40% EtOH / 60% PBS for 3 min in the dark. This was followed by immersion in 50% EtOH / 50% PBS (10 min), followed by four rinses in PBS (5 min each). Next, nuclei were stained with the Hoechst reagent (0.003 μM; Hoechst 33258, bisBenzimide) in 0.3% Triton X-100, followed by a final 5-min rinse in water. Stained sections were then dried and coverslipped and viewed with epifluorescent microscopy (Olympus IX73, Pittsburgh PA).

Image analyses

For the infrared measurements of tyrosine hydroxylase (TH) levels, regions of interest were traced in three sections by a blinded observer along the boundaries of the striatum, using the anterior commissure, lateral ventricle, and corpus callosum as anatomical landmarks. For the measurements of nigral TH or FluoroGold levels, the nigra was defined by the dorsal boundaries of the TH immunostaining, the lateral boundaries of the ventral tegmental area, and the ventrolateral outer surface of the brain. The ventral tegmental area was distinguished from the substantia nigra by the location of the medial terminal nucleus and the medial lemniscus. For the bilateral cell counts in the substantia nigra, images of the ipsilateral and contralateral nigrae were stitched on the Olympus microscope and a blinded observer counted all nigral TH^+ cells in three ventral midbrain sections per animal using the manual count tool in ImageJ software (NIH Image, Bethesda, MD). For the infrared measurements of NeuN levels, regions of interest were traced in three sections by a blinded observer along the outer boundaries of the hippocampus. Photographs from all experimental groups were captured at the same exposures and with the same intensity scaling. The cell counts of two independent and blinded raters were always found to be in agreement. Finally, sections from FluoroGold-infused animals were viewed under confocal microscopy to assess colocalization of FluoroGold with TH (Olympus Fluoview 1200 confocal system on an IX83 inverted frame). All confocal images were captured using a 40× silicone oil objective (NA 1.25) with a gain of 1.0. In the confocal studies, the UV-illuminated FluoroGold staining was pseudocolored red to contrast with the green TH. Higher resolution epifluorescent images were captured with 40× or 100× objectives. Sections from control and experimental groups were processed, photographed, and analyzed in parallel.

Blocking peptide experiments

Preadsorption controls were employed to confirm the specificity of the primary antibodies against pathologically phosphorylated alpha-synuclein (pSer129). Preadsorption controls are not useful for monoclonal antibodies, as they always will be adsorbed out by their antigen leading to inevitable loss of labeling regardless of which proteins they bind in tissue (Saper, 2005). Thus, we incubated the polyclonal pSer129 with 10-fold excess blocking peptide (Cat.no. 188826, Abcam, Cambridge, MA) for 24h at 4 ^{o}C prior to application to tissue. Adjacent sections from the same animals were exposed to free primary antibodies or blocked primary antibodies for 24h at 4 ^{o}C, followed by secondary antibody incubations. To control for secondary antibody specificity, primary antibodies were omitted from the immunohistochemical protocol, and this led to loss of fluorescent signal as expected.

Behavioral testing: Novel object (NOR) and novel place recognition (NPR) tests

Object and place recognition tasks consisted of four phases including an initial acclimation (habituation) phase of 10 minutes conducted in an open-field arena (45 cm × 60 cm × 60cm) constructed of green polyvinylchloride plastic. Three identical floors were prepared—a bare floor that was used during the acclimation phase, and two identical floors that contained brackets to fix objects into place. A dim diffusive light from two lamps was utilized to minimize shadows within the field. A video camera (JVC) was positioned over the arena to record behavior during the retention phases for subsequent analysis by blinded observers. The stimulus objects were made of glass or plastic with different shapes and textures, such as light bulbs, mugs, coffee

cups, and saline bottles. The animals were not able to displace the objects or hide in or under them. Also, objects were selected that did not have accessories that could stimulate play behaviors such as handles. Objects were washed with 70% isopropyl alcohol to remove olfactory cues between trials.

The acclimation phase was followed 24 h later by a familiarization phase, during which the animals were exposed to two identical objects in fixed in opposite corners of the arena 10 cm distant from the adjacent walls. The familiarization phase lasted 5 minutes for the animals to acquire recognition memories of the objects and their locations within the arena. Twenty-four hours later, recognition testing took place over a 5 min period, during which the animals were allowed to explore both the familiar object from the previous phase and a novel object that was substituted for one of the identical familiar objects. The time animals spent exploring the familiar and novel objects was recorded. The head of the animal must be within 4 cm and oriented within 45 degrees of the object to be considered engaged in object exploration.

Twenty-four hours later, the animals were returned to the arena for an additional trial to investigate the ability of the animal to recognize the novel place. The arena contained the two identical familiar objects from the familiarization phase, but one object was moved to a different location out of the corner and farther toward the center of the arena. The exploration time for each object place was recorded. Exploration ratio was calculated by dividing the time animal spent exploring the novel object/place by the total time exploring both the novel and familiar objects/places. Results were reported as mean ± SEM. Animals that spent a total of less than 10 sec exploring objects during the testing phases were excluded from the data analysis.

Behavioral testing: Buried Pellet Test

The buried peanut test was performed to measure olfactory function, as previously described in the literature (Lehmkuhl et al., 2014). Briefly, mice were habituated for one hour prior to all test days. During habituation, the animal was placed in a cage with evenly distributed clean bedding for an hour. Next, the animal was placed in a new cage in which a peanut was hidden 0.5 cm below the bedding so that it is not visible. The latency to find a buried peanut immediately following entry into a clean mouse cage was videotaped and measured by a blinded observer.

Statistical analyses

Data are presented as the mean and SEM in all figures. Depending on the number of independent variables, data were analyzed by one, two, or three-way ANOVA followed by the Bonferroni *post hoc* correction (SPSS Version 20, Armonk, NY). When there were only two groups, the two-tailed, unpaired Student's *t* test was performed. Differences were reported significant only when $p \leq 0.05$. The Grubb's outlier test did not reveal any significant outliers. The Mann-Whitney U test was employed for the inclusion count measurements due to heterogeneity of variance. The Pearson correlation was performed to compute correlation between inclusion counts and behavioral functions. The unpaired Student's *t* test was employed for the behavioral analysis.

Chapter 1

Rationale

The glutathione precursor NAC has been shown to be protective in multiple experimental models of injury and to benefit patients with various neurological conditions, ranging from Parkinson's and Alzheimer's disease to traumatic brain injury, schizophrenia, and bipolar disorder (Adair et al., 2001, Berk et al., 2008a, Berk et al., 2008b, Hoffer et al., 2013). NAC increases glutathione levels in the brain of patients with Parkinson's disease, supporting the view that NAC can cross the blood-brain barrier (Holmay et al., 2013, Katz et al., 2015). Recently, the Leak lab has shown that NAC may also facilitate a stress-induced increase in heat shock protein 70 (Hsp70) in cellular models of neurodegeneration (Jiang et al., 2013). As discussed further below, NAC may raise Hsp70 expression through thiol exchanges with heat shock factor 1, which contains multiple cysteine residues and facilitates Hsp70 gene transcription. Hsp70 is known to promote proteasomal degradation of oxidized proteins by binding to oxidized proteins and mediating their interaction with the 20S proteasome (Reeg et al., 2016). NAC therefore appears to protect neuronal and glial cells through both glutathione-dependent and independent manners. In order to define the mechanism of action of NAC in an animal model of neurodegeneration, the first goal of the present study was to establish an *in vivo* model of the protective effects of NAC. Before we could test the hypothesis that NAC is protective against neurodegeneration, we had to establish a robust and reproducible animal model of neurodegeneration.

Multiple models were examined because no one model can mimic all the pathologies of such a complex disorder and every model suffers from unique limitations. Furthermore, if a neuroprotectant can ameliorate multiple types of injury, it is far more likely to succeed in the

clinic. Our models included: 1) proteasome inhibitor infusions into the mouse hippocampus to inhibit the degradation of misfolded proteins and elicit cell death, 2) alpha-synuclein fibril infusions into the mouse and rat hippocampus and/or striatum to seed the misfolding of endogenous alpha-synuclein into Lewy bodies and Lewy neurites, and 3) 6-OHDA infusions into the mouse striatum to elicit oxidative stress and kill dopaminergic neurons.

Proteotoxic stress from protein misfolding is a central feature of neurodegenerative diseases and can lead to hallmark protein inclusions (Morimoto, 2008). For example, both Parkinson's and Alzheimer's disease are characterized by protein inclusions in the hippocampus (Goedert et al., 2010). Lewy pathology in the hippocampal and entorhinal cortex, first observed in Braak stages 3 or 4, have profound implications for cognitive dysfunction in Parkinson's patients (Braak et al., 2003a, Russell et al., 2014) Therefore, we first sought to develop animal models of hippocampal proteotoxicity using the proteasome inhibitor lactacysytin and alpha-synuclein fibrils.

6-OHDA has been used to model nigrostriatal cell loss for many decades. Recent studies have relied on immunostaining for the dopaminergic marker TH to confirm dopaminergic cell death. However, TH mRNA and protein levels are well known to be subject to modulation by stress (Baruchin et al., 1990, Kumer and Vrana, 1996, Chang et al., 2000, Tank et al., 2008, Tekin et al., 2014). There are limitations to relying only on TH expression by itself, because changes in TH expression can occur independently of changes in actual dopaminergic cell numbers. Therefore, the retrograde tract tracer FluoroGold was used to specifically label nigrostriatal projection neurons, which form the pathway known to degenerate in Parkinson's disease. FluoroGold is an exogenous molecule and therefore not subject to stress-induced changes in

gene transcription. However, the use of FluoroGold as a tracer in the 6-OHDA model has not been properly validated.

Specific Aim 1: Establish the 6-OHDA model of Parkinson's disease and validate the tools used to define nigrostriatal degeneration *in vivo*. Test the hypothesis that FluoroGold does not change the impact of 6-OHDA toxicity on loss of nigrostriatal somata and terminals. Test the hypothesis that retrograde tract-tracing is a more sensitive tool to quantify nigrostriatal degeneration than TH^+ cell loss. Examine whether relatively high-throughput screening of FluoroGold or TH levels on an infrared 16-bit imager can serve as an initial screen for nigrostriatal pathway loss.

Results

Develop a model of proteotoxic stress in the mouse hippocampus in vivo

Male CD1 mice were infused with the proteasome inhibitors MG132 and lactacystin in the hippocampus. Animals were perfused 7 days post-injection and stained for $NeuN^+$ neurons and $GFAP^+$ astrocytes. Sections were imaged at high resolution on an EVOS microscope or at low resolution on an Odyssey Infrared Imager. First, we showed loss of immunofluorescent signal when primary antibodies were omitted (Figure 3), revealing the specificity of the secondary antibodies. The primary antibodies also result in single bands at the expected molecular weight on Western blots and stain cellular structures consistent with the appearance of neuronal nuclei (NeuN) or stellate astrocytes (GFAP).

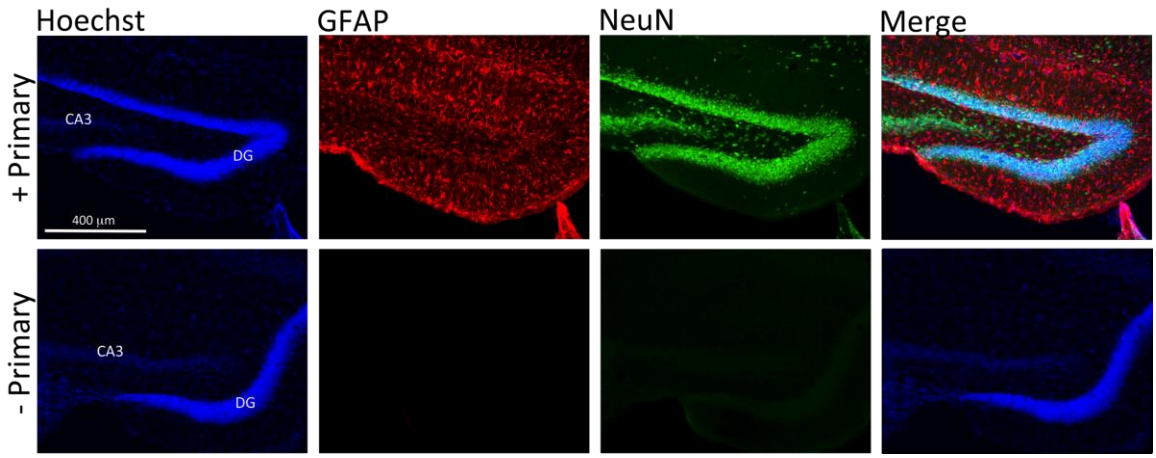

Fig. 3. Hoechst-GFAP-NeuN triple staining in the hippocampus. Coronal brain tissue from male CD1 mice was collected and stained with antibodies against NeuN and GFAP and the nuclear marker Hoechst. NeuN antibodies labeled neuronal nuclei and GFAP antibodies labeled reactive astrocytes as expected. Omission of primary antibody caused the expected loss of signal.

Proteotoxicity induced by MG132 and lactacystin

Although we tried to infuse MG132 into the mouse hippocampus, we discovered that MG132 failed to dissolve in PBS or DMSO followed by addition of PBS. Pure DMSO infusions into the rodent brain can lead to toxicity (Hanslick et al., 2009). Therefore, we abandoned MG132 and infused lactacystin, which is readily dissolved in PBS.

We discovered that infusions of 5-10 µg lactacystin elicited severe loss of NeuN in the ipsilateral hippocampus *in vivo* (Figure 4). However, lactacystin was too toxic in a small fraction of the animals, and led to tissue necrosis and a hole in the hippocampus. It was therefore abandoned as a model of hippocampal neurodegeneration.

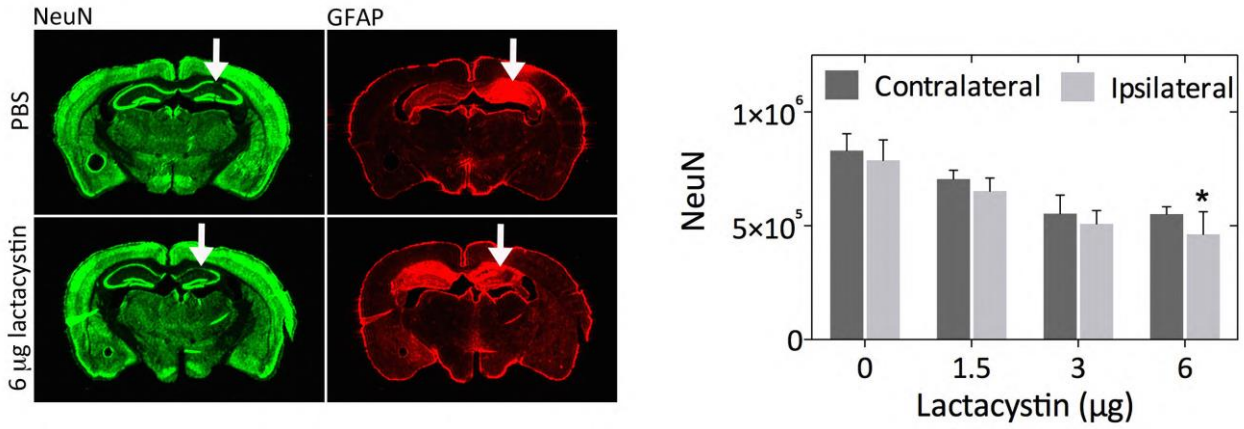

Fig. 4. Lactacystin elicits gliosis and loss of NeuN. The dorsal hippocampus was infused with phosphate buffered saline (PBS) or the proteasome inhibitor lactacystin (10 µg) in adult mice (top). Animals were killed after 7d and sections stained for NeuN and GFAP and imaged on an infrared Odyssey imager. Hippocampal NeuN$^+$ signal was quantified in Odyssey software. N=10 mice per group. *p≤0.001 vs 0 µg lactacystin, Bonferroni post hoc following two-way ANOVA.

Chronic proteotoxic stress from the fibrillized protein alpha-synuclein

As lactacystin was overly toxic to a small fraction of animals at ED_{50} doses, we decided to employ the alpha-synuclein fibril model instead. Hippocampal neurons are known to develop dense alpha-synuclein$^+$ Lewy pathology in Parkinson's disease and Lewy body dementia (Braak et al., 2003a, Russell et al., 2014). Previous studies have shown that injections of alpha-synuclein fibrils into CA1 of the hippocampus lead to Lewy-like pathology in areas that project to the hippocampus (Luk et al., 2012a, Sacino et al., 2013). However, those infusions were unilateral and failed to lead to cognitive deficits, perhaps because the unlesioned hemisphere could compensate against the unilateral injury. Therefore, we began this study by infusing the hippocampus with fibrils. Mice injected with alpha-synuclein fibrils were perfused 30d post-injection and brains were immunostained for the neuronal marker NeuN and the astrocyte marker

GFAP. There was mild loss of NeuN following infusion of 12.5μg fibrils (Figure 5), but the response was slight and not highly dose-dependent. In this study we used higher doses of alpha-synuclein fibrils compared to the literature, in which 5 μg fibrils were infused in 2.5 μl PBS (Luk et al., 2012a). However, our goal was to accelerate and increase the spread of alpha-synucleinopathy to model the cognitive deficits of dementia with Lewy bodies.

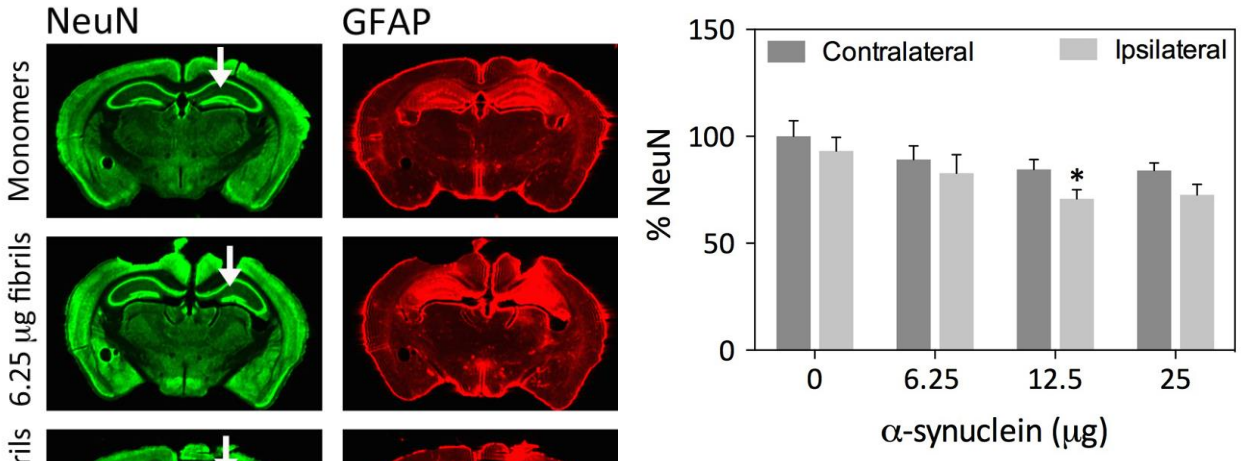

Fig. 5. Alpha-synuclein fibrils elicit mild loss of NeuN signal in the ipsilateral hippocampus. The dorsal hippocampus was stereotaxically infused with phosphate buffered saline (PBS) or α-synuclein fibrils in adult mice. Animals were killed after 1 month. Brain sections were stained for NeuN and GFAP and imaged on an infrared imager. Hippocampal $NeuN^+$ signal was quantified in Odyssey software by a blinded observer. N=10 mice per group. *p≤0.001 vs 0 μg α-synuclein, Bonferroni *post hoc* following two-way ANOVA

Formation of Lewy-like pathology following infusions of alpha-synuclein fibrils

Mice were infused with alpha-synuclein fibrils or PBS into the hippocampus. One month later, coronal brain sections from both groups were immunostained in parallel for pathologically phosphorylated alpha-synuclein (pSer129) and imaged at the same exposure and intensity scaling (Fujiwara et al., 2002, Anderson et al., 2006). Nuclei were labeled blue with Hoechst. As expected, alpha-synuclein fibrils elicited Lewy-like inclusions in the mouse hippocampus in a dose-dependent manner (Figure 6). Fibril infusions into the hippocampus led to dense accumulations of $pSer129^{+}$ inclusions in CA1, CA2, and the dentate gyrus. Lewy-like inclusions were formed within neurites and somata (Figure 7). However, the pathology was sparse and was not transmitted to afferent or efferent sites that project to or are innervated by the hippocampus. At this time, we had not yet discovered that increasing the duration of sonication greatly facilitates the transmission of Lewy pathology across the brain. For this reason, we decided to use the well-established 6-OHDA model of nigrostriatal cell loss in order to test the mechanism of action of NAC.

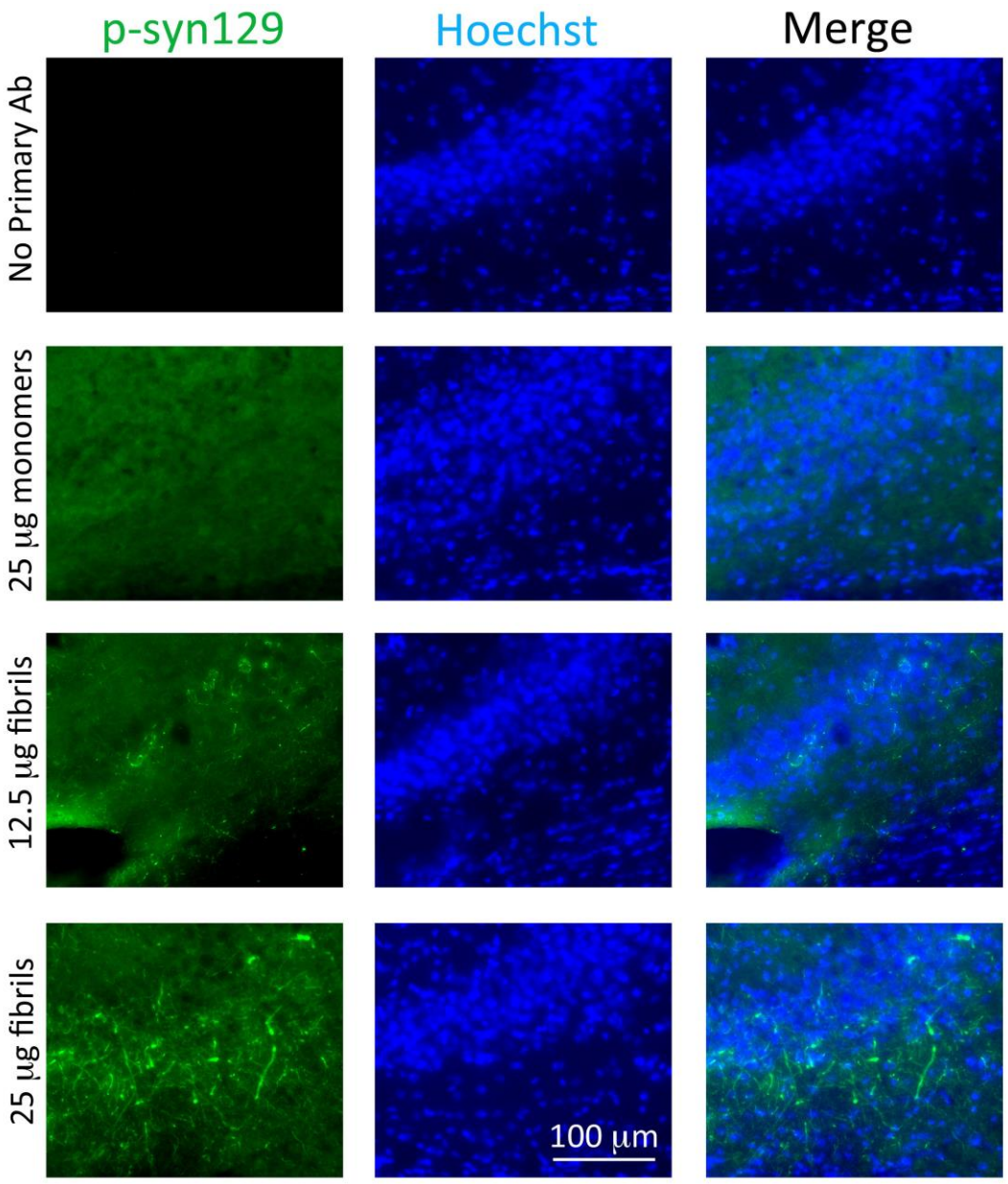

Fig. 6. Alpha-synuclein fibrils elicit Lewy-like inclusions in the mouse hippocampus. Mice were infused with the indicated doses of alpha-synuclein fibrils or monomers and sacrificed 1 month later. Hippocampal sections were immunostained for phosphorylated alpha-synuclein (pSer129), a modification associated with Lewy pathology. Lewy-like pathology was elicited in a dose-dependent manner as expected. Hoechst labeling of nuclei is shown in blue.

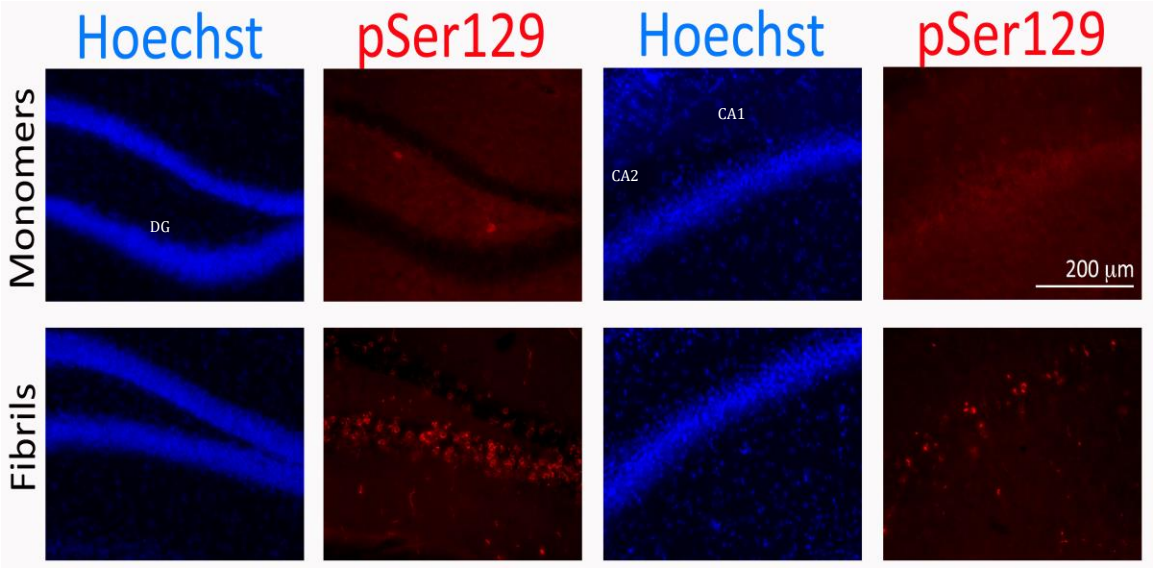

Fig. 7. **Alpha-synucleinopathy following fibril injections.** Mice were infused with 5 ug alpha-synuclein fibrils or monomers and sacrificed 1 month later. Coronal brain sections were collected and immunostained for pathologically phosphorylated alpha-synuclein (pSer129). Nuclei were labeled with Hoechst. The fibril injection in this animal extended from CA1 into CA2 and the dentate gyrus (DG). Dense Lewy-like pathology was elicited by one month post-infusion.

Impact of the retrograde tracer FluoroGold on 6-OHDA toxicity in the striatum

As mentioned earlier, the phenotypic marker TH is known to be modulated by stress (Baruchin et al., 1990, Kumer and Vrana, 1996, Chang et al., 2000, Tank et al., 2008, Tekin et al., 2014). As a result, loss of TH may not reflect true loss of dopaminergic terminals or cell bodies. In order to address this potential confound, we infused the retrograde tracer FluoroGold into the striatum to label dopaminergic cell bodies in the ipsilateral substantia nigra, pars compacta. We expected 6-OHDA-induced loss of FluoroGold in the nigra to be a more sensitive measurement of dopaminergic cell death than measurements relying on TH, as only those terminals that project to the infusion site would be retrogradely labeled. In contrast, measurements of all TH^+ neurons in the nigra would include those neurons that do not project to the center of the injection and are not

killed by the circumscribed 6-OHDA infusions. Furthermore, in contrast to TH, FluoroGold is not an endogenous protein and loss of FluoroGold immunoreactivity is expected to reflect true loss of dopaminergic cell numbers (Sauer and Oertel, 1994). Thus, we began this study by validating the use of this retrograde tracer (Fig.8A). Infusions of FluoroGold into the striatum retrogradely labeled neurons in the substantia nigra, pars compacta as expected. Next, we infused FluoroGold or vehicle into the striatum one week before 6-OHDA, at the same stereotaxic coordinates. This protocol permitted tracer uptake without any disruption from 6-OHDA-induced oxidative stress. The dose of 6-OHDA (4 ug) was based on a pilot study showing ~50% loss of dopaminergic terminals (not shown). As an initial screen for 6-OHDA-induced loss of the nigrostriatal pathway, we measured TH and FluoroGold label in both the ipsi and contralateral striata and nigra using an infrared Odyssey imager (Fig. 8 and 9). The results reveal a slight but significant loss in ipsilateral TH levels in the vehicle-treated striatum in the absence of FluoroGold, as shown in the first two bars in Figure 8B. Importantly, FluoroGold did not alter the impact of 6-OHDA on striatal TH loss. This finding suggests that FluoroGold can be used in conjunction with 6-OHDA with no alteration in its toxic effects. However, FluoroGold infusions led to a slight decrease in striatal area in the contralateral hemisphere (Fig. 8C). This effect was not apparent in the 6-OHDA group, possibly due to astrocytosis or some other form of hypertrophy or hyperplasia in response to loss of dopaminergic terminals. Finally, the most important measurement—TH expression as a function of striatal area—showed no significant impact of FluoroGold in any group (Fig. 8D).

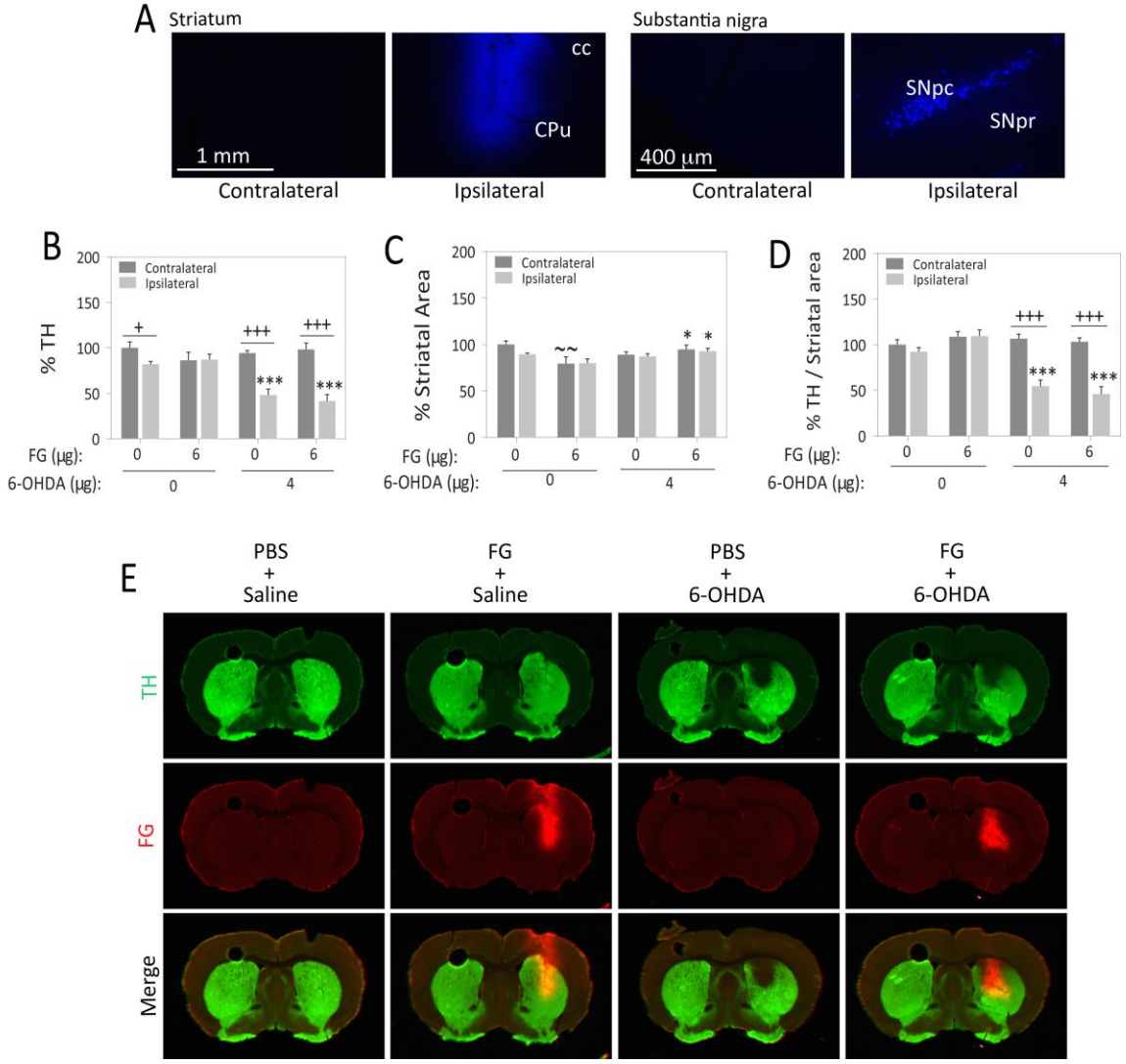

Fig. 8. Impact of the retrograde tracer FluoroGold on 6-OHDA toxicity in the striatum. (A) Mice were stereotaxically infused with 6 μg FluoroGold (FG). Seven days later, mice were sacrificed and brain sections viewed under UV illumination on an epifluorescent microscope. The ipsilateral nigrostriatal pathway was retrogradely labeled. cc, Corpus callosum; CPu, caudatoputamen; SNpc, substantia nigra, pars compacta; SNpr, substantia nigra, pars reticulata. (B) In a separate series of experiments, mice were infused with 6 μg FluoroGold or an equivalent volume of phosphate-buffered saline (PBS) into the right striatum. Seven days after FluoroGold infusions, mice were infused with 4 μg 6-OHDA or an equivalent volume of vehicle (0.02% ascorbic acid in saline) in the same striatal location. One week following 6-OHDA infusions, forebrain sections were immunostained for the dopaminergic terminal marker tyrosine hydroxylase (TH) and FluoroGold and scanned on the Odyssey Imager. (b) The impact of 6-OHDA toxicity on overall striatal TH levels was not affected by FluoroGold. (C) FluoroGold slightly reduced striatal area in the hemisphere contralateral to the infusion. 6-OHDA prevented this effect. (D) FluoroGold did not change TH levels per unit area in the striatum of vehicle or 6-OHDA-infused animals. (E) Representative coronal sections through the forebrain, immunolabeled for TH^+ dopaminergic terminals (green) and FluoroGold (red). Shown are the mean and SEM of 5–6 mice per group. $^*p \leq 0.05$, $^{**}p \leq 0.01$, $^{***}p \leq 0.001$ versus 0 μg 6-OHDA; $^{+}p \leq 0.05$, $^{++}p \leq 0.01$, $^{+++}p \leq 0.001$ ipsilateral versus contralateral; $^{\sim}p \leq 0.05$, $^{\sim\sim}p \leq 0.01$, $^{\sim\sim\sim}p$

≤ 0.001 versus 0 μg FG; three-way ANOVA followed by Bonferroni post hoc correction. Copyright 2016 by Nouraei *et al* 2016. Reprinted with permission.

Next, we focused on the ventral mesencephalon to investigate whether FluoroGold could alter loss of nigral TH in response to 6-OHDA. Our results suggested that FluoroGold infusions did not change TH expression in the nigra of 6-OHDA or vehicle-infused animals (Fig. 9A). We also demonstrated that FluoroGold decreased nigral area in the 6-OHDA group (Fig. 9B). However, FluoroGold had no effect on TH expression as a function of nigral area (Fig. 9C). As expected, FluoroGold loss in the nigra in response to 6-OHDA toxicity was more dramatic than TH loss (Fig.9D vs A, G). Cell counts confirmed that loss of $FluoroGold^+$ cells was greater than TH^+ cell loss in the nigra (Fig. 9E vs F, H vs I). Thus, the FluoroGold tracer was a more sensitive tool to measure the toxicity of 6-OHDA than measurements relying on expression of TH protein alone.

Damier and colleagues described the topographic pattern of nigral degeneration in patients with Parkinson's disease (Damier et al., 1999). Those studies revealed that the ventrolateral nigra is the most vulnerable to dopaminergic cell loss in this condition. Our 6-OHDA model exhibited the same pattern as in patients (see white arrows in Fig. 9H and I). Furthermore, we also showed with a confocal analysis that some, but not all $FluoroGold^+$ cells expressed the dopaminergic marker TH, consistent with previous FluoroGold studies (Sauer and Oertel, 1994). It is possible that FluoroGold uptake suppressed TH transcription or translation in nigrostriatal cells, as there are previous reports showing that FluoroGold can exert mild toxicity (Naumann et al., 2000). The colocalization studies also confirmed that the cells projecting to the dorsal neostriatum, the epicenter of the infusion, were clustered in the ventral tier of the substantia nigra, pars compacta (see merged images in Fig. 9G, J).

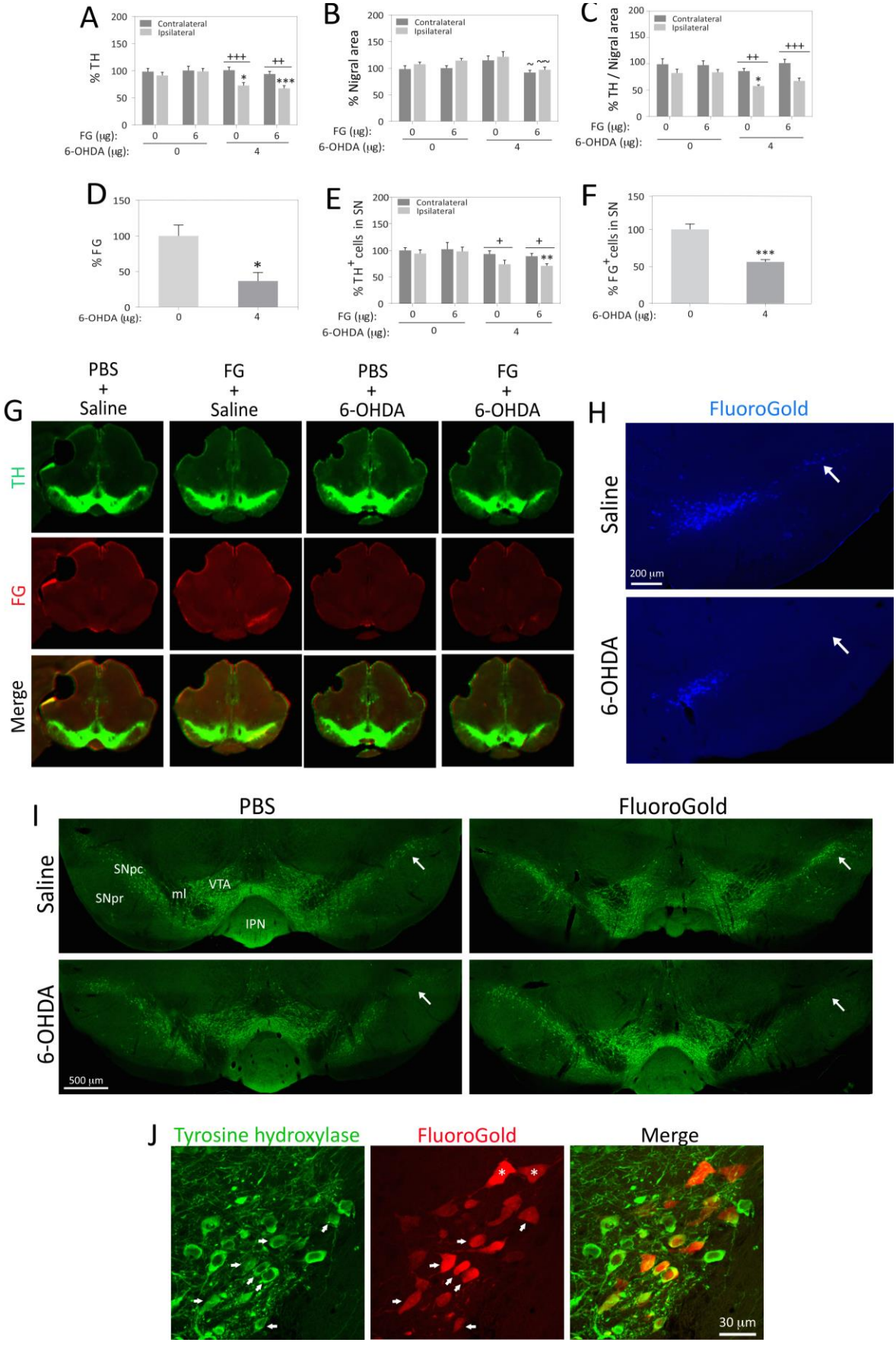
A
% TH
Contralateral
Ipsilateral
FG (µg):
6-OHDA (µg):
B
% Nigral area
C
% TH / Nigral area
D
% FG
E
% TH+ cells in SN
F
% FG+ cells in SN
PBS + Saline
FG + Saline
PBS + 6-OHDA
FG + 6-OHDA
G
TH
FG
Merge
H
FluoroGold
Saline
6-OHDA
200 µm
I
PBS
FluoroGold
SNpc
SNpr
ml
VTA
IPN
500 µm
J
Tyrosine hydroxylase
FluoroGold
Merge
30 µm

Fig. 9. Impact of the retrograde tracer FluoroGold on 6-OHDA toxicity in the substantia nigra. Mice were stereotaxically infused with 6 μg FluoroGold (FG) or an equivalent volume of phosphate-buffered saline (PBS) into the right striatum. Seven days later, mice were infused in the same location with 4 μg 6-OHDA or an equivalent volume of vehicle (0.02% ascorbic acid in saline). One week later, brain sections were stained for the dopaminergic terminal marker tyrosine hydroxylase (TH) and FluoroGold. (A) The impact of 6-OHDA on overall TH levels in the nigra was not affected by FluoroGold. (B) FluoroGold slightly reduced nigral area in both hemispheres of 6-OHDA-infused animals. (C) FluoroGold did not change TH levels per unit area in the nigra of vehicle or 6-OHDA-infused animals. (D) Overall FluoroGold levels in the nigra were significantly reduced by 6-OHDA. (E) FluoroGold did not significantly change TH^+ cell counts in the nigra in vehicle or 6-OHDA-infused animals. (F) The number of $FluoroGold^+$ cells of the nigrostriatal pathway was significantly reduced by 6-OHDA. (G) Representative coronal sections through the midbrain, immunolabeled for TH^+ dopaminergic neurons (green) and $FluoroGold^+$ cells (red) and scanned on the Odyssey Imager. (H–I) Microscopic images of $FluoroGold^+$ (h) and TH^+ (i) cells in the ventral midbrain in 6-OHDA/saline and FluoroGold/PBS-infused animals. The arrow points to the lateral nigra, the area most vulnerable to loss in Parkinson's disease. (J) Confocal analysis of FluoroGold and TH dual labeling. Arrows point to some of the cells that contain both FluoroGold and TH. Asterisks overlie FluoroGold-labeled nigrostriatal cells that do not express TH. $FluoroGold^+$ cells were viewed under UV illumination and pseudocolored red for presentation. Shown are the mean and SEM of 5–6 mice per group. $^*p \leq 0.05$, $^{**}p \leq 0.01$, $^{***}p \leq 0.001$ versus 0 μg 6-OHDA; $^{+}\ p \leq 0.05$, $^{++}\ p \leq 0.01$, $^{+++}\ p \leq 0.001$ ipsilateral versus contralateral; $^{\sim}\ p \leq 0.05$, $^{\sim\sim}\ p \leq 0.01$, $^{\sim\sim\sim}\ p \leq 0.001$ versus 0 μg FG; three-way ANOVA followed by Bonferroni post hoc correction or two-tailed Student's t-test for panels d and f. IPN, interpeduncular nucleus; ml, medial lemniscus; SNpc, substantia nigra, pars compacta; SNpr, substantia nigra, pars reticulata; VTA, ventral tegmental area.

Discussion

In this aim, multiple models of Parkinson's disease that mimic oxidative or proteotoxic stress were developed in order to test the efficacy of neuroprotective molecules. This was accomplished because no one model can mimic all different pathological aspects of a complex disorder such as Parkinson's disease. Importantly, if a neuroprotectant can ameliorate multiple types of injury, it is far more likely to succeed in the clinic. The models established in this study include the following: 1) proteasome inhibitor infusions into the mouse hippocampus to inhibit the degradation of misfolded proteins and elicit cell death within 7 days, 2) 6-OHDA infusions into the mouse striatum to elicit oxidative stress and kill dopaminergic neurons within 7-10 days, and 3) alpha-synuclein fibril infusions into the mouse and rat hippocampus and/or striatum to seed the misfolding of endogenous alpha-synuclein and elicit the formation of Lewy bodies and Lewy neurites. We have fully reproduced the 6-OHDA model of Parkinson's disease, a robust and reproducible method of inducing dopaminergic neurodegeneration in a pattern that mimics the topography of nigrostriatal cell loss in the human condition. Nigrostriatal degeneration was verified by a blinded observer with four rigorous techniques: 1) measurements in overall TH expression levels in both the striatum and nigra using the 16-bit Odyssey Imager and 2) TH^+ nigral cell counts in large, high-quality stitched montages of the substantia nigra, 3) measurements of FluoroGold levels using the Odyssey imager, and 4) counts of individual $FluoroGold^+$ nigral neurons in high-quality stitched images.

We have found that FluoroGold is a more sensitive tool than measurements of either TH cell numbers or TH levels, consistent with our original hypotheses. We have also gathered data suggesting that FluoroGold exerts some mild toxicity, as evident in nigral area measurements, but that it did not significantly affect the toxicity of 6-OHDA in either the striatum or the nigra. Thus, we have validated the use of the 16-bit, high sensitivity Odyssey imager as an initial screening tool to measure loss of the nigrostriatal pathway. The 16-bit depth (2^{16}) of the grayscale Odyssey imager translates to a wide dynamic range, because 2^{16} (65,536) potential shades of gray afford high resolution, especially compared to 8-bit color imagers, which perceive only 2^8 (256) shades of color. The overall TH level measurements in the striatum and nigra with the Odyssey imager are in general agreement with higher resolution cell count data from stitched images, which facilitates future studies of this pathway.

Finally, we were also able to report measurements of striatal and nigral area, which the majority of Parkinson's studies fail to show, even though striatal TH measurements are highly dependent upon the size of the region of the interest (i.e., larger tracings result in higher TH values) and changes in nigral and striatal area provide additional information about the toxicity of treatments.

Chapter 2

Rationale

The glutathione precursor NAC has been shown to be beneficial in many clinical trials. For example, NAC improved some aspects of cognition in patients with Alzheimer's disease (Adair et al., 2001). NAC increased the chances of symptom resolution form 42% to 86% (with no reported side effects) in soldiers experiencing mild traumatic injury compared to those who received placebo (Hoffer et al., 2013). NAC also has been shown to improve the depressive component of bipolar disorder (Berk et al., 2008a) and to mitigate the negative symptoms and akathisia associated with schizophrenia (Berk et al., 2008b). Recent studies have suggested that administration of NAC increases glutathione levels in the brains of patients with Parkinson's disease (Holmay et al., 2013, Katz et al., 2015). These findings support the view that NAC can cross the blood-brain barrier in humans. Additionally the neuroprotective properties of NAC have been investigated in Parkinson's patients (Monti et al., 2016). The results of this preliminary study demonstrate that patients receiving the NAC showed a ~10% increase in dopamine transporter binding in the caudate and putamen and improvements in the Unified Parkinson's Disease Rating Scale (UPDRS), a standardized measurement of clinical symptoms, as compared to the placebo group.

NAC is one of the most frequently used positive controls in cellular and animal studies of neuroprotection due to its well-established antioxidant properties. Recent studies in our lab showed that NAC prevents neurodegeneration in multiple cellular models of neurodegenerative disorders (Jiang et al., 2013; Posimo et al., 2013; Unnithan et al., 2012; Unnithan et al., 2014).

Consistent with these observations, Clark and colleagues have shown that oral NAC attenuates alpha-synucleinopathy and dopaminergic loss in alpha-synuclein overexpressing mice (Clark et al., 2010). However, they did not establish the mechanism of action. Second, Berman and colleagues have shown that NAC substantially reduced the loss of dopaminergic neurons in EAAC1−/− mice, which have impaired neuronal cysteine uptake, reduced neuronal glutathione content, and chronic oxidative stress (Berman et al., 2011). Third, neuroprotective effects of NAC against dopaminergic loss have been reported in the MPTP model of Parkinson's disease (Perry et al., 1985, Sharma et al., 2007, Pan et al., 2009). Fourth, Munoz and colleagues reported that subcutaneous NAC robustly protects against 6-OHDA-induced dopaminergic degeneration (Munoz et al., 2004), consistent with studies showing that NAC protects dopaminergic neurons against 6-OHDA toxicity *in vitro* (Choi et al., 2008) and that NAC reduces oxidative stress in 6-OHDA-treated animals (Aluf et al., 2010).

6-OHDA infusions into the striatum are known to lead to progressive dopaminergic cell death over the course of several weeks (Sauer and Oertel, 1994). However, the Munoz study does not address whether systemically administrated NAC will prevent nigral cell loss against 6-OHDA toxicity at longer time-points. Another limitation of the Munoz study is that the impact of systemic NAC on dopaminergic cells in the contralateral substantia nigra and striata was not addressed. Furthermore, this study did not report measurements of dopaminergic neurons in animals treated with NAC by itself (in the absence of 6-OHDA). This is an important control group, because if NAC raises TH expression in both the absence and presence of 6-OHDA, one cannot conclude then that it alters the impact of 6-OHDA.

The Clark study mentioned above did not examine dopaminergic cell bodies and only reported TH measurements in the striatum (Clark et al., 2010). We filled this gap by examining dopaminergic cell loss at the level of the axon terminal in the striatum and the soma in the substantia nigra to determine if the neuroprotection spanned the entire nigrostriatal pathway (Clark et al., 2010). In addition, we examined protection of nigral cell bodies by multiple methods to improve the rigor of our study: 1) overall expression of the dopaminergic marker TH in the ventral mesencephalon with a low-resolution, high-sensitivity infrared Odyssey imager, 2) counts of TH^+ cell bodies in the substantia nigra by higher-resolution microscopy, and 3) retrograde labeling of nigrostriatal proiections neurons with FluoroGold (Schmued and Fallon, 1986, Wessendorf, 1991). Furthermore, the protective effects of NAC were measured at two separate timepoints: 10 days and 3 weeks after 6-OHDA infusions. This served to determine whether the protective properties of NAC were long lasting or merely transient, which is especially relevant for the treatment of chronic, progressive neurodegenerative disorders such as Parkinson's disease. For example, the Stroke Therapy Academic Industry Roundtable (STAIR) proposal published in 1999 recommended that investigators sacrifice animals between 2 and 3 weeks after injury (Fisher et al., 2009), as accomplished here.

The mechanism underlying NAC-mediated neuroprotection of the nigrostriatal pathway has not been fully established. NAC can elicit neuroprotection in both glutathione-dependent and glutathione-independent manners. For example, Clark and colleagues reported that NAC protected striatal dopaminergic terminals with no sustained effect on glutathione levels (Clark et al., 2010). NAC can activate NFkB and elevate Mn superoxide dismutase gene expression (Das et al., 1995). NAC also protect cells by activation of the extracellular signal–regulated

kinase (ERKs) cascade (Yan and Greene, 1998, Zhang et al., 2011, Sun et al., 2012). Finally, NAC can also induce AP-1 activity by activation of ERK and the transcription factor Elk-1, thereby leading to an increase in c-Fos expression (Meyer et al., 1993, Muller et al., 1997). The Leak lab has shown that NAC can blunt proteotoxicity in a heat shock protein 70-dependent manner (Jiang et al., 2013), perhaps through thiol exchanges with transcription factors such as heat shock factor 1 that regulate transcription of Hsp70 mRNA. Another potential mechanism whereby NAC may increase Hsp70 gene induction is by facilitating the nuclear translocation of Nrf2 (Kwak et al., 2003, Dinkova-Kostova et al., 2004, Dinkova-Kostova, 2012). Nrf2 is normally bound to Keap1, which has cysteine residues that nucleophiles such as NAC may interact with in thiol exchange reactions. When Nrf2 is released from Keap2, it is no longer degraded by the proteasome and is free to enter the nucleus and increase the transcription of Hsp70 and related genes (Kwak et al., 2003, Dinkova-Kostova et al., 2004, Dinkova-Kostova, 2012).

In summary, beneficial effects of NAC have been reported in multiple neurological conditions but the underlying mechanisms are poorly understood. Therefore, it is essential to establish animal models of the therapeutic effects of NAC in order to 1) shed light on disease etiology and 2) accelerate the discovery of novel drug targets by identifying the underlying neuroprotective mechanisms. Thus, the goal of the present study was to develop an animal model in which the molecular mechanisms underlying the neuroprotective properties of NAC could be investigated. Specifically, we hypothesized that NAC would protect dopaminergic cells against 6-OHDA toxicity for at least 3 weeks and that the sustained protection would be associated with a long-term increase in Hsp70 expression in the striatum.

Specific Aim 2: Test the hypothesis that NAC protects the somata and terminals of the nigrostriatal pathway against 6-OHDA toxicity *in vivo*.

Results

NAC protects dopaminergic terminals of the nigrostriatal pathway 10 days following 6-OHDA exposure

In the present study, NAC was injected intraperitoneally on a daily basis beginning immediately after 6-OHDA surgeries until sacrifice 10 days later (Fig. 10). Brain sections were then immunohistochemically stained for TH and imaged on the Odyssey imager. Ipsilateral TH levels were divided by contralateral TH levels and expressed as a ratio, a common method of presenting striatal TH in the literature. As expected, 6-OHDA elicited significant toxicity in dopaminergic terminals of the ipsilateral striatum (Fig. 10A). Unexpectedly, NAC had no effect on 6-OHDA-induced loss of ipsilateral/contralateral TH. Next, we examined the right and left hemispheres individually. As mentioned earlier, the impact of NAC on dopaminergic neurons in the contralateral hemisphere have not been reported in the literature. We discovered that NAC raised TH expression in the contralateral hemisphere in 6-OHDA-treated animals (Fig. 10B). Furthermore, there was a trend towards a NAC-mediated increase in TH levels in the ipsilateral hemisphere in 6-OHDA-treated animals ($p = 0.058$, two-way ANOVA followed by Bonferroni *post hoc* correction). There was no significant difference in striatal area between treatment groups (Fig. 10C). TH signal in the striatum is sensitive to changes in striatal area, because tracing a bigger region of interest results in a greater TH signal in proportion to the larger size of the trace. Therefore, TH levels were expressed per unit striatal area, in order to approximate the

level of TH expression per dopaminergic axon terminal, i.e., the "density" of striatal TH. NAC raised TH expression in both hemispheres in 6-OHDA-infused mice when striatal TH signal was expressed as a function of striatal area (Fig. 10D). Consistent with previous work by Munoz et al., our data therefore suggest that NAC can cross the blood-brain barrier and protect against 6-OHDA-induced oxidative stress 10 days post-injury (Munoz et al., 2004).

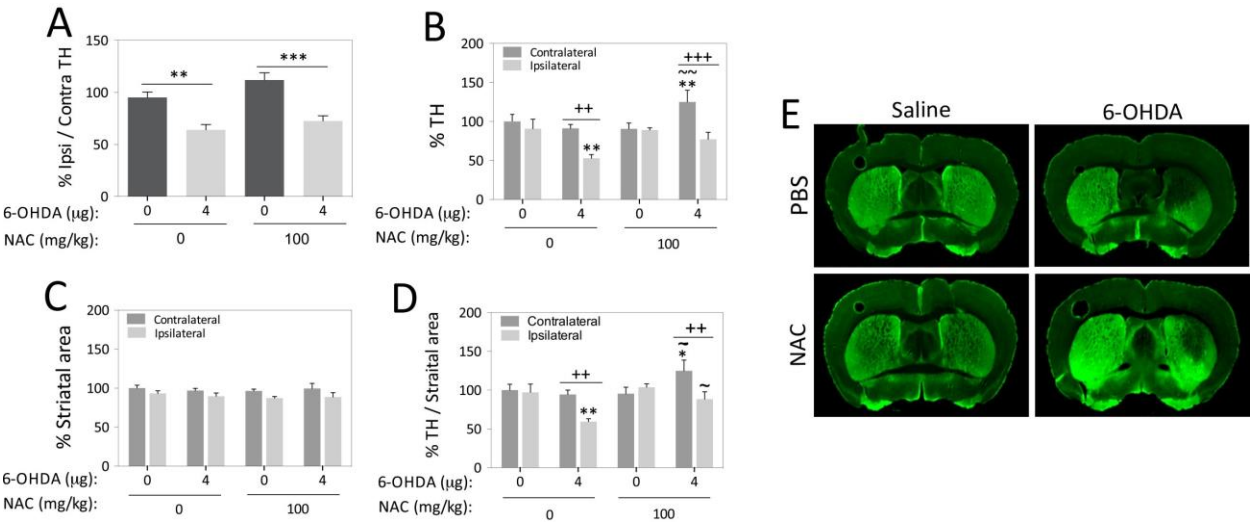

Fig. 10. NAC raises TH levels in the striatum 10 days after 6-OHDA infusions. Mice were stereotaxically infused with 4 µg 6-OHDA or an equivalent volume of vehicle (0.02% ascorbic acid in saline) into the right striatum. For the next 10 days, mice received daily intraperitoneal injections of 100 mg/kg NAC or an equivalent volume of phosphate-buffered saline (PBS). Forebrain sections were immunostained for the dopaminergic terminal marker tyrosine hydroxylase (TH) and scanned on a high-sensitivity Odyssey Imager. (A) 6-OHDA significantly reduced ipsilateral/contralateral striatal TH levels. NAC did not affect this ratio. (B) Overall TH levels in the contralateral and ipsilateral striata. 6-OHDA reduced TH levels on the side ipsilateral to the infusion. NAC raised TH levels in the contralateral striatum of 6-OHDA-infused animals. There was a trend towards a NAC-mediated increase in TH levels in the ipsilateral hemisphere in 6-OHDA-treated animals ($p = 0.058$). (C) Striatal area was not affected by 6-OHDA or NAC. (D) TH levels were expressed as a function of striatal area, a measurement that reflects average dopaminergic terminal density (TH per unit area). NAC significantly raised TH density in both hemispheres after 6-OHDA infusions. (E) Representative coronal sections through the forebrain, immunolabeled for TH+ dopaminergic terminals and scanned on the Odyssey imager. Shown are the mean and SEM of 7–8 mice per group. $^{*}p \leq 0.05$, $^{**}p \leq 0.01$, $^{***}p \leq 0.001$ versus 0 µg 6-OHDA; $^{+}p \leq 0.05$, $^{++}p \leq 0.01$, $^{+++}p \leq 0.001$ ipsilateral versus contralateral; $^{\sim}p \leq 0.05$, $^{\sim\sim}p \leq 0.01$, $^{\sim\sim\sim}p \leq 0.001$ versus 0 mg/kg NAC; two or three- way ANOVA followed by Bonferroni post hoc correction. Copyright 2016 by Nouraei et al. Reprinted with permission.

NAC protects dopaminergic cell bodies of the nigrostriatal pathway 10 days following 6-OHDA exposure

Next we investigated the neuroprotective effect of NAC in the substantia nigra by screening for changes in the density of nigral TH labeling (Fig. 11). In contrast to the striatum, overall TH expression in the nigra was not significantly affected by NAC treatment (Fig. 11A). Instead, 6-OHDA led to a significant loss of ipsilateral nigral TH compared to the contralateral side in both PBS and NAC-treated animals (Fig. 11A). Furthermore, there was a significant reduction in the areas of the ipsilateral and contralateral substantia nigra by 6-OHDA in both the saline and NAC-infused mice. This could be attributed to commissural effects of 6-OHDA (Fig. 11B). When we expressed TH levels as a function of nigral area, 6-OHDA elicited an increase in TH density in the contralateral nigra, a potentially compensatory effect that would not be apparent had we only performed higher resolution dopaminergic cell counts (Fig. 11C). Next, we expressed the ipsilateral TH signal density as a function of TH levels in the contralateral hemisphere and found no significant toxicity by 6-OHDA in the NAC-treated animals (Fig. 11D). On the other hand, NAC did not significantly raise this measure relative to the PBS treated animals and the preponderance of evidence collected in this study does not support long-term protective effects of NAC in this model. Therefore, we conclude that NAC failed to protect dopaminergic neurons in the substantia nigra from 6-OHDA toxicity 10 days post-infusion. Blinded TH^+ cell counts in the nigra also revealed no significant neuroprotective effect of NAC (Fig. 11F).

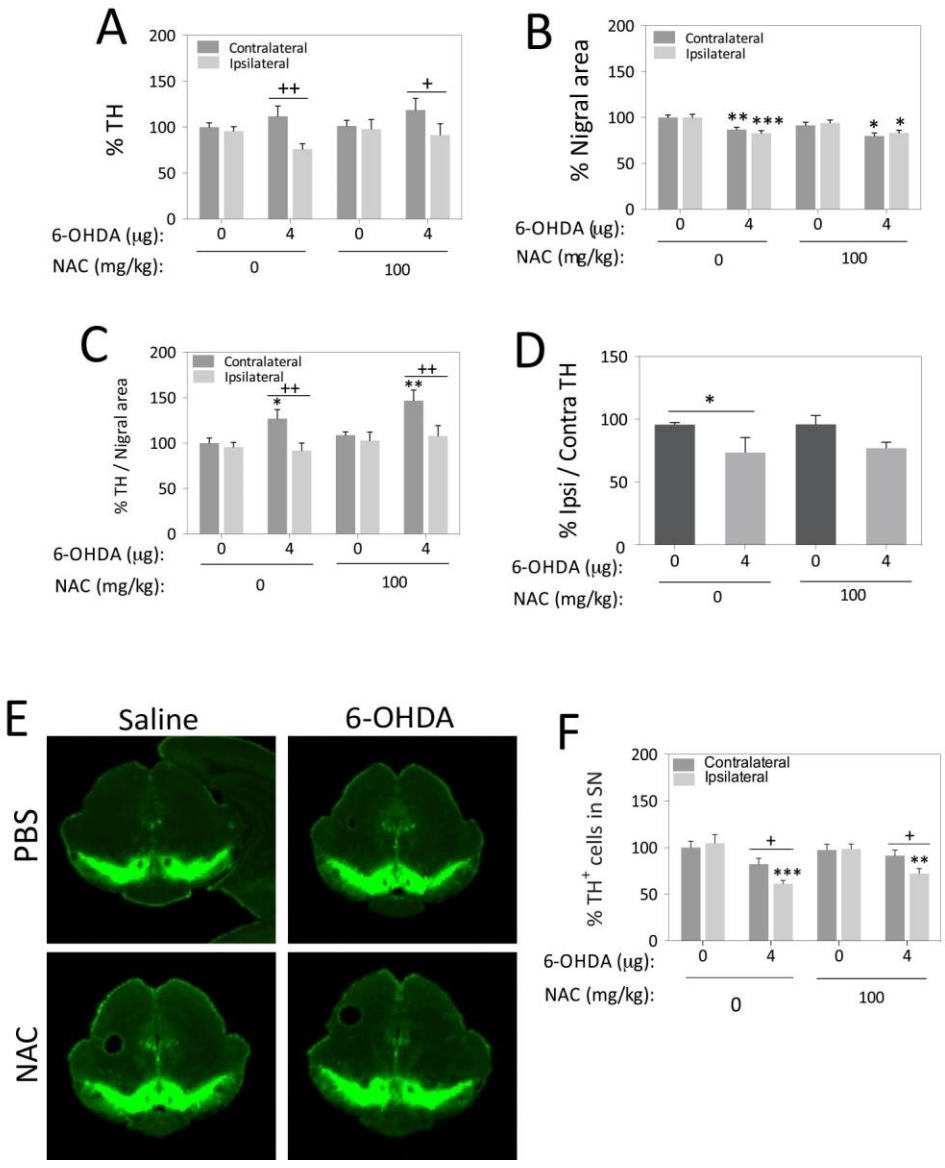

Fig. 11. NAC fails to protect dopaminergic neurons in the substantia nigra from 6-OHDA toxicity. Mice were stereotaxically infused with 4 μg 6-OHDA or an equivalent volume of vehicle (0.02% ascorbic acid in saline) into the right striatum. For the next 10 days, mice received daily intraperitoneal injections of 100 mg/kg NAC or an equivalent volume of phosphate- buffered saline (PBS). Midbrain sections were stained for the dopaminergic terminal marker tyrosine hydroxylase (TH). (A) Overall TH levels in the contralateral and ipsilateral nigrae. The ipsilateral nigra had lower TH levels than the nigra contralateral to the 6-OHDA infusion site. (B) Nigral area was significantly reduced by 6-OHDA in both hemispheres in the absence or presence of NAC. (C) TH levels were expressed as a function of nigral area, a measurement that reflects average TH density (TH per unit area). 6-OHDA raised TH density in the contralateral nigra and NAC did not significantly affect this measure. (D) 6-OHDA significantly reduced ipsilateral/contralateral nigral TH levels. Although 6-OHDA did not cause a significant loss of this measure in NAC-treated animals, NAC did not significantly increase this ratio. (E) Representative coronal sections through the mesencephalon, immunolabeled for TH+ cell bodies and scanned on the Odyssey Imager. (F) TH cell counts in the nigra reveal that NAC has no impact on the loss of dopaminergic cells in this structure. Shown

are the mean and SEM of 7–8 mice per group. *$p \leq 0.05$, **$p \leq 0.01$, ***$p \leq 0.001$ versus 0 μg 6-OHDA; + $p \leq 0.05$, ++ $p \leq 0.01$, +++ $p \leq 0.001$ ipsilateral versus contralateral; ~ $p \leq 0.05$, ~~ $p \leq 0.01$, ~~~ $p \leq 0.001$ versus 0 mg/kg NAC; two or three-way ANOVA followed by Bonferroni post hoc correction.

NAC does not protect dopaminergic terminals of the nigrostriatal pathway three weeks following 6-OHDA exposure

The progressive neurotoxicity associated with striatal 6-OHDA infusions has been reported previously (Sauer and Oertel, 1994). In the Munoz study, the examination of TH^+ structures in NAC-treated animals was completed only 1 week following 6-OHDA infusions (see Fig. 8 in Munoz et al., 2004). Because the Munoz study only examined the short-term effects of NAC and 6-OHDA continues to elicit slowly progressive degeneration, we examined whether the neuroprotective effect of NAC was long lasting. In order to address this important question, we repeated the intraperitoneal NAC experiments in 6-OHDA infused mice and sacrificed them 3 weeks following surgeries. NAC led to no significant protection in these animals (Fig. 12A). However, NAC reduced TH expression in the contralateral hemisphere of the animals receiving the ascorbic acid vehicle (0 μg 6-OHDA group or third set of bars in Fig. 12A). Striatal area was not affected by 6-OHDA or NAC at this timepoint (Fig. 12B). As a result, TH staining density followed the same pattern as in Fig. 12A (Fig. 12C). Finally, NAC had no effect on the ipsilateral/contralateral ratio of striatal TH expression (Fig. 12D). Thus, we conclude that intraperitoneal NAC does not protect dopaminergic terminals of the nigrostriatal pathway against the oxidative toxicity of 6-OHDA for the long term.

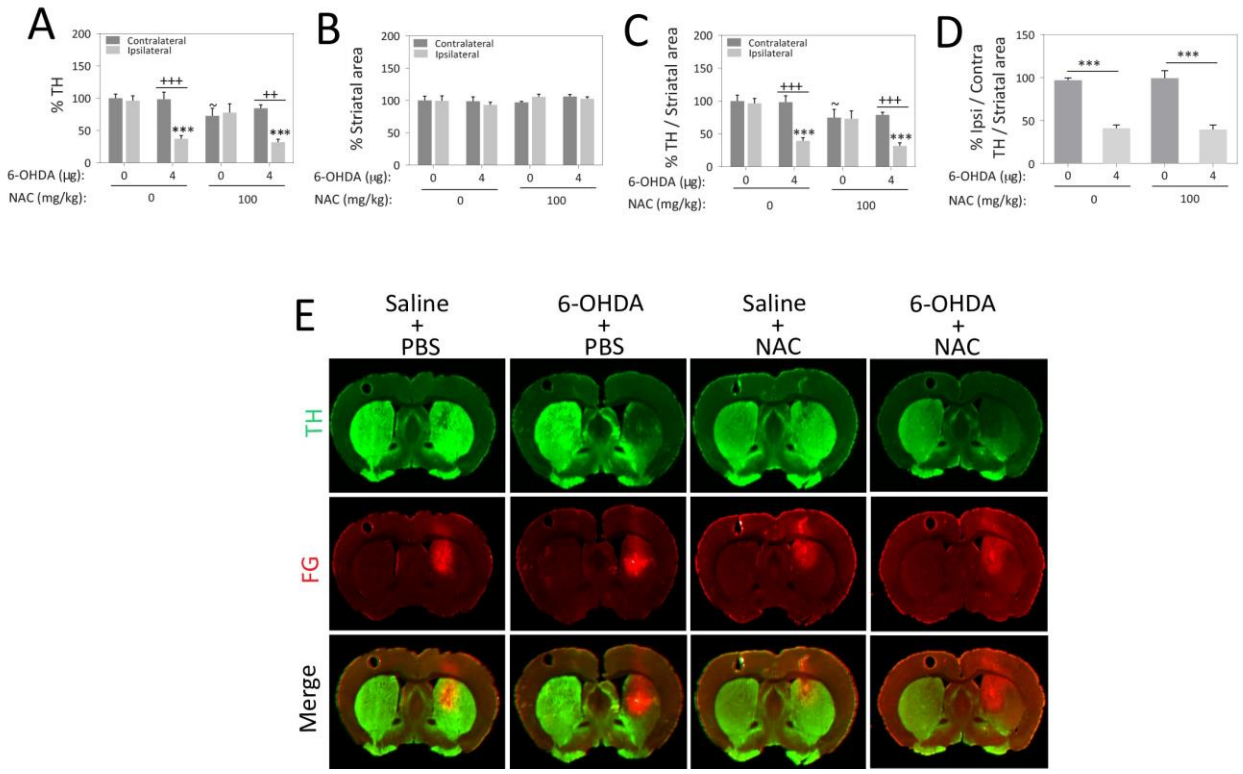

Fig. 12. NAC fails to protect dopaminergic terminals in the striatum three weeks following 6-OHDA infusions. Mice were stereotaxically infused with 6 µg FluoroGold (FG) into the right striatum. Seven days later, mice were infused in the same location with 4 µg 6-OHDA or an equivalent volume of vehicle (0.02% ascorbic acid in saline). For the next three weeks, mice received daily intraperitoneal injections of 100 mg/kg NAC or an equivalent volume of PBS. Forebrain sections were stained for the dopaminergic terminal marker tyrosine hydroxylase (TH) and FluoroGold (FG). (A) NAC reduced overall TH levels in the striatum contralateral to vehicle infusion and did not protect against 6-OHDA-induced loss of TH. (B) Striatal area was not significantly affected by NAC or 6-OHDA. (C) TH levels were expressed as a function of striatal area, reflecting TH density (TH per unit area). NAC reduced this measure in the contralateral hemisphere of vehicle-infused animals. (D) 6-OHDA significantly reduced ipsilateral/contralateral striatal TH levels and NAC did not impact this measure. (E) Representative coronal sections through the forebrain, immunolabeled for TH+ terminals (green) and FluoroGold (red). Shown are the mean and SEM of 5–8 mice per group. *$p \leq 0.05$, **$p \leq 0.01$, ***$p \leq 0.001$ versus 0 µg 6-OHDA; + $p \leq 0.05$, ++ $p \leq 0.01$, +++ $p \leq 0.001$ ipsilateral versus contralateral; ~ $p \leq 0.05$, ~~ $p \leq 0.01$, ~~~ $p \leq 0.001$ versus 0 mg/kg NAC; two or three-way ANOVA followed by Bonferroni post hoc correction. Copyright 2016 by Nouraei et al. Reprinted with permission.

NAC does not protect dopaminergic cell bodies of the nigrostriatal pathway three weeks following 6-OHDA exposure

Next we examined the effect of NAC on dopaminergic cell bodies by screening TH and FluoroGold signal in the ventral midbrain, as we had previously shown that these measurements are in agreement with higher resolution cell counts. As expected from the striatal TH results, 6-OHDA led to a decrease in nigral TH levels in both NAC and PBS-treated groups (Fig. 13A), confirming that NAC did not protect nigral dopamine neurons against 6-OHDA toxicity at longer timepoints. NAC elicited some degree of toxicity by reducing overall TH levels in all but ipsilateral hemisphere of the control group. In this study, the area of the nigra in the ipsilateral hemisphere was slightly increased by infusions of the vehicle ascorbic acid in both the PBS and NAC-treated animals (Fig. 13B). The increase in the area of TH expression could be due to a hormetic response to the mild stress induced by the acidic vehicle, and this would be abolished by the additional stress of 6-OHDA, consistent with the J-shaped nature of hormetic dose-response curves (Calabrese and Baldwin, 2002, Kendig et al., 2010). TH expression per unit area was slightly reduced in the ipsilateral hemisphere of the animals treated with the ascorbic acid vehicle, an effect that was significant in the presence of NAC (Fig. 13C). Finally, the ratio of ipsilateral over contralateral TH expression in the substantia nigra was not altered by NAC (Fig. 13D). NAC also did not increase FluoroGold signal in the 6-OHDA infused animals (Fig. 13E). Instead, NAC led to a reduction in FluoroGold immunoreactivity in the ascorbic acid-treated group. This finding may suggest some toxicity induced by NAC, leading to some neuronal cell death in the nigrostriatal pathway, which is consistent with the Odyssey imaging results in Fig. 13A.

Given the lack of protective effects of NAC on nigral TH or FluoroGold levels after 3 weeks, we did not proceed with dopaminergic neuronal counts or with glutathione or heat shock protein 70 measurements in this study.

We have presented the strengths and limitations of the tools used to define nigrostriatal degeneration in **Table 2.**

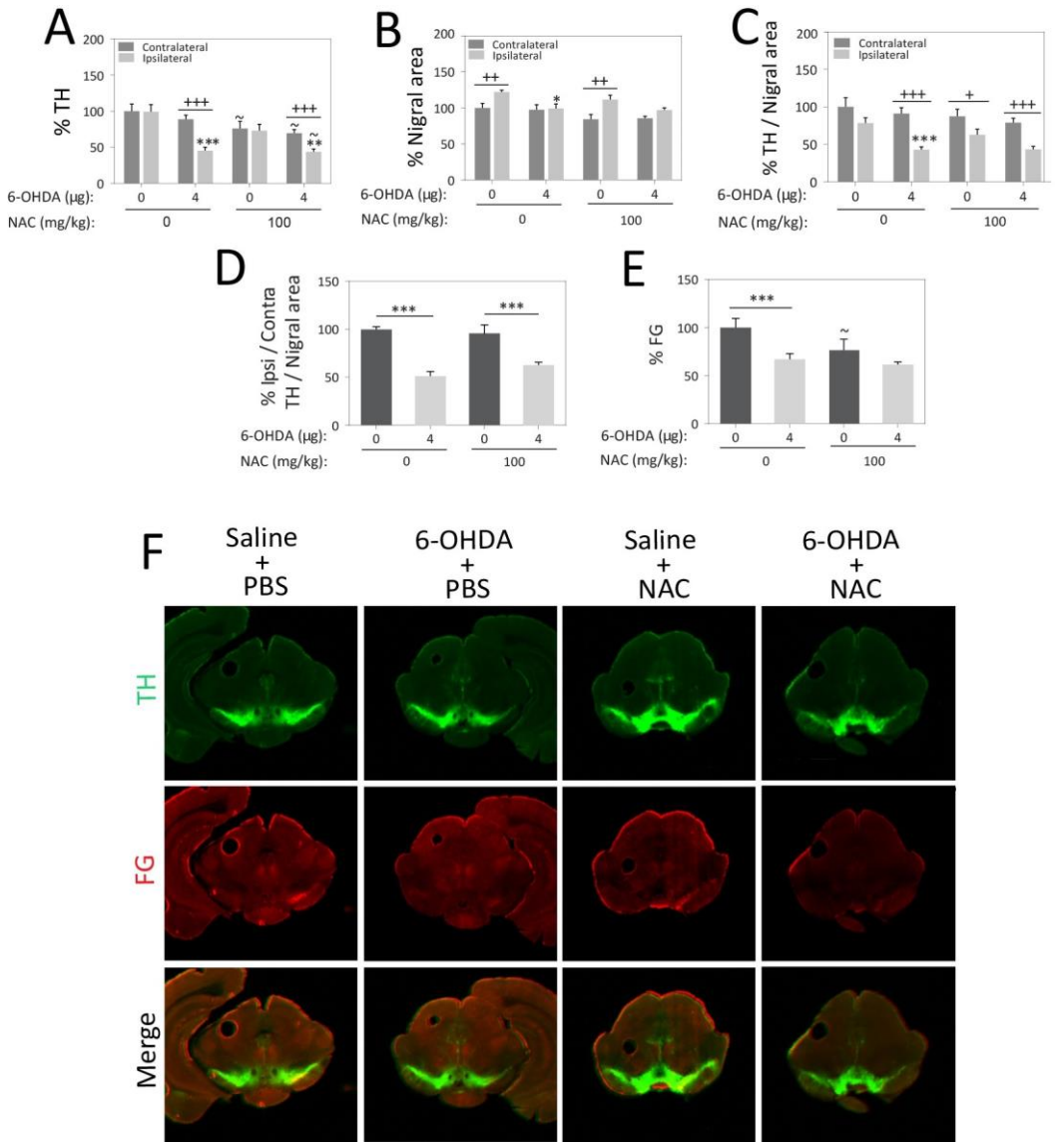

Fig. 13. NAC fails to protect dopaminergic neurons in the substantia nigra three weeks following 6-OHDA infusions. Mice were stereotaxically infused with 6 µg FluoroGold (FG) into the right striatum. Seven days later, mice were infused in the same location with 4 µg 6-OHDA or an equivalent volume of vehicle (0.02% ascorbic acid in saline). For the next three weeks, mice received daily intraperitoneal injections of 100 mg/kg NAC or an equivalent volume of PBS. Midbrain sections were stained for the dopaminergic terminal marker tyrosine hydroxylase (TH) and FluoroGold (FG). (A) NAC reduced overall TH levels in the nigra in all groups except for the vehicle-infused ipsilateral striatum. (B) Nigral area was increased by infusion of vehicle into the ipsilateral hemisphere and 6-OHDA prevented this effect. NAC had no impact on this measure. (C) TH levels were expressed as a function of nigral area, reflecting TH density (TH per unit area). NAC did not raise TH density in the ipsilateral nigra. (D) 6-OHDA significantly reduced ipsilateral/contralateral nigral TH levels and NAC did not impact this ratio. (E) Overall FluoroGold levels were reduced by 6-OHDA in the ipsilateral nigra. NAC decreased FluoroGold levels in vehicle-infused animals. (F) Representative coronal sections through the mesencephalon, immunolabeled for TH+ (green) and FluoroGold+ (red) cells. Shown are the mean and SEM of 5–8 mice per group. *$p \leq 0.05$, **$p \leq 0.01$, ***$p \leq 0.001$ versus 0 µg 6-OHDA; + $p \leq 0.05$, ++ $p \leq 0.01$, +++ $p \leq 0.001$ ipsilateral versus contralateral; ~ $p \leq 0.05$, ~~ $p \leq 0.01$, ~~~ $p \leq 0.001$ versus 0 mg/kg NAC; two or three-way ANOVA followed by Bonferroni post hoc correction. Copyright 2016 by Nouraei et al. Reprinted with permission.

Table 2: Strengths and limitations of the techniques to quantify nigrostriatal degeneration.

Strengths	Limitations
• Striatal and nigral TH measurements were completed on a 16-bit imager with high sensitivity	• The Odyssey imager has low resolution (21 μm) and individual cells cannot be resolved
• Blinded TH+ cell counts were performed by higher resolution microscopy to overcome the spatial limits of the Odyssey Imager and to complement the measurements of striatal TH	• The higher resolution counts were not performed with stereological techniques
• Measurements of the area of the striatum and nigra were included	• None
• TH levels in the striatum and nigra were expressed per unit area to approximate TH density and to avoid the confounding effect of different-sized tracings of the region of interest	• TH levels may be modulated by stress such that a drop in TH density may not reflect a true loss in dopaminergic terminals or neurons
• FluoroGold was used to overcome the limitation of stress-induced modulation of TH expression	• FluoroGold exhibited some toxicity
• FluoroGold can be labeled immunohistochemically so that it can be viewed in more channels than under UV illumination and can also be labeled more permanently with diaminobenzidine	• None
• Measurements of nigral TH levels on the Odyssey Imager were consistent with nigral TH+ cell counts, suggesting that high-throughput Odyssey imaging can be an efficient screening tool in models of Parkinson's disease	• Loss of protein does not necessarily indicate loss of cell numbers
• Measurements of loss of FluoroGold+ structures in the nigra were more sensitive than loss of TH+ structures	• FluoroGold exhibited some toxicity
• FluoroGold was infused 7d before 6-OHDA and specifically labeled healthy projection neurons that form the nigrostriatal pathway and project to the site of infusion	• None
• Neuroprotection was assessed at two different survival periods	• None
• We included an ascorbic acid/saline control for every 6-OHDA group and a PBS control for every NAC group	• None
• We included measurements of the contralateral hemisphere as an additional control	• None
• NAC was given intraperitoneally instead of orally to overcome low oral bioavailability and potential variability from different degrees of food intake due to the strong thiol odor of NAC	• Daily intraperitoneal injections are much more stressful than daily food intake

Discussion

NAC has been investigated in many experimental models of injury and has been used in multiple clinical trials with positive outcomes. Because of these successful experiments, there are currently 333 ongoing clinical trials on NAC. Results from our *in vitro* studies demonstrate that NAC can protect cortical neurons and neuroblastoma cells against proteasome inhibitors and oxidative stress (Jiang et al., 2013; Posimo et al., 2013; Unnithan et al., 2012; Unnithan et al., 2014). For example, we demonstrated that NAC can prevent cell death in response to severe, dual hits of the proteasome inhibitor MG132 and hydrogen peroxide (Unnithan et al., 2012; Unnithan et al., 2014). We also discovered that NAC can prevent loss of heat shock protein defenses in neuroblastoma cells treated with high concentrations of MG132. The protective effects of NAC were abolished in the presence of inhibitors of Hsp70 (Jiang et al., 2013). In the present study, we gathered support for the hypothesis that NAC protects dopaminergic terminals against 6-OHDA toxicity at short timeframes. However, we also discovered that the protective effects of NAC wane by three weeks post-infusion. Previous studies of NAC in the 6-OHDA model did not examine dopaminergic cell bodies at longer timeframes, did not report contralateral values, were not blinded, and failed to include a control group with NAC alone (in the absence of 6-OHDA). If NAC raises TH expression to equal degrees in the presence or absence of 6-OHDA, one cannot conclude that it changes the impact of 6-OHDA. We have observed that this issue is a common limitation of many neuroprotection studies. Therefore, we included a saline control group for 6-OHDA, a PBS control group for FluoroGold delivery, and a PBS control group for NAC. Both ipsilateral and contralateral values were measured. We examined both short and long timepoints. We were blinded in all our analyses. Finally, we used

four rigorous methods to quantify nigrostriatal cell loss to increase confidence in our interpretations of the data.

We established that NAC raises TH expression only in the 6-OHDA group (showing that it does change the impact of 6-OHDA), but that this effect was transient. As NAC exhibits low (~9.1%) oral bioavailability (Olsson et al., 1988), we delivered NAC intraperitoneally at a dose of 100 mg/kg based on numerous previous studies (Munoz et al., 2004, Chakraborti et al., 2008, Bachle et al., 2011, Smaga et al., 2012, Comparsi et al., 2014, Gunay et al., 2014, Jaccob, 2015, Prakash et al., 2015, Soleimani Asl et al., 2015, Truini et al., 2015). Furthermore, The World Health Organization guidelines for NAC administration in acetaminophen overdose are 150 mg/kg intravenously over 1 h, followed by 50 mg/kg intravenously over 4 h, and 100 mg/kg intravenously over 16 h (Pauley et al., 2015). NAC has been delivered intravenously at doses as high as 150 mg/kg in clinical trials on Parkinson's patients (Holmay et al., 2013). NAC was delivered intravenously at 100 mg/kg daily for 21 days in patients undergoing hematopoietic stem cell transplantation (Ataei et al., 2015). In patients with myocardial infarction, NAC was delivered via the intracoronary route at 100 mg/kg (Eshraghi et al., 2016). In order to prevent oral mucositis in patients who receive high-dose chemotherapy, NAC was delivered intravenously at 100 mg/kg per day for at least 2 weeks (Moslehi et al., 2014). Thus, our 100 mg/kg dose is in accordance with the clinical literature. However, our data suggest that 100 mg/kg intraperitoneal NAC can lead to mild nigrostriatal degeneration on its own—even in the absence of 6-OHDA—raising significant concerns about its long-term use in humans. Other authors have similarly argued that NAC may have toxic properties after chronic treatments (Munoz et al., 2004, Zaeri and Emamghoreishi, 2015). Thus, in future studies, we aim to deliver

NAC orally at lower doses, either in food or water. Daily intraperitoneal injections may be much more stressful than food intake even if NAC has an unpleasant, strong thiol odor that makes it less palatable. Preliminary data in the Leak lab show that the addition of NAC does not change food intake rates in mice (Mason and Leak, unpublished).

The lack of sustained neuroprotective effects of NAC in the present study has important implications for the long-term clinical use of NAC, which would be necessary in patients with progressive neurodegenerative disorders such as Parkinson's disease. Although clinical trials of NAC in Parkinson's patients led to positive outcomes, the effect sizes were relatively small (Monti et al., 2016). One possibility is that mild toxicity of NAC, as shown by the present work, reduced the sizes of the protective effects. However, in the Monti *et al* study, NAC was delivered intravenously at a dose of 50 mg/kg once a week and orally at 1200 mg/person on a daily basis. Thus, we delivered a higher daily dose of NAC than in the Monti study, as our dose was based on earlier animal and human studies that had employed the 100 mg/kg dose or higher (Munoz et al., 2004, Chakraborti et al., 2008, Bachle et al., 2011, Smaga et al., 2012, Holmay et al., 2013, Comparsi et al., 2014, Gunay et al., 2014, Moslehi et al., 2014, Ataei et al., 2015, Jaccob, 2015, Pauley et al., 2015, Prakash et al., 2015, Soleimani Asl et al., 2015, Truini et al., 2015, Eshraghi et al., 2016).

It is worth noting in this context that NAC mediated long-term protection of striatal TH in alpha-synuclein overexpressing mice in the Clark study (Clark et al., 2010). Clark and colleagues further showed that the NAC-mediated increase in nigral glutathione was no longer apparent at the time of the striatal neuroprotection assay. In the present study, there may also be only

transient upregulation of glutathione with dietary NAC, as in the Clark study, although further studies would be necessary to confirm this. This could explain why the protection of dopaminergic terminals was not sustained. Glutathione is known to inhibit glutathione synthetase by a negative feedback loop, thereby limiting its own production (Lushchak, 2012) Glutathione would be expected to reduce oxidative injury in the 6-OHDA model, but have less impact on proteinopathic stress. Therefore, we hypothesized that an upregulation of Hsp70 by NAC might underlie the protective effects of NAC in multiple *in vitro* models of proteotoxic cell death (Jiang et al., 2013; Posimo et al., 2013; Unnithan et al., 2012; Unnithan et al., 2014). Hsp70 has been shown to protect cells against both oxidative and proteotoxic stress (Jiang et al., 2013; Posimo et al., 2013; Unnithan et al., 2012; Unnithan et al., 2014). It is possible that there was no upregulation of Hsp70 *in vivo* in the present study or that the upregulation of Hsp70 *in vivo* was transient. Hsp70 is also known to inhibit its own production in a negative feedback loop with HSF1 (Zorzi and Bonvini, 2011, Vjestica et al., 2013).

In the present study, NAC only increased TH expression in the 6-OHDA-treated animals at early timepoints. That is, there was no basal effect of NAC delivered on its own (in the absence of 6-OHDA). One possible explanation for this specificity is that 6-OHDA reduces the levels of reduced glutathione and increases the levels of oxidized glutathione. This would release glutamate-cysteine ligase from feedback inhibition and thereby allow NAC to provide the rate-limiting precursor (cysteine redisue) for additional glutathione synthesis, at least at early timpoints, but only in the 6-OHDA group.

In our *in vivo* studies, we used multiple rigorous methods to quantify nigrostriatal degeneration

and validated the tools. First, we used an Odyssey imager to measure loss of TH protein in the striatum and expressed the data in multiple ways to ensure that changes in striatal area did not confound our interpretations. Next, changes in dopaminergic neurons in the substantia nigra were measured by four techniques: 1) measurements of TH expression levels and nigral area using the Odyssey Imager and 2) dopaminergic cell counts using a higher resolution microscopy, 3) measurements of FluoroGold levels using the Odyssey imager, and 4) counts of individual FluoroGold^{+} nigral neurons. Many studies in the 6-OHDA model report TH or dopamine values only as an ipsilateral/contralateral ratio without reporting the contralateral values. As explained in the classic stereology literature, expressing data as a ratio is subject to the "reference trap" (Braendgaard and Gundersen, 1986, Hyde et al., 2007). Thus, one cannot determine from a ratio whether the changes are attributable to the numerator or the denominator, or both. The investigator is usually inclined to assume that the ratio reflects the numerator and not the denominator because the latter is the reference value. Our results clearly show that contralateral TH levels can change in response to the treatments to the same degree as ipsilateral TH levels (Fig. 10). Therefore, the most appropriate control for this type of study of the basal ganglia is the ipsilateral hemisphere in the vehicle-treated animals. As we expected, it was important to examine the therapeutic potential of NAC at multiple timepoints, to report contralateral values, and to examine the cell bodies in addition to the terminals.

We have included a list of the strengths and limitations of the techniques used here to assess nigrostriatal degeneration (**Table 2**). Here, we will only highlight some of the major points mentioned in **Table 2** to avoid repetition. We found that FluoroGold is a highly sensitive tool to quantify nigrostriatal degeneration. Because it is such a robust tract-tracer, it has been employed

in many studies (Sauer and Oertel, 1994, Mandel et al., 1997, Choi-Lundberg et al., 1998, Yamada et al., 1999, Kozlowski et al., 2000, Aymerich et al., 2006, Ebert et al., 2008, Anastasia et al., 2009, Cohen et al., 2011). Consistent with one study showing that FluoroGold may be toxic (Naumann et al., 2000), we found that FluoroGold slightly reduces nigral area (see Fig. 9B). Therefore, it might be worth examining more inert tract-tracers, such as biotinylated dextran amines. However, the dextran amines are transported in both retrograde and anterograde directions. This would preclude using the Odyssey imager to measure overall tracer levels in the nigra as a specific measure of the nigrostriatal efferent pathway. Another option would be the retrograde tracer True Blue. Although it fades quickly, this tracer has been reported to be less toxic than FluoroGold over long survival timeframes (Garrett et al., 1991).

One of the limitations of using the Odyssey imager to screen overall TH levels is that loss of protein expression may not necessarily represent loss of axon terminals or soma numbers. *For example, in response to stress, neurons may retract their dendrites or lose TH expression without any degeneration.* Thus, it is important to include dopaminergic cell counts to accompany measurements of striatal and nigral TH. Nevertheless, the degree of overall loss of nigral TH expression according to the infrared imager was consistent with the degree of loss of TH^+ cell counts. Thus, the Odyssey imager is useful as a rapid screening tool prior to more low-throughput measurements and the two types of measurements should be viewed as complementary. For example, increases in TH expression per unit area, as detected by the Odyssey imager, may suggest that individual nigral cells are producing more TH if there is no parallel change in cell numbers. Another advantage of using the Odyssey imager is that nigral and striatal areas are easily measured, loss of which can also reveal some form of toxicity. In the

present study we did not use stereological techniques for cell counts. However, we counted all TH^+ neurons in three enormous stitched microscopic images at mid levels of the nigra. Non-stereological counting techniques are subject to over or under-reporting cell numbers. However, such errors would be expected to occur at same rates for both the experimental and control groups in the present study.

As with stereological studies of dopamine neurons, TH cell counts in the present report are highly dependent on TH expression levels. For example, it is possible that dopamine cells of the nigrostriatal pathway may express TH at levels too low to be detected by immunohistochemistry and would therefore not be counted even by stereological techniques. To address this problem, previous studies have reported cell counts of Cresyl Violet-stained nigral cells. However, Nissl substance is also expressed in glial cells and glial cells can undergo hyperplasia in response to stress, which would result in higher nigral cell counts with the Cresyl Violet technique. To circumvent this issue, we employed FluoroGold to specifically label dopamine neurons of the nigrostriatal pathway. Another alternative would be to use a neuronal marker such as NeuN. However, NeuN is not a reliable marker of dopamine neurons in the substantia nigra, as it is not even present in some TH-expressing dopamine neurons (Cannon and Greenamyre, 2009) Additionally, neuronal markers such as NeuN would not specifically label the efferent projection neurons of the nigrostriatal pathway, the loss of which is an important variable for modeling Parkinson's disease**.**

In summary, we used multiple independent measurements of nigrostriatal degeneration to rigorously study the therapeutic potential of NAC. NAC offered transient protection in our

model, but the protective effects were diminished at longer timepoints. The strengths and limitations of using an established retrograde tracer to quantify nigrostriatal degeneration have been described in detail. Alternatives for future studies, such as delivering NAC by food or water and switching to less toxic tracers have been proposed. Finally, chronic treatment with NAC may even exert toxic effects of its own. This has important implications for clinical trials of NAC in patients with Parkinson's disease, a severe, progressive, neurodegenerative disorder that would demand long-term treatment strategies.

Chapter 3

Rationale

Progressive cognitive decline is evident in many patients in mid-to-late stage Parkinson disease (Braak et al., 2003, (Lue et al., 2016). Indeed, Parkinson's patients have a 4-6 fold greater incidence of dementia compared to healthy individuals (Hobson and Meara, 2004, Metzler-Baddeley, 2007). Clinical studies following patients with Parkinson's disease for 8 or 20 years found cumulative cognitive deficit prevalence rates of 78% and 83%, respectively (Aarsland et al., 2003, Hely et al., 2008). A combination of motor dysfunction and cognitive dementia increase mortality 3-8 fold and greatly impact quality of life (Xu et al., 2014).

In Parkinson's disease, motor symptoms typically occur prior to the onset of cognitive impairments (Aarsland, 2016). The hippocampus develops Lewy pathology in Braak stages III and IV (Braak et al., 2003a). Stages V and VI are associated with the formation of alpha-synuclein inclusions in the neocortex. Alpha-synucleinopathy in the hippocampus and neocortex are strongly correlated with cognitive deficits in Parkinson's disease (Kalaitzakis and Pearce, 2009). A similar topographical pattern has been reported in Lewy body dementia, a condition where symptoms of cognitive impairment appear before movement deficits. To date, there are few models of Parkinson's disease dementia and of Lewy pathology in the hippocampus. Furthermore, current treatments for cognitive deficits in Parkinson's disease are not very effective and are largely limited to cholinesterase inhibitors and Memantine, a partial NMDA-antagonist (Aisen et al., 2012). It is essential to diagnose cognitive deficits at early stages in

order to improve the effectiveness of the limited treatment options (Caviness et al., 2011). Therefore, there is an urgent need for agents to improve cognitive function and/or to delay the rate of cognitive decline in Parkinson's disease dementia and Lewy body dementia.

Dehydroepiandrosterone (DHEA) and its sulfated ester DHEAS are two of the most abundant neurosteroids synthesized within the nervous system (Flood et al., 1988, Migues et al., 2002). Some studies suggested that the levels of DHEAS are significantly reduced in the brains of patients with Alzheimer's disease compared with the healthy individuals (Nasman et al., 1991, Leblhuber et al., 1993, Solerte et al., 1999, Murialdo et al., 2000). However, the link between reduced levels of DHEAS and neurodegenerative diseases is still controversial. *In vivo* studies in rats indicate that intraperitoneal injections of DHEAS enhance hippocampal acetylcholine release, as measured by *in vivo* microdialysis (Rhodes et al., 1996). Consistent with these findings, our lab showed that DHEAS improved memory function in rats with a selective cholinergic lesion of the septohippocampal tract (data unpublished). Furthermore, inhibition of the steroid sulfatase enzyme, which increases DHEAS levels by preventing its conversion back to DHEA, can facilitate the memory-enhancing effects of DHEAS (Johnson et al., 1997, Li et al., 1997, Johnson et al., 2000). Other studies have also demonstrated that DHEAS protects hippocampal neurons against glutamate-induced neurotoxicity in the hippocampus while little protection is obtained from the equivalent doses of DHEA (Mao and Barger, 1998). These results suggest that DHEAS is a neuroprotective agent with the potential to alleviate dementia associated with Parkinson's disease or related neurodegenerative disorders. Therefore, we hypothesized that DHEAS may improve memory function in rats infused with alpha-synuclein fibrils into the hippocampus and/or striatum, a model of Parkinson's disease dementia.

Specific Aim 3: Test the hypothesis that DHEAS will improve memory function in an alpha-synuclein model of Parkinson's disease dementia.

Results – Preliminary Study

Hippocampal and/or striatal injection of alpha-synuclein fibrils impaired novel place and novel object recognition respectively in rats (preliminary data)

Male Sprague Dawley rats (3 months old) were bilaterally infused with alpha-synuclein fibrils into the hippocampus and/or striatum. Seven months later the animals were tested for declarative memory using novel object (NOR) and novel place (NPR) recognition paradigms. Pilot results demonstrate significant impairments in novel object recognition (Fig. 14) but not novel place recognition in animals injected in the dorsal striatum with alpha-synuclein ($P<0.01$) and a trend toward impairment in novel place recognition but not object recognition in rats injected in the hippocampus ($P=0.06$) (Fig. 14).

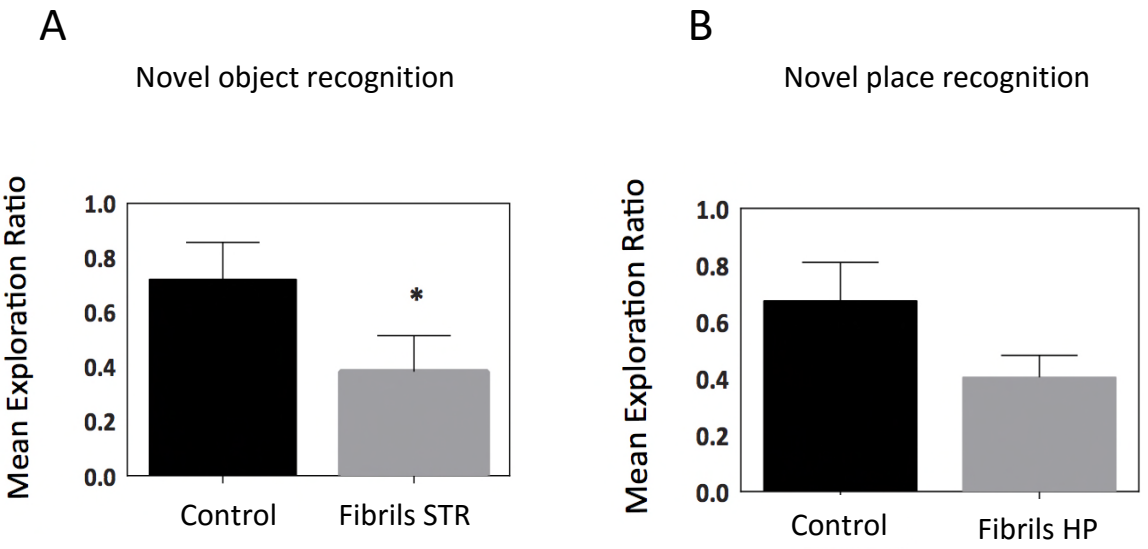

Fig.14. ***Novel object and novel place recognition test at seven months.*** Rats were infused with alpha-synuclein fibrils into the hippocampus and/or striatum bilaterally. Seven months later the animals were tested for declarative memory using novel object and novel place recognition paradigms. (A) Novel object recognition but not novel place recognition was significantly impaired in animals injected in the dorsal striatum with alpha-synuclein ($P<0.01$). (B) There was a trend toward impairment of novel place recognition but not object recognition in rats injected in the hippocampus ($P=0.06$). *$p \leq 0.05$ versus control, n=3-4 rats per group.

Alpha-synuclein fibrils led to mild loss of NeuN in the hippocampus (preliminary data)

Animals were then perfused and brains were immunostained for the neuronal marker NeuN. Sections were imaged on an Odyssey Infrared Imager and quantified in blinded fashion. Histological examination of hippocampi injected with alpha-synuclein fibrils revealed a significant loss of NeuN signal in the hippocampus by seven months after infusion ($P<0.01$) (Fig. 15). These preliminary results suggest that specific cognitive impairments in Parkinson's disease may be related to loss of NeuN signal associated with alpha-synucleinopathy in cortical and subcortical structures.

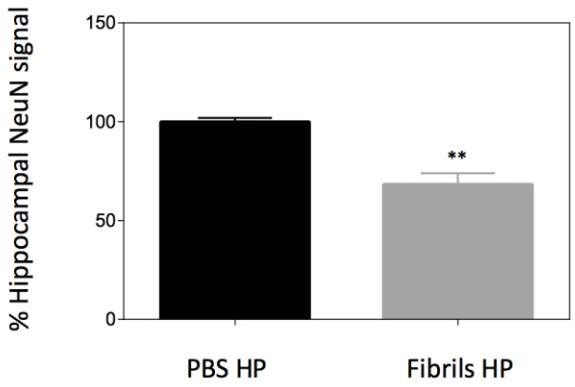

Fig.15. ***Alpha-synuclein fibrils elicit NeuN loss in the rat hippocampus at seven months***. Rats were infused with alpha-synuclein fibrils into the hippocampus and/or striatum bilaterally. Seven months later the animals were perfused and brains were immunostained for the neuronal marker NeuN. ** $p \leq 0.01$ versus control, n=3-4 rats per group.

Alpha synuclein infusions had no effect on memory function or NeuN signal

As the preliminary results were promising, more animals were injected with alpha-synuclein fibrils or PBS into the hippocampus and/or striatum bilaterally. Six to seven months post-surgery, we injected DHEAS (10 mg/kg) intraperitoneally immediately before the novel object/place recognition tests to investigate whether memory functions would be improved. Neither alpha-synuclein infusions nor DHEAS injections led to significant effects on NOR or NPR in this study (Fig. 16). Subsequent immunohistochemical analyses revealed only sparse accumulations of $pSer129^{+}$ inclusions (Fig.17) and no significant changes in the dopaminergic marker TH in the striatum or the neuronal marker NeuN in the striatum or hippocampus (Fig.18 A-F), due to technical limitations such as improper sonication parameters and application of low doses of fibrils.

A

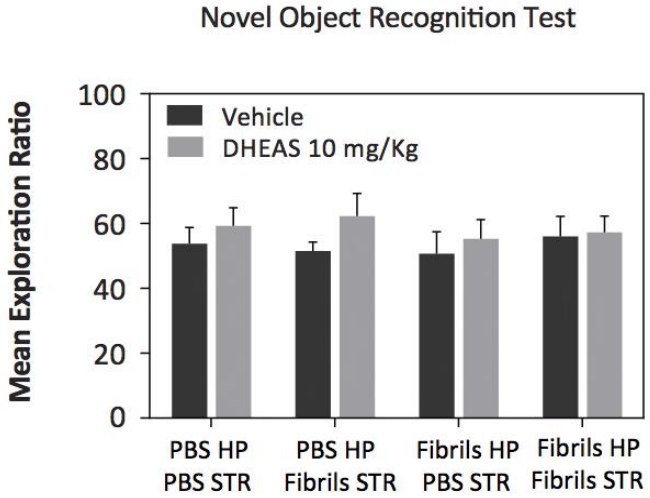

B

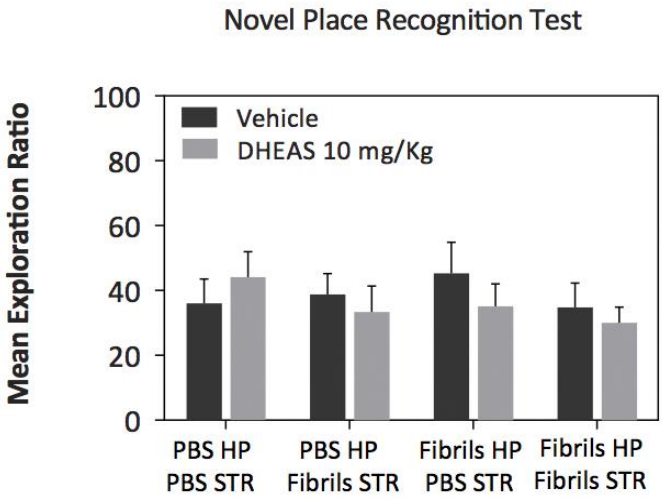

Fig.16. Novel object and novel place recognition test at seven months. Rats were infused with alpha-synuclein fibrils into the hippocampus and/or striatum bilaterally. Seven months later the animals were tested for declarative memory using novel object (NOR) and novel place (NPR) recognition paradigms. (A) Neither alpha-synuclein infusions nor DHEAS injections had significant effects on NOR. (B) Neither alpha-synuclein infusions nor DHEAS injections had significant effects on NPR in this study, n=8 rats per group.

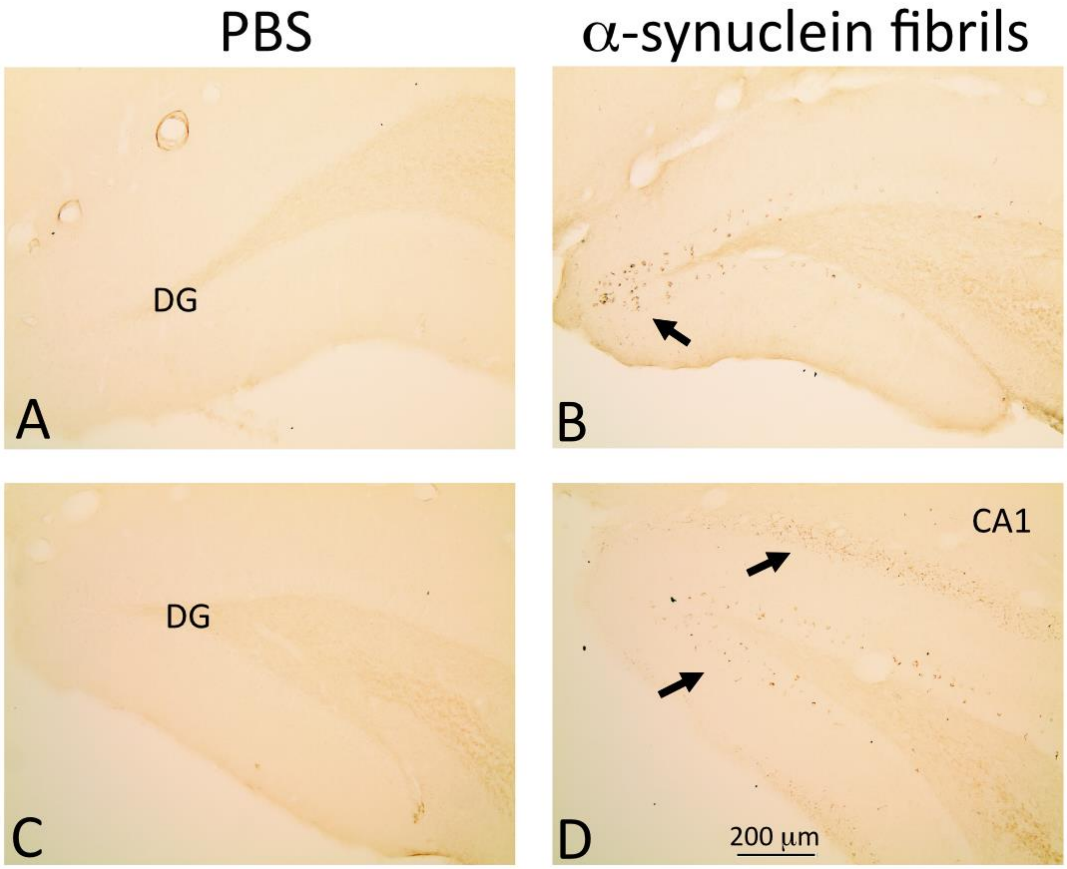

Fig. 17. Alpha-synuclein fibrils led to only mild alpha-synuclein pathology in dentate gyrus and CA1. Rats were infused with alpha-synuclein fibrils into the hippocampus and/or striatum bilaterally. Seven months later the animals were perfused and brains were immunolabeled for pathologically phosphorylated alpha-synuclein (pSer129) Alpha-synuclein fibrils led to only mild alpha-synuclein pathology in the dentate gyrus and CA1.

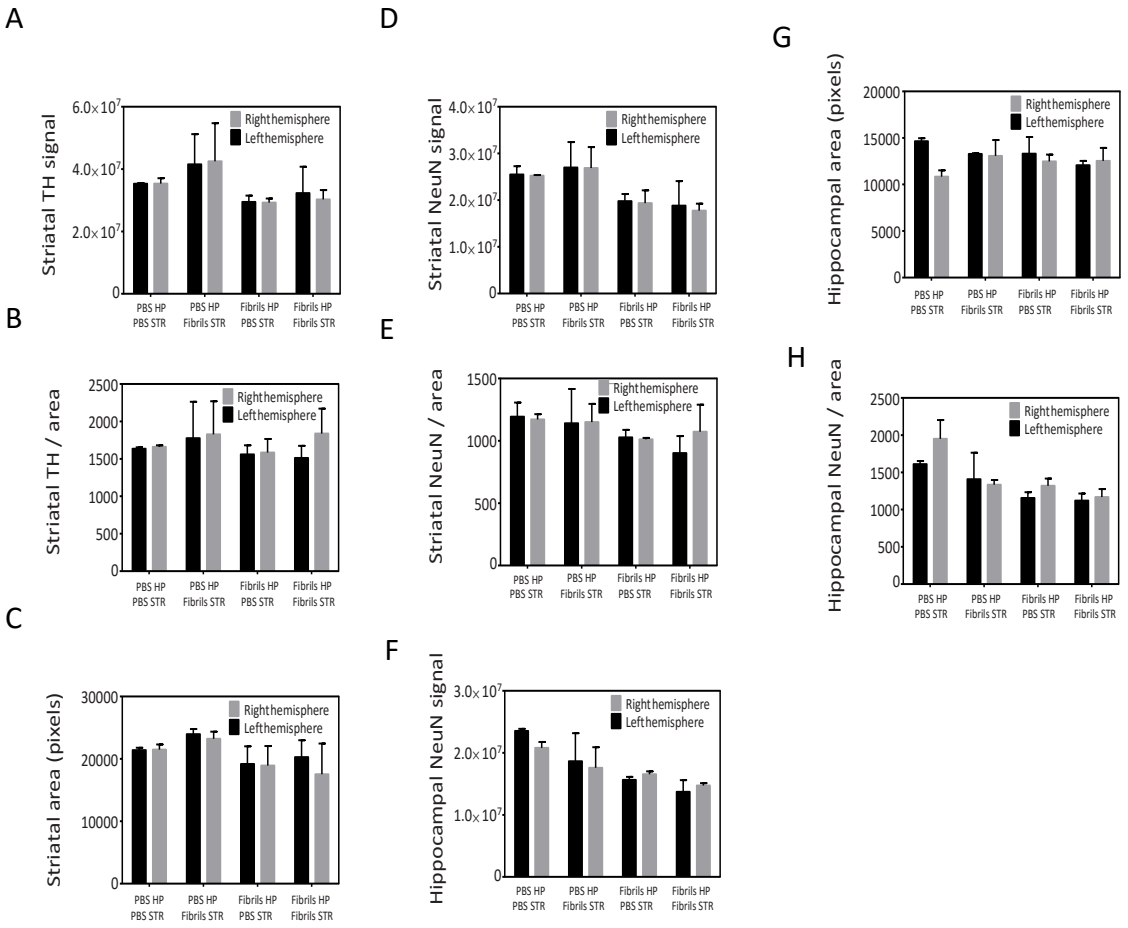

Fig.18. Alpha-synuclein infusions injections failed to affect levels of the dopaminergic marker TH or the neuronal marker NeuN in the striatum or hippocampus. Rats were bilaterally infused with alpha-synuclein fibrils into the hippocampus and/or striatum. Seven months later the animals were perfused and brains were immunostained for the neuronal marker NeuN, dopaminergic marker TH, hippocampal / striatal area, TH and NeuN density. (A-C) Alpha-synuclein infusions had no significant effects on striatal TH signal, striatal area or striatal TH / area. (D-E) Alpha-synuclein infusions had no significant effects on striatal NeuN signal or striatal NeuN /area. (F-H) Alpha-synuclein infusions had no significant effects on hippocampal NeuN signal, hippocampal area. or hippocampal NeuN /area. n=8 rats per group.

Discussion

First, we injected alpha-synuclein fibrils bilaterally into the rat hippocampus and/or striatum to elicit protein-misfolding stress, the major hallmark of all neurodegenerative disorders. The novel object recognition and novel object place recognition tests were employed after 7 months. In a pilot study, mice injected with alpha-synuclein fibrils exhibited significant loss of memory compared to PBS-treated controls. Alpha-synuclein injections in the striatum led to loss of novel object recognition skills whereas injections in the hippocampus impaired novel place recognition. Next, we injected DHEAS intraperitoneally immediately before the novel object/place recognition tests to investigate whether memory functions would be improved. Neither alpha-synuclein infusions nor DHEAS injections exerted significant effects on novel object/place recognition tests in this study. Immunohistochemical analyses suggested only mild alpha-synuclein pathology and no significant changes in levels of the dopaminergic marker TH or the neuronal marker NeuN in the striatum or hippocampus.

Although the preliminary data were promising, there can be differences in the concentrations of the fibrils from batch to batch or even within the same batch, as the fibrils may settle to the bottom of the tube quickly during the aliquoting procedure. At the time of this study, the Leak lab had not yet optimized the parameters of sonication. Fibril sonication parameters are important in the formation and transmission of Lewy-like pathology (Volpicelli-Daley et al., 2014). Furthermore, in the present study, we used lower doses of fibrils (2 μg per site injection) compared to the 5 μg per site injection that was reported previously (Luk et al., 2012a), as we

had limited access to fibrils in this study. All of these technical limitations may explain our negative results.

Chapter 4

Rationale

The classical neuropathological feature of Lewy body disorders is the accumulation of the synaptic protein alpha-synuclein in fibrillar aggregates (Wakabayashi et al., 2007). Lewy pathology commences in the olfactory bulb and medulla oblongata and is known to reach the basal forebrain and mesocortex in Braak stage IV (Braak et al., 2003a). This appearance of Lewy pathology in the telencephalon is correlated with the emergence of cognitive impairments or dementia. Dementia is a common nonmotor symptom in Parkinson's disease, with a prevalence of ~50% (Kalaitzakis and Pearce, 2009). Furthermore, 24-36% of patients with newly diagnosed Parkinson's disease exhibit some form of memory deficits (Foltynie et al., 2004, Muslimovic et al., 2005, Kalaitzakis and Pearce, 2009). Parkinson's disease patients with dementia exhibit neuronal loss in several brain regions, including the locus coeruleus, nucleus basalis of Meynert, dorsal raphe, ventral tegmental area, and the medial substantia nigra (Kalaitzakis and Pearce, 2009). There is a correlation between the severity of clinical dementia and the number of Lewy bodies in the entorhinal cortex and the density of Lewy neurites in hippocampal CA2 (Nagano-Saito et al., 2005). Alpha-synucleinopathy reaches CA2 of the hippocampus in Braak stages III-IV (Parkkinen et al., 2008). Magnetic resonance imaging (MRI) studies have shown that hippocampal atrophy is associated with cognitive deficits in nondemented Parkinson's disease patients (Nagano-Saito et al., 2005). Dementia with Lewy bodies, a condition distinct from Parkinson's disease dementia, is also known to be associated with dense alpha-synucleinopathy in CA2 of the hippocampus (Del Ser et al., 2001). The distinction between dementia with Lewy

bodies and Parkinson's disease dementia is based on the temporal sequence of cognitive versus motor symptoms (Mrak and Griffin, 2007). If motor symptoms appear prior to dementia by more than one year, the patient is diagnosed with Parkinson's disease dementia. However, when dementia appears within 12 months of motor symptoms, a diagnosis of dementia with Lewy bodies should be considered.

The importance of the hippocampus in memory and learning is well established by many animal and clinical studies. For example, long-term potentiation in synaptic function has been well studied in the hippocampus (Bliss and Collingridge, 1993). It is therefore not surprising that many studies report a correlation between Lewy neurite density in CA2 and cognitive impairments (Churchyard and Lees, 1997, Pagani et al., 2005, Kalaitzakis et al., 2009). However, there are few available models of hippocampal alpha-synucleinopathy with which to mimic the memory deficits seen in Parkinson's disease dementia and dementia with Lewy bodies.

For the last 40 years, the majority of research in Parkinson's disease was limited to motor symptoms, which are generally attributed to the loss of dopaminergic neurons (Alexander, 2004). Recently, the importance of non-motor parkinsonian symptoms has become increasingly evident and animal models have been developed that exhibit some, but not all, of the non-motor features of this condition. For example, many different transgenic lines of mice over-expressing alpha-synuclein have been generated (Fleming and Chesselet, 2006, Lim et al., 2011, Paumier et al., 2013). Lim and colleagues showed that the impairments in contextual fear memory in mice over-expressing alpha-synuclein at 8 months is correlated with accumulation of abnormal alpha-synuclein in limbic areas, especially in the hippocampus (Lim et al., 2011). Other groups

demonstrated that mice overexpressing human A53T mutant alpha-synuclein develop fine sensorimotor and synaptic impairments before the onset of late-stage gross motor and memory deficits related to Parkinson's disease (Paumier et al., 2013). The A53T transgenic mice exhibit spatial memory deficits at 6 and 12 months, as measured by Y-maze cognitive testing. One important limitation of this model is that behavioral impairments do not seem to progress with time, but rather develop in an all or none fashion with extensive variability across animals. The early-onset deficits also do not correlate with the accumulation of alpha-synuclein, suggestive of additional mechanisms responsible for early symptoms. In sum, this transgenic model shows fine sensorimotor and synaptic dysfunction long before alpha-synuclein accumulation or obvious motor symptoms become evident. The transgenic models cannot be used to answer whether hippocampal Lewy pathology is responsible for cognitive deficits, as gene expression is increased in neurons throughout the brain. Human studies can also not address whether the link between hippocampal Lewy pathology and cognitive dysfunction is causal or merely correlative.

All of the transgenic animal models are based on the genetics of familial Parkinson's disease. However, most cases of Parkinson's disease are sporadic in nature, in that only 10–15% of patients have a positive family history of the condition (Papapetropoulos et al., 2007). Therefore, another concern with employing transgenic models is the relevance of the pathophysiological mechanisms triggered by rare mutations to the non-familial sporadic cases. Recently, researchers have infused recombinant alpha-synuclein fibrils into CA1/CA2 of the hippocampus and the striatum (Luk et al., 2012a, Sacino et al., 2013). However, as mentioned above, hippocampal Lewy pathology in Parkinson's disease is centered in CA2/3 (Del Ser et al., 2001). Luk and colleagues did not report any memory deficits following hippocampal injection of fibrils, as

assessed using the Y maze (Luk et al., 2012a). Sacino *et al*. failed to measure cognitive functions after hippocampal fibril injections, and reported severely limited spread of alpha-synucleinopathy from the injection site (Luk et al., 2012a, Sacino et al., 2013). Furthermore, none of these previous studies involved bilateral injections, even though it is possible that the unlesioned hemisphere may compensate against unilateral injuries. Therefore, the first goal of this aim is to develop a model of bilateral hippocampal alpha-synucleinopathy with greater potential for behavioral impairments and that could be used to test therapies aimed at ameliorating cognitive deficits in Parkinson's disease dementia or dementia with Lewy bodies. In order to accomplish this goal, two month-old CD1 mice were bilaterally infused with alpha-synuclein fibrils (5 μg) or PBS into CA2/3 of hippocampus. We measured behavioral impairments at 2 and 3 months post-infusion. As mentioned above, although hippocampal alpha-synucleinopathy is known to be correlated with cognitive deficits in Lewy body disorders (Churchyard and Lees, 1997, Pagani et al., 2005, Kalaitzakis et al., 2009), it is not known if this link is causal or correlative. If the link is indeed causal, this would significantly influence drug development by providing a clinically relevant model of parkinsonian dementia. Therefore, we also aimed to investigate whether hippocampal alpha-synucleinopathy following bilateral infusions of fibrils leads to the emergence of memory deficits as in Parkinson's disease dementia or dementia with Lewy bodies.

Alpha-synuclein is thought to be endocytosed into endosomes and degraded via autophagy or proteasomal degradation systems (Luk et al., 2009, Volpicelli-Daley et al., 2011). However, fibrillar structures may poke holes in vesicular membranes such as lysosomes and endosomes and then have access to the cytosol, where misfolded and fibrillar alpha-synuclein may act as a

template to seed similar misfolding in native, endogenous alpha-synuclein molecules that are nearby. This fibrillar template may therefore seed pathology that is self- gating and spreads throughout the central nervous system via synaptic contacts over time (Glabe and Kayed, 2006, Goedert et al., 2010). Indeed, several investigators have hypothesized that the pattern of transmission of Lewy pathology following fibril injections is based on established neuroanatomical connections, even though the transmission through neuroanatomical circuits has not been investigated rigorously (Luk et al., 2012a, Sacino et al., 2013). Therefore, we assessed the pattern of spread of alpha-synucleinopathy after fibril infusions into CA2/CA3 and compared that to the literature on hippocampal afferents and efferents.

According to the tract-tracing literature, major afferents of the hippocampal formation arise in the medial septum, diagonal band of Broca, and entorhinal cortex (Segal, 1977, Swanson and Cowan, 1977, Swanson, 1982, Vertes, 1992, Conde et al., 1995, Yoshida and Oka, 1995, Gasbarri et al., 1997, Risold and Swanson, 1997, Acsady et al., 1998, Naber and Witter, 1998, McKenna and Vertes, 2001, O'Mara et al., 2001, Francisco E. Olucha-Bordonau, 2015, Natalie L.M. Cappaert, 2015, Paxinos, 2015). More minor projections arise in the supramammillary nucleus and the monoaminergic cell groups in the locus coeruleus and raphe (Segal, 1977, Swanson and Cowan, 1977, Swanson, 1982, Vertes, 1992, Conde et al., 1995, Yoshida and Oka, 1995, Gasbarri et al., 1997, Risold and Swanson, 1997, Acsady et al., 1998, Naber and Witter, 1998, McKenna and Vertes, 2001, O'Mara et al., 2001, Francisco E. Olucha-Bordonau, 2015, Natalie L.M. Cappaert, 2015, Paxinos, 2015). Septal projections terminate in all fields of the hippocampal formation but are particularly prominent in the dentate gyrus (Swanson and Cowan, 1977). The septal projection to CA3 originates mainly in the medial septal nucleus and nucleus

of the horizontal diagonal band of Broca, similar to the septal projections to the dentate gyrus (Yoshida and Oka, 1995). Cells in the medial septum and the dentate gyrus both receive collaterals from the same cells in the medial raphe nucleus (McKenna and Vertes, 2001). The dentate gyrus also receives a minor and diffusely distributed projection from cells located in the ventral tegmental area (Swanson, 1982, Gasbarri et al., 1997). As mentioned above, a hypothalamic projection to the dentate gyrus arises from supramammillary area (Segal, 1977, Vertes, 1992).

There are several reports of amygdalar projections into the hippocampus (Pikkarainen et al., 1999, Cenquizca and Swanson, 2007). The amygdaloid complex projects to the hippocampus and parahippocampal areas, including to the subiculum (Pikkarainen et al., 1999). The basolateral division of amygdala targets the stratum oriens and stratum radiatum of CA3 and CA1 as well as the subiculum. The basomedial division of the amygdala projects to the stratum lacunosum-moleculare of CA1 (Pikkarainen et al., 1999). The amygdala also receives significant reciprocal projections from the hippocampal formation (ventral regions of field CA1) and prefrontal cortex (Cenquizca and Swanson, 2007).

Swanson and colleagues have shown that most of the hippocampal efferent projections originate from the subiculum (Swanson and Cowan, 1977), and that the only subcortical projection from CA3 terminates in the lateral septal nucleus. The pattern of the projections from CA3 to the lateral septum differs from that of CA1 projections, as CA3 preferentially projects to more caudal levels of the lateral septum (Risold and Swanson, 1997). The major projections arising from CA1 pyramidal cells descend into the stratum oriens or the alveus and then extend towards

the subiculum (Finch and Babb, 1981, Finch et al., 1983, Amaral et al., 1991). The projections of the subiculum target a number of cortical and subcortical regions, including medial portions of the anterior olfactory nucleus and the agranular insular cortex (Conde et al., 1995, Naber and Witter, 1998, O'Mara et al., 2001). In addition, the ventral CA1/subiculum region of the hippocampus provides prominent inputs to medium spiny neurons of the nucleus accumbens (Floresco et al., 2001).

Hippocampal commissural projections arise mainly from mossy cells in the hilar region of the dentate gyrus and from CA3 pyramidal cells (Swanson et al., 1980, Zappone and Sloviter, 2001). Injections of the retrograde tracer FluoroGold that are centered in the dentate gyrus of the medial hippocampus elicit contralateral retrograde labeling exclusively in dentate hilar neurons, whereas larger injections spanning CA3 and CA1 (and the dentate gyrus) lead to contralateral labeling in CA3 as well as the hilum (Zappone and Sloviter, 2001). The existence of specific axonal pathways connecting the two hippocampi allows us to examine the spread of Lewy-like pathology across commissural circuits. Therefore, in addition to the bilateral infusions of fibrils into CA2/CA3, we also infused fibrils unilaterally in order to study the topographical pattern of inclusion formation within commissural and associational circuits. Understanding the mechanisms of propagation and transmission of the Lewy-like pathology could lead to the design of novel therapeutic interventions in Parkinson’s disease and other alpha-synucleionopathies.

Specific Aim 4: Determine if Lewy-like pathology in CA2/CA3 will lead to cognitive deficits in an experimental model of Parkinson’s disease dementia or dementia with Lewy bodies.

Results

Unilateral injections of alpha-synuclein fibrils into CA2/3 lead to the formation of dense pSer129^{+} inclusions in the hippocampus and entorhinal cortex

Fibril sonication parameters are important in the formation and transmission of the pathology (Volpicelli-Daley et al., 2014). We have recently conducted an animal study to optimize the fibril sonication protocol and discovered that 1h sonication renders the alpha-synuclein model more aggressive and robust (Mason et al., 2016). In that study, we showed that infusions of 1 hour-sonicated fibrils into the OB/AON led to transmission of alpha-synucleinopathy from olfactory structures deep into the limbic rhinencephalon, including all major afferent brain regions—such as the piriform and entorhinal cortices, amygdala, and hippocampus. Thus, we used these validated sonication parameters to investigate whether infusions of 1 hour waterbath-sonicated alpha-synuclein fibrils into hippocampal CA2/3 lead to the formation of Lewy-like pathology in the hippocampus and transmission through neuroanatomical circuits such as the perforant and septohippocampal pathways. Animals were sacrificed three months post-infusion and brains were immunolabeled for pSer129, the pathologically phosphorylated form of alpha-synuclein (Sato et al., 2013). Nuclei were labeled with the DRAQ5 or Hoechst nuclear stains. These mice developed robust alpha-synucleinopathy in the hippocampus and at some, but not all the afferent sites that send first-order projections to the hippocampus, such as the amygdala, entorhinal cortex, and lateral septum (Figure 19) (Segal, 1977, Swanson and Cowan, 1977, Swanson, 1982, Vertes, 1992, Conde et al., 1995, Yoshida and Oka, 1995, Gasbarri et al., 1997, Risold and Swanson, 1997, Acsady et al., 1998, Naber and Witter, 1998, McKenna and Vertes,

2001, O'Mara et al., 2001, Francisco E. Olucha-Bordonau, 2015, Natalie L.M. Cappaert, 2015, Paxinos, 2015). Fibril infusions centered in CA2/3 led to dense Lewy-like pathology in cornu ammonis and the dentate gyrus of the hippocampal formation and layer II of the entorhinal cortex, demonstrating successful transmission of alpha-synucleinopathy through the perforant path, consistent with previous work (Sacino et al., 2014a). Additional Lewy-like pathology was detected in the ectorhinal/perirhinal cortex, which projects into the hippocampus and is an important gateway for the spread of Lewy pathology from the mesocortex into neocortex in Braak stages V and VI (Braak et al., 2003a, Braak et al., 2003b). Extrahippocampal pSer129^{+} inclusions were also found in the lateral septum (dorsal and ventral divisions) and amygdaloid complex (central, cortical, and basal nuclei). PBS injections did not result in any alpha-synucleinopathy (Figure 19).

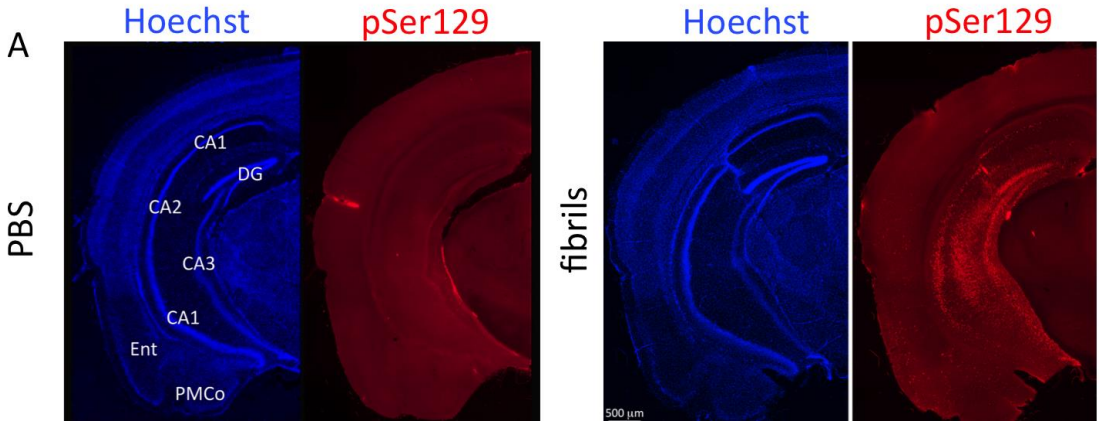

B

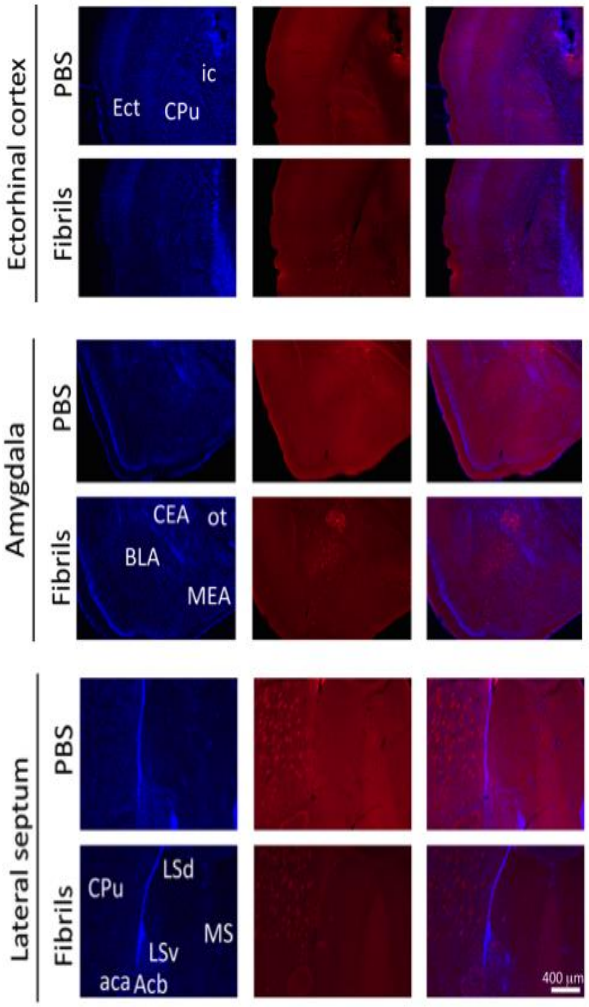

Fig. 19. Transmission of alpha-synucleinopathy after infusions of waterbath-sonicated fibrils into CA2/3 of the hippocampus. Two month-old mice were unilaterally infused with alpha-synuclein fibrils (5 µg) or an equal volume of phosphate-buffered saline (PBS) into CA2/CA3. Fibrils were sonicated for 1 h in a waterbath prior to infusion. Three months later, coronal brain sections were collected. (A) Shown are images of pSer129 and Hoechst staining in the hippocampus and entorhinal cortex in PBS and fibril-infused animals. (B-D) The pathology was transmitted into extrahippocampal regions such as the ectorhinal cortex, amygdala, accumbens, and lateral septum. All groups were stained in parallel and captured at the same exposure and intensity scaling. All abbreviations are listed in **Table 5.**

Most perinuclear pSer129^{+} inclusions are formed within cells expressing the neuronal nuclear marker NeuN

Next we characterized the nature of the inclusions formed three months following fibril injections into CA2/3. We confirmed that most perinuclear inclusions were wrapped around NeuN^{+} nuclei (Figure 20A). This was verified with confocal microscopy (Figure 20B). The morphology of these inclusions is similar to that exhibited by some Lewy bodies in mouse and human tissue (Osterberg et al., 2015).

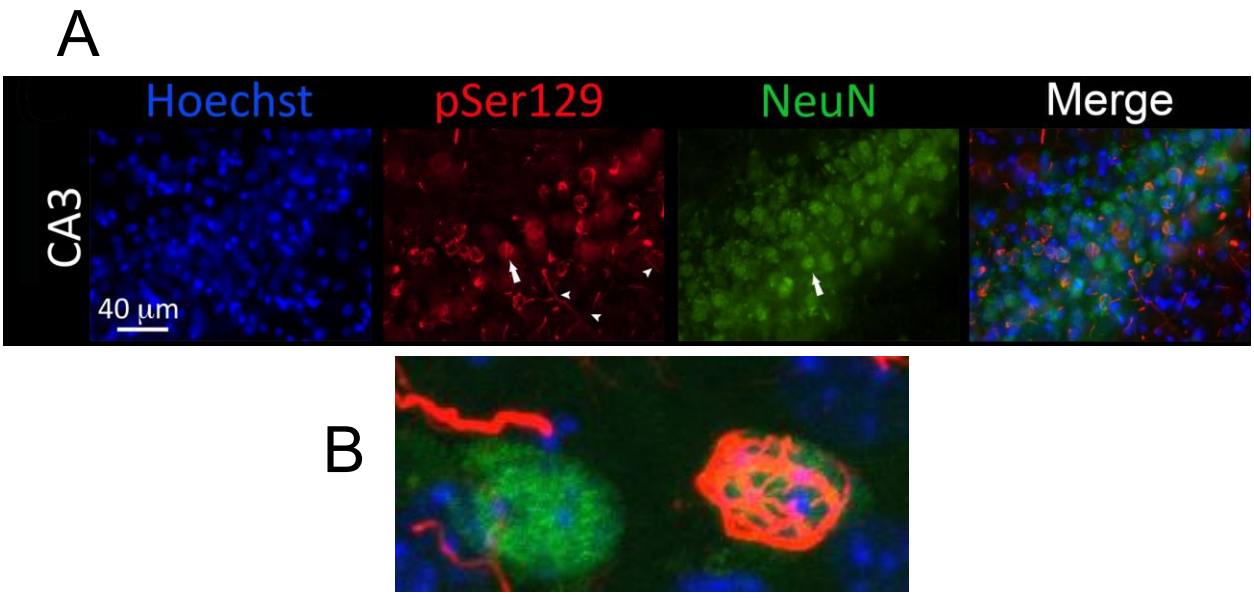

Fig. 20. The development of dense perinuclear and neuritic inclusions following fibril infusions. (A) Two month-old mice were unilaterally infused with 1 h waterbath-sonicated alpha-synuclein fibrils (5 µg) or an equal volume of phosphate-buffered saline (PBS) into the CA2/3 of hippocampus. Three months later, sagittal brain sections were collected and stained with antibodies against pSer129 and the neuronal

nuclear marker NeuN. Hoechst-labeled nuclei are shown in blue. The pSer129^{+} inclusions were perinuclear or found in processes. Arrows point to pSer129^{+} somal inclusions and arrowheads to neuritic inclusions. (B) Confocal microscopy confirmed the perinuclear localization of pSer129^{+} structures.

Preadsorption of pSer129 antibodies with pSer129 blocking peptides lead to loss of immunoreactivity

To confirm the specificity of the primary antibody raised against phosphorylated alpha-synuclein, we performed two sets of control experiments. First, we preadsorbed the primary antibody with 10-fold excess pSer129 blocking peptide. Sections were then exposed to free or antigen-bound primary antibodies. The preadsorption control was performed on the polyclonal pSer129 antibody because preadsorption controls on monoclonal antibodies always lead to loss of labeling regardless of which proteins they bind in tissue (Saper, 2005). Preincubation of polyclonal pSer129 antibodies with pSer129 blocking peptide led to dramatic loss of immunoreactivity relative to adjacent sections from the same animal that were exposed to unbound primary antibodies (Figure 21). These findings support the specificity of the primary antibody.

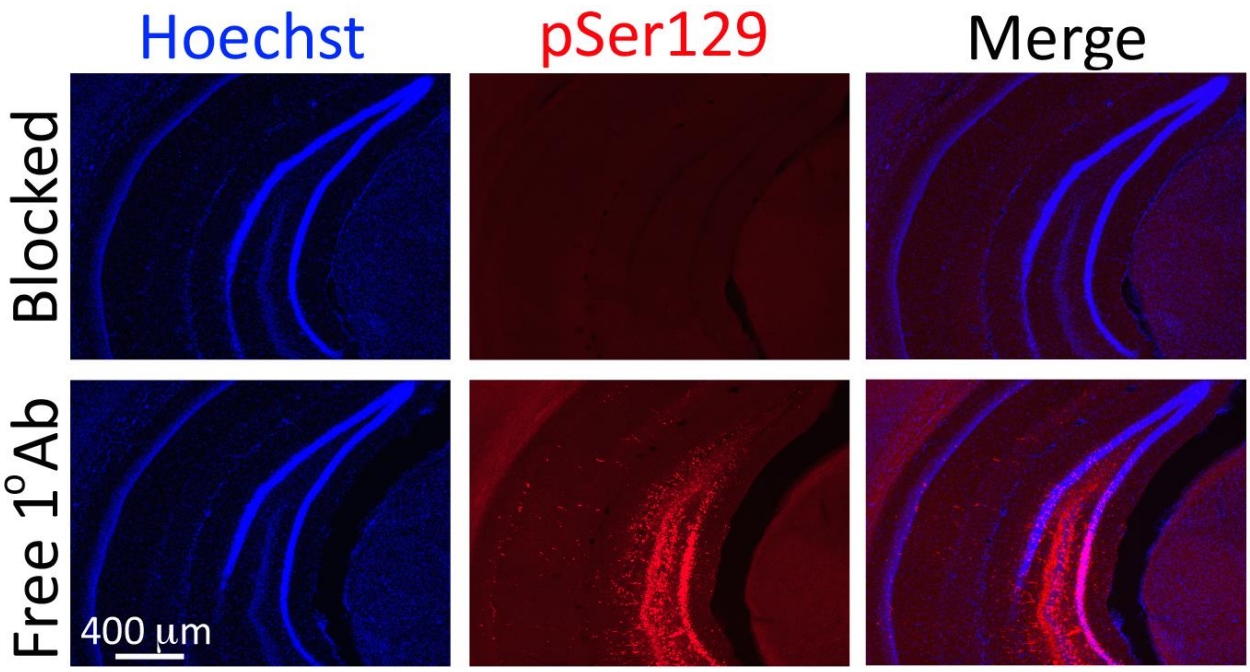

Fig. 21. Preadsorption of pSer129 antibodies with blocking peptide led to loss of immunoreactivity. Two month-old mice were unilaterally infused with 1 h waterbath-sonicated alpha-synuclein fibrils (5 µg) or an equal volume of phosphate-buffered saline (PBS) into the CA2/3 of hippocampus. Three months later, sagittal brain sections were collected. Polyclonal antibodies against pSer129 were preadsorbed with pSer129 blocking peptide or incubated alone for 24 h prior to application to tissue. Hoechst-labeled nuclei are shown in blue. Shown are adjacent sections from the same fibril-infused animal, captured with equivalent exposures and intensity scaling.

The second control for antibody specificity was to use two independent antibodies against the same phosphorylation site, but with slightly different epitope sizes (for the sequence of the immunogens, please see antibody **Table 3**). These polyclonal and monoclonal pSer129 antibodies led to the same patterns of staining, as expected (Figure 22). The staining overlap was nearly complete, similar to what we reported previously (Mason et al., 2016). However, the colocalization was not 100%, likely due to heterogeneity of the antibody clones, competition between the two types of IgG clones, or exposure of slightly distinct epitopes within aggregated and misfolded protein clumps.

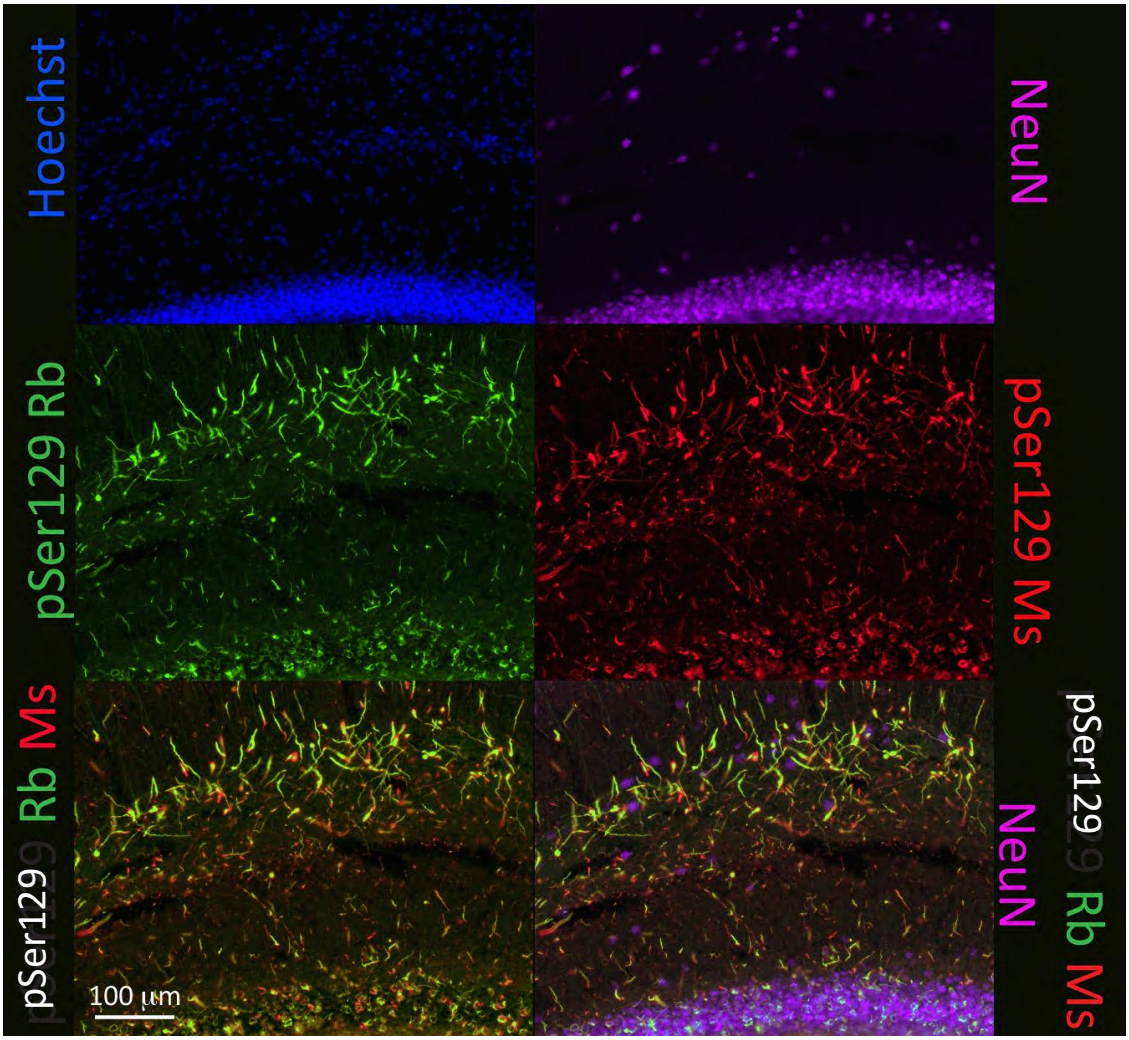

Fig. 22. Overlap of polyclonal and monoclonal pSer129 staining patterns. Mice were infused in CA2/3 with PBS or 5 µg alpha-synuclein fibrils. Sagittal brain sections were collected three months later. Shown are dense inclusions in the hippocampus, labeled with polyclonal pSer129 antibodies (green) and monoclonal pSer129 antibodies (red). The NeuN neuronal nuclear immunostain (purple) and Hoechst nuclear stain (blue) are also shown to delineate cytoarchitectonic boundaries and identify neuronal elements. Polyclonal pSer129 antibodies and monoclonal pSer129 antibodies were applied simultaneously in this experiment, followed by the appropriate secondary antibodies.

The proteasomal degradation tag ubiquitin is present in some, but not all pSer129^{+} structures

Most, but not all Lewy bodies and Lewy neurites contain ubiquitin (Kuzuhara et al., 1988, Spillantini et al., 1998b). Indeed, prior to general availability of alpha-synuclein antibodies, investigators employed ubiquitin immunostaining to demark Lewy pathology. For example, the neuritic pathology in CA2/CA3 in Lewy body disease is densely immunoreactive for ubiquitin (Dickson et al., 1991, Dickson et al., 1994, Mattila et al., 1999). Therefore, we investigated whether the pSer129^{+} inclusions formed in our model are also Lewy-like in nature. Mice were sacrificed 3 months after fibril infusions in the CA2/3. Sagittal sections were collected and immunostained for K48-linked ubiquitin and pSer129. Cellular proteins conjugated to K48-linked ubiquitin chains are specifically targeted for proteasomal degradation (Nathan et al., 2013). Alpha-synuclein is thought to clog the proteasome and inhibit its proteolytic function, leading to a buildup of misfolded and aggregated proteins that are tagged with ubiquitin (Cuervo et al., 2004, Ebrahimi-Fakhari et al., 2011a). Some, but not all pSer129^{+} structures were colocalized with the ubiquitin marker of protein aggregates, as expected based on Spillantini's classic work that ubiquitin antibodies label fewer Lewy bodies than alpha-synuclein antibodies (Kuzuhara et al., 1988, Spillantini et al., 1998b). (Figure 23). These findings are also consistent with the work of Osterberg et al. showing pSer129^{+} inclusions at progressive stages of maturity, with only mature inclusions bearing hallmarks of Lewy pathology (Osterberg et al., 2015).

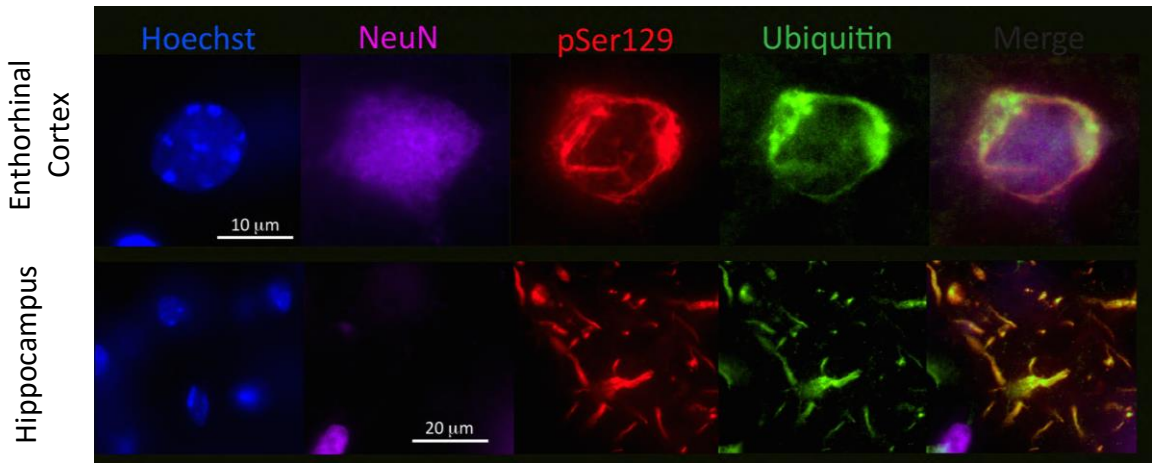

Fig. 23. pSer129^{+} inclusions harbor the ubiquitin tag for proteasomal degradation. Mice were infused in the CA2/3 with PBS or 5 µg alpha-synuclein fibrils. Brain sections were collected three months later. Shown are somal and neuritic inclusions in the hippocampus and entorhinal cortex, respectively. Inclusions were labeled with pSer129 (red) and ubiquitin (green) antibodies. The NeuN neuronal nuclear immunostain (purple) and Hoechst nuclear stain (blue) were employed to show cytoarchitectonic boundaries and identify neuronal structures. Some, but not all pSer129^{+} structures were ubiquitin^{+}.

Thioflavin-S reactive amyloid structures are present at the infusion site in fibril-treated animals

Lewy bodies are known to harbor proteins with β-sheet structures that form a dense core of amyloid (Gallea and Celej, 2014). Therefore, we stained PBS or fibril-infused animals with the Thioflavin S amyloid stain. Our experiments demonstrated the presence of Thioflavin S^{+} structures at the infusion site that were completely absent in PBS control mice (Figure 24). High-magnification images of the Thioflavin^{+} structures revealed a similar morphology as perinuclear and neuritic pSer129^{+} inclusions. However, as in our previous study, extrahippocampal regions did not develop these dense Thioflavin^{+} structures. This suggests that inclusions at afferent sites have not formed mature amyloid structures by three months post-infusion.

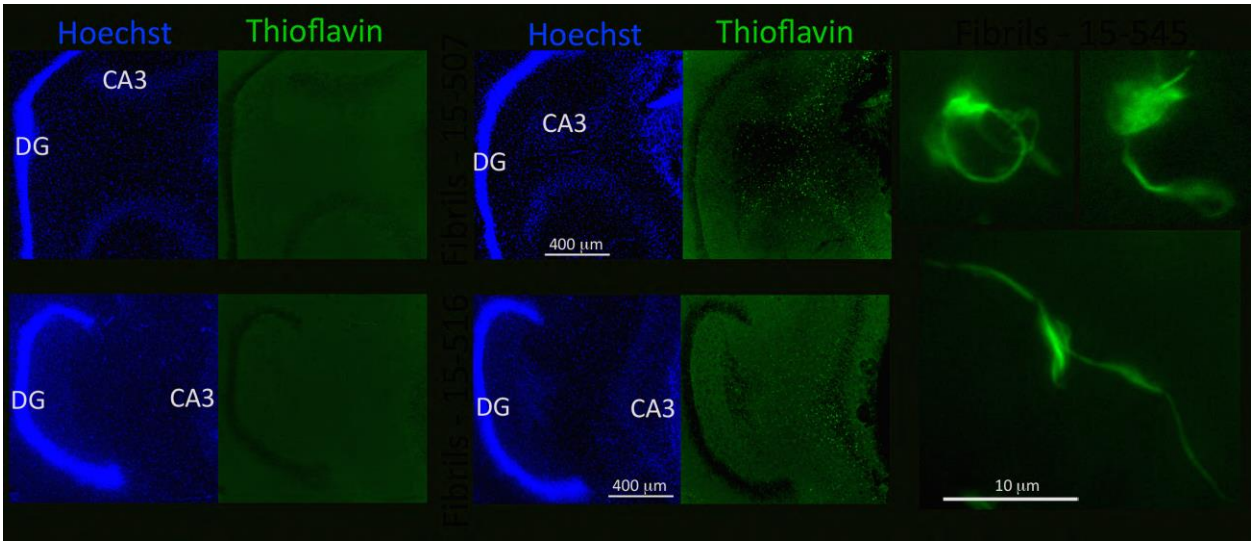

Fig. 24. Amyloid structures at the fibril infusion site. Mice were infused in CA2/3 with PBS or 5 µg alpha-synuclein fibrils. Brain sections were collected three months later. Shown are Thioflavin S^+ structures (green) at the infusion site that were absent in PBS control mice. The Hoechst nuclear stain (blue) was employed to delineate cytoarchitectonic boundaries. High-magnification views of the Thioflavin S^+ structures revealed a similar morphology as the perinuclear and neuritic $pSer129^+$ inclusions. Photos were captured from fibril and PBS-treated animals at the same exposures and intensity scaling.

Alpha-synucleinopathy spreads through neuroanatomical circuits following infusion of fibrils into CA2/3

In order to investigate the pattern of transmission of alpha-synucleinopathy following infusion of fibrils into CA2/3, we investigated the topographical distribution of inclusions across the entire brain. All fibril-infused animals exhibited dense inclusions that were immunopositive for pathologically phosphorylated alpha-synuclein. As mentioned above, major afferents of the

hippocampal formation include the septum, diagonal band, and entorhinal cortex, whereas minor projections arise in the supramammillary nucleus, locus coeruleus, raphe, and ventral tegmental area (Segal, 1977, Swanson and Cowan, 1977, Swanson, 1982, Vertes, 1992, Conde et al., 1995, Yoshida and Oka, 1995, Gasbarri et al., 1997, Risold and Swanson, 1997, Acsady et al., 1998, Naber and Witter, 1998, McKenna and Vertes, 2001, O'Mara et al., 2001, Francisco E. Olucha-Bordonau, 2015, Natalie L.M. Cappaert, 2015, Paxinos, 2015). Perinuclear or somal inclusions appeared in the pyramidal cell layer of Ammon's horn and the granule cell layer of the dentate gyrus after fibril treatment (Fig 25 A and B). In addition, neuritic inclusions were found in the stratum radiatum of CA3 and in the polymorph layer of the dentate gyrus, likely labeling the mossy fiber pathway, because granule cells of the dentate gyrus send unmyelinated axons along the mossy fiber pathway to the CA3 subregion of the hippocampus (Acsady et al., 1998). Neuritic and perinuclear pSer129^{+} pathology following CA2/CA3 injections also extended into the subiculum and presubiculum. Alpha-synucleinopathy was transmitted along the dorsoventral axis of the hippocampus, with some interindividual variability in the extent of spread, possibly due to slight differences in the placement of the infusate in this highly laminar structure.

In fibril-infused animals, there was evidence of extra-hippocampal pathology in various amygdalar subnuclei, including the posteromedial cortical amygdala, the amygdalohippocampal area, and the basal amygdaloid nuclei. Dense pathology was observed in the amygdalopirifom transition area. Some animals exhibited sparse pathology in the dorsal nucleus of the endopiriform claustrum, the lateral septum, and the rostral extent of the nucleus accumbens. The pathology in the accumbens was found in the processes and not cell bodies, suggestive of some, albeit limited anterograde transmission, consistent with the known projections of the

hippocampus to the accumbens (Floresco et al., 2001). Very little, if any pathology was evident in the medial septum, although this is a major source of hippocampal afferents (Acsady et al., 1998, Natalie L.M. Cappaert, 2015, Paxinos, 2015). These findings strongly suggest some degree of selective vulnerability to alpha-synucleinopathy, as has been discussed extensively in the human literature (Braak et al., 2003a). According to Braak's hypothesis, unmyelinated axons require higher levels of energy to maintain axonal function compared to myelinated axons. High energy demands could result in oxidative stress at the level of the mitochondrion, which would be expected to increase neuron vulnerability to alpha-synuclein aggregation in PD (Braak et al., 2003a, Braak et al., 2003b).

Had widespread diffusion of fibrils through the extracellular space been solely responsible for the emergence of Lewy-like pathology, we would have expected to see inclusions in all areas close the lateral ventricle by the site of infusion, such as the caudoputamen and thalamus, but this was not the case (Figure 25A, B, D-Q).

In order to better understand the neuroanatomy of projections terminating at the site of fibril infusion, we infused tracers at the same CA2/CA3 stereotaxic coordinates. For example, we injected animals with biotinylated dextran amines (BDA) and collected the brains 7d post-infusion for exposure to a streptavidin-linked fluorophore. The 10kDa dextran amines travel preferentially in the anterograde directions, although they are not exclusively transported only in one direction. Following 10 kDa dextran amine injections, there was dense retrograde labeling in layer II of the entorhinal cortex, as would be expected from the dense projections of the perforant pathway, which originates in layer II of the entorhinal cortex and terminates in the dentate gyrus

and CA3, among other hippocampal subregions (Acsady et al., 1998, Baks-Te Bulte et al., 2005, Natalie L.M. Cappaert, 2015, Paxinos, 2015). In addition to the retrograde labeling of somata, there was also dense anterograde BDA labeling of fibers in the deeper layers of the entorhinal cortex (Figure 25 C, see white arrow). The existence of somal pSer129^{+} inclusions in the superficial layers of the entorhinal cortex and the relative scarcity of pSer129^{+} fiber labeling in the deeper layers may suggest preferential retrograde transmission of alpha-synucleinopathy in these brain regions. In addition, the entorhinal pathology was mainly located in the ventromedial part of the entorhinal cortex in our model, which suggests retrograde labeling from the ventral hippocampus based on previous anatomical work (Fyhn et al., 2004). Only sparse, if any, pathology was detected in the dorsal entorhinal cortex in some animals. Tract-tracing studies using biotinylated dextran amines have demonstrated that the dorsolateral entorhinal cortex projects to the dorsal hippocampus whereas the ventromedial portion of the entorhinal cortex projects to the ventral hippocampus (Fyhn et al., 2004). Considered together with the pattern of pSer129^{+} inclusions in the present study, these findings suggest that the ventromedial entorhinal cortex develops Lewy-like pathology due to anterograde projections to the ventral parts of the hippocampus, which exhibited dense inclusions in virtually all fibril-infused animals. These findings support Braak's hypothesis that most of the Lewy pathology is transmitted retrogradely in humans. However, the clinical studies by Braak cannot answer this question as definitively as our rodent work, because the pathology is initiated in multiple locations in humans, whereas in mice the pathology was initiated in the hippocampus (Braak et al., 2003a, Braak et al., 2003b). Understanding the direction of the transmission of the pathology has clinical implications, as it might shed light on the mechanisms underlying inclusion spread and identify targets for novel therapies. In this context, retrograde and anterograde transport mechanisms along the axon

involve distinct molecular motors, dynein and kinesin, respectively, which may confer selectivity to the direction of travel of alpha-synuclein (Colin et al., 2008).

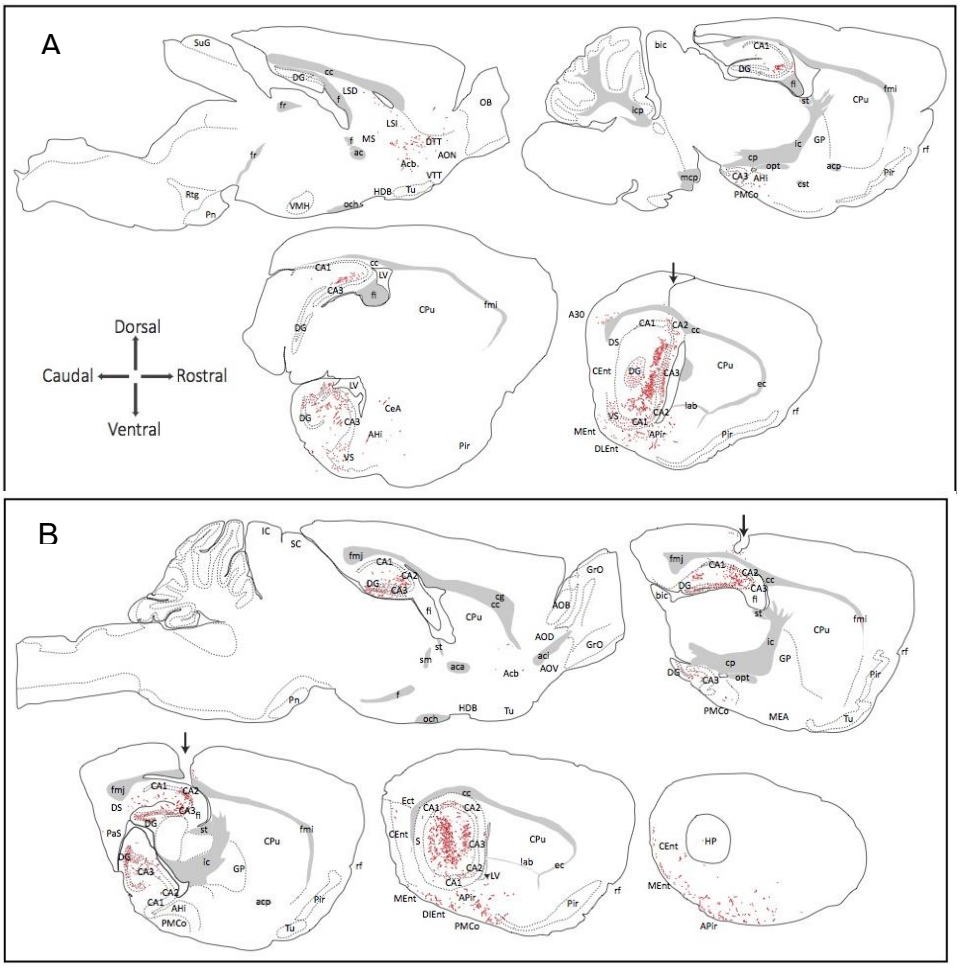
A
B
Dorsal
Caudal
Rostral
Ventral

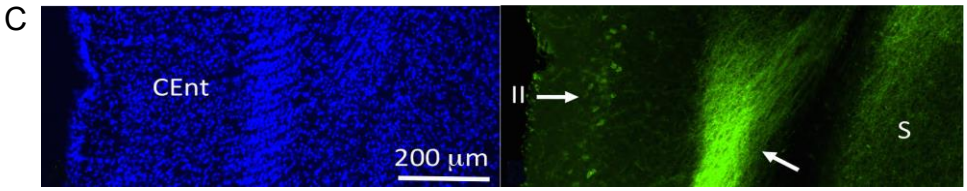
C
CEnt
200 µm
II
S

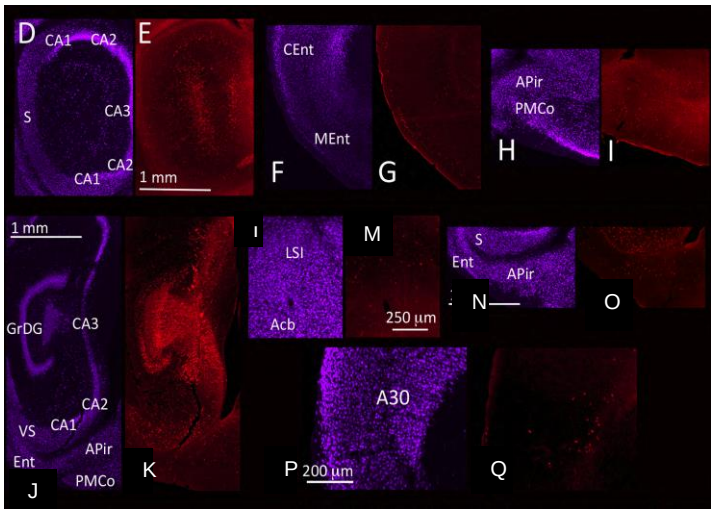
D
E
F
G
H
I
J
K
L
M
N
O
P
Q
1 mm
250 µm
200 µm
CEnt
MEnt
APir
PMCo
LSI
Acb
A30
GrDG
CA1
CA2
CA3
VS
Ent

Fig. 25. Alpha-synucleinopathy is transmitted through neuroanatomical circuits following infusion of fibrils into CA2/3. Two month-old CD1 mice were unilaterally infused with alpha-synuclein fibrils (5 μg) into CA2/3 of hippocampus. Three months later, sagittal brain sections were collected and immunostained for pathologically phosphorylated alpha-synuclein (pSer129; red). Large, high-quality microscopic photomontages of pSer129 and nuclear labeling were stitched together and viewed with Adobe Illustrator software on a tablet. (A and B) Sagittal schematics of only obvious and clearly visible brain cytoarchitectonics (solid lines), myelinated fiber bundles (gray shading), $pSer129^{+}$ neurites (red flourishes), and $pSer129^{+}$ somal inclusions (red dots) were then traced with the pencil and paintbrush tools. All abbreviations are listed in **Table 5.** (C) Dense retrograde labeling in layer II, as would be expected from the dense projections of the perforant pathway, and anterograde labeling in the deep layers of the entorhinal cortex following injections of 10 kDa biotinylated dextran amines (BDA) in CA2/3. BDA labeling is shown in green and Hoechst nuclear staining in blue. (D-Q) Examples of stitched photomontages of pSer129 immunostaining and DRAQ5 nuclear labeling following fibril infusions in CA2/CA3. These montages were used to generate the schematics shown in panels A and B.

Commissural spread of alpha-synucleinopathy

Early Parkinson's disease is characterized by unilateral onset of clinical symptoms. However, the reasons underlying the asymmetric nature of the disorder are poorly understood (Djaldetti et al., 2006). One hypothesis is that there is unilateral exposure to a disease-precipitating insult, and that the pathology is then transmitted along commissural fibers to the contralateral side only after a delay. However, it is not yet known if Lewy pathology can travel through commissural networks. In this study, we sought to investigate the commissural spread of alpha-synucleinopathy through neuroanatomical circuits following unilateral infusions of alpha-synuclein fibrils into CA2/3. As mentioned above, hippocampal commissural projections arise largely from excitatory mossy cells in the hilar region of the dentate and from CA3 pyramidal cells (Swanson et al., 1980, Zappone and Sloviter, 2001). FluoroGold tract-tracing studies reveal that retrograde tracer injections in the medial hippocampus (that encompass the dentate gyrus) elicit contralateral FluoroGold labeling that is exclusively in dentate hilar neurons, whereas larger injections (that also involve CA3 and CA1) lead to contralateral labeling in CA3 as well as

the hilum (Zappone and Sloviter, 2001). In the present study, mice were unilaterally infused with alpha-synuclein fibrils or PBS into CA2/3 of hippocampus and sacrificed after three months. Immunostaining for pathologically phosphorylated alpha-synuclein in coronal brain sections revealed the formation of somal inclusions in contralateral CA3 pyramidal cells as well as neuritic inclusions in the stratum oriens, lucidum, radiatum, and lacunosum moleculare (Figure 26). However, dentate hilar neurons only developed sparse, if any pathology, which again suggests some degree of selective vulnerability to alpha-synucleinopathy. pSer129^{+} structures were completely absent in PBS control mice. This spread of pathology through commissural projections in our model suggests that similar neuroanatomical spread may explain the presence of Lewy pathology in CA3 in patients. Had non-specific and widespread diffusion of fibrils through the extracellular space been responsible for the emergence of Lewy-like pathology in the contralateral hippocampus, we would have expected to see labeling in other contralateral hippocampal subfields in addition to CA3.

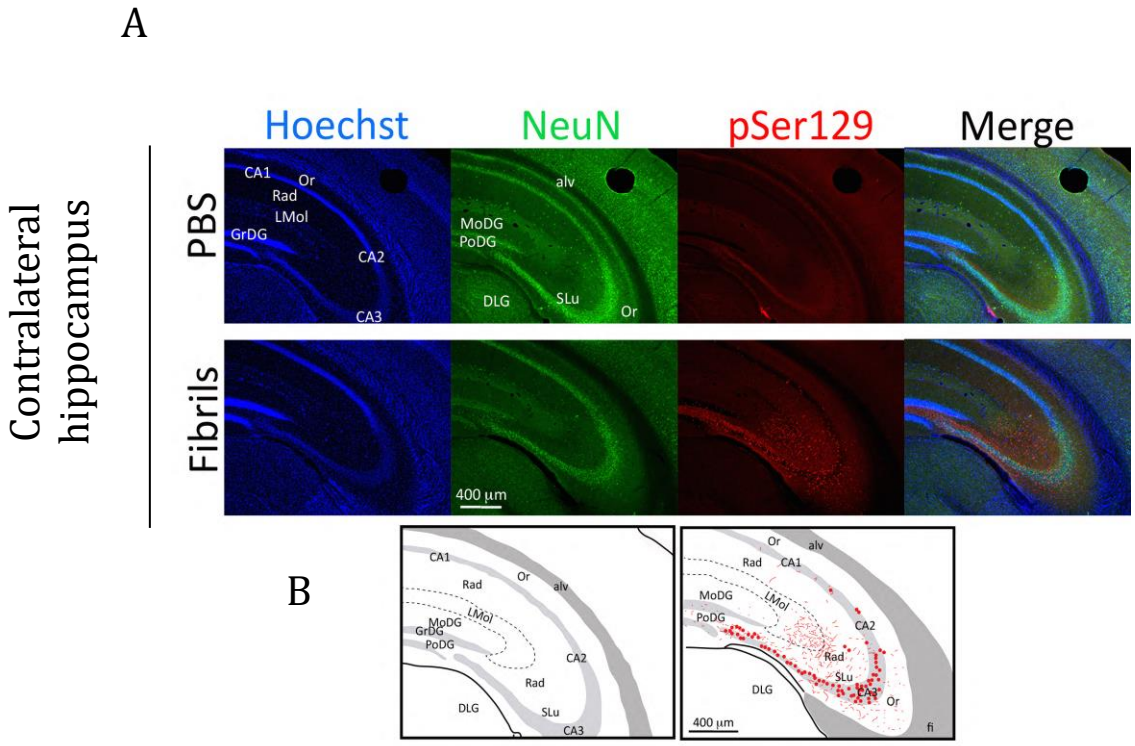

Fig. 26. Commissural spread of alpha-synucleinopathy through neuroanatomical circuits following infusion of fibrils into CA2/3. Two month-old CD1 mice were unilaterally infused with alpha-synuclein fibrils (5 µg) or PBS into CA2/3 of hippocampus. Three months later, coronal brain sections were collected and immunostained for pathologically phosphorylated alpha-synuclein (pSer129; red). The Hoechst neuronal stain (blue) was used to show cytoarchitectonic boundaries. (A) Shown are images of pSer129 and Hoechst staining in the contralateral hippocampus in PBS and fibril-infused animals. Mice infused with fibrils exhibited alpha-synucleinopathy in CA3 of the contralateral hippocampus. pSer129^{+} structures were absent in PBS control mice. All groups were stained in parallel and captured at the same exposure and intensity scaling. (B) High-quality microscopic photomontages of pSer129 and nuclear labeling were stitched together and viewed with Adobe Illustrator software on a tablet. Coronal schematics of only obvious and clearly visible brain cytoarchitectonics (solid lines), myelinated fiber bundles (gray shading), pSer129^{+} neurites (red flourishes), and pSer129^{+} somal inclusions (red dots) were then traced with the pencil and paintbrush tools. Immunostaining for pathologically phosphorylated alpha-synuclein revealed formation of somal inclusions in contralateral CA3 pyramidal cells as well as neuritic inclusions in the stratum oriens, lucidum, radiatum and lacunosum moleculare. Dentate hilar neurons only develop sparse, if any pathology, suggesting some degree of selective vulnerability. All abbreviations are listed in **Table 5.**

pSer129^{+} inclusions were formed in structures known to harbor anatomical connections with the hippocampus and were dramatically higher in bilateral fibril-injected mice compared to PBS-treated animals

Previous studies either did not report any memory deficits following unilateral hippocampal injection of fibrils or never measured cognitive function (Luk et al., 2012a, Sacino et al., 2013). Thus, we sought to develop a model of bilateral hippocampal alpha-synucleinopathy to increase the potential for behavioral impairments and to avoid any possible compensatory effects in the unlesioned hemisphere. Similar to unilateral injections, mice that were bilaterally infused with fibrils into CA2/3 exhibited dense alpha-synucleinopathy in the hippocampal formation and subiculum. Extrahippocampal pSer129^{+} inclusions were also located in the superficial layers of the entorhinal cortex, the lateral septum, the nucleus accumbens, and in many amygdaloid subnuclei, as with unilateral injections (see above). No inclusions were formed in the medial septum. Thus, pSer129^{+} inclusions were again formed in some, but not all structures known to harbor anatomical connections with the hippocampus (Segal, 1977, Swanson and Cowan, 1977, Swanson, 1982, Vertes, 1992, Conde et al., 1995, Yoshida and Oka, 1995, Gasbarri et al., 1997, Risold and Swanson, 1997, Acsady et al., 1998, Naber and Witter, 1998, McKenna and Vertes, 2001, O'Mara et al., 2001, Francisco E. Olucha-Bordonau, 2015, Natalie L.M. Cappaert, 2015, Paxinos, 2015). Bilateral PBS infusions did not result in any alpha-synucleinopathy (Fig 27A). Next, a blinded analysis revealed that the number of pSer129^{+} inclusions in CA1, CA2, CA3, dentate gyrus, subiculum, and the amygdala (posteromedial cortical amygdala) of fibril-treated mice were dramatically higher than PBS-infused mice (Figure 27B). However, there was great variability in the number of inclusions, which we leveraged with a statistical correlation analysis, as described further below.

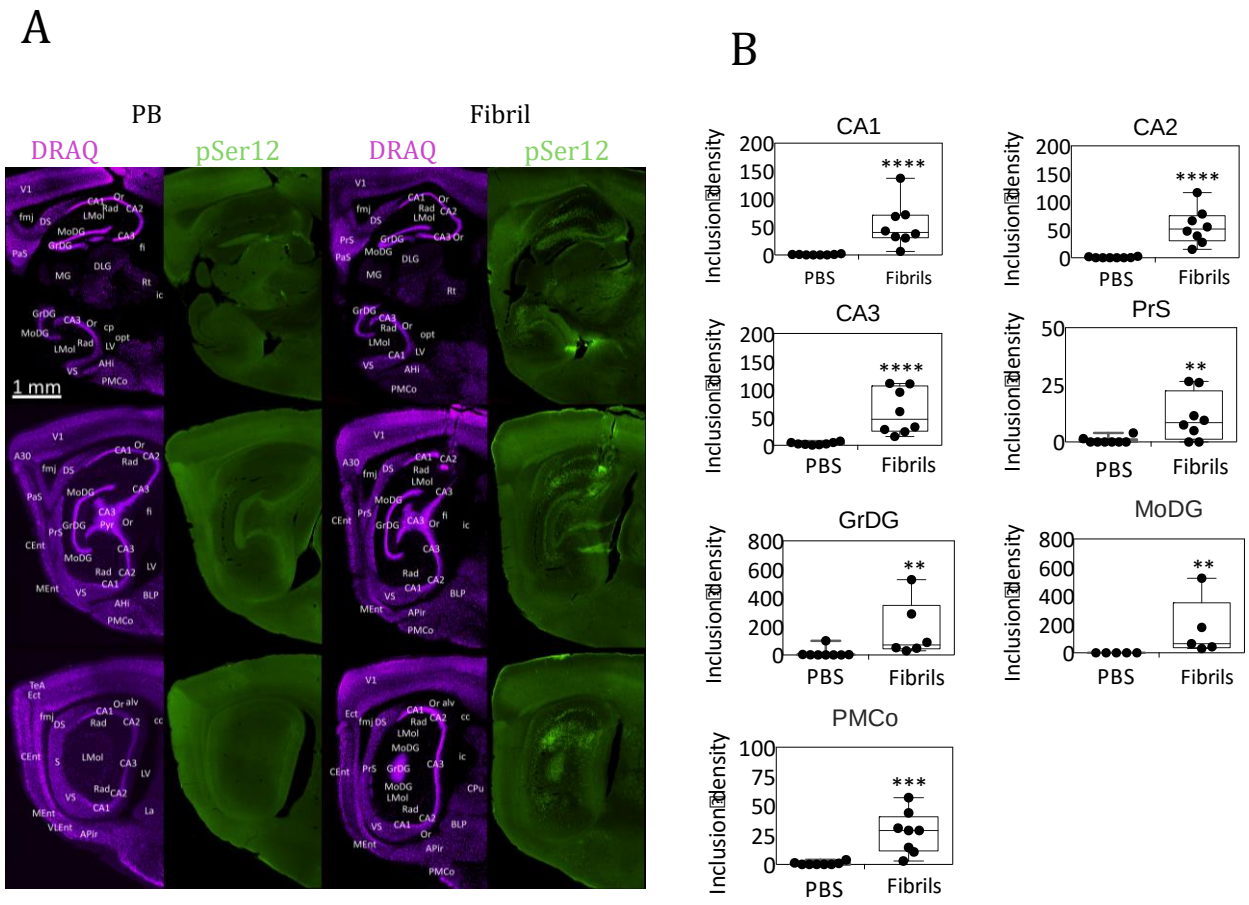

Fig. 27. pSer129^{+} inclusion counts are dramatically higher in bilateral fibril-injected mice compared to PBS-treated animals. (A) Two month-old CD1 mice were bilaterally infused with alpha-synuclein fibrils (5 µg) or PBS into CA2/3 of hippocampus. Three months later, sagittal brain sections were collected and immunostained for pathologically phosphorylated alpha-synuclein (pSer129; green). The DRAQ5 neuronal stain (purple) was used to show cytoarchitectonic boundaries. Mice infused with fibrils into CA2/3 of both hemispheres exhibited dense alpha-synucleinopathy in the hippocampal formation and subiculum. Extrahippocampal pSer129^{+} inclusions were also located in the superficial layers of the entorhinal cortex, the lateral septum, the nucleus accumbens, and in many amygdaloid subnuclei. pSer129^{+} structures were absent in PBS control mice. (B) pSer129^{+} inclusion numbers were counted manually by a blinded observer. *p ≤ 0.05, **p ≤ 0.01, ***p ≤ 0.001 vs PBS, Mann-Whitney U, (n = 8-10 mice/group). GrDG: granule cell layer of the dentate gyrus; MoDG: molecular layer of the dentate gyrus; PMCo: posteromedial cortical amygdala; PrS: presubiculum. All other abbreviations are listed in **Table 5.**

Alpha synuclein fibril infusions had no effect on Hoechst^{+} and NeuN^{+} cell numbers

Two studies suggest that there is no neuron loss in CA1, CA2/CA3, the dentate gyrus, or the subiculum in Parkinson's disease (Ince et al., 1991, Joelving et al., 2006). However, there is selective neuron loss in lower presubiculum pyramidal neurons of the hippocampal formation in dementia with Lewy bodies (Harding et al., 2002). Moreover, the amygdala is significantly atrophied in Parkinson's disease and in dementia with Lewy bodies (Cordato et al., 2000). Therefore, we sought to quantify all cells (*i.e.* Hoechst$^+$) and specifically neurons (*i.e.* NeuN$^+$) in the regions with the densest alpha-synucleinopathy, in order to investigate the similarities of this model with the human condition. Mice were bilaterally infused with alpha-synuclein fibrils (5 μg) or PBS into CA2/3 of hippocampus. Three months later, sagittal brain sections were collected and stained for neuronal nuclear marker NeuN and the nuclear marker Hoechst. NeuN$^+$ and Hoechst$^+$ cells were counted by a blinded observer. Alpha-synuclein infusions had no effect on cell numbers in this model, including in the presubiculum (Figure 28). Thus, this model does not recapitulate all the features of Lewy body dementia. However, the general lack of cell loss in the hippocampal formation is similar to the absence of cell death in the hippocampal formation in Parkinson's disease.

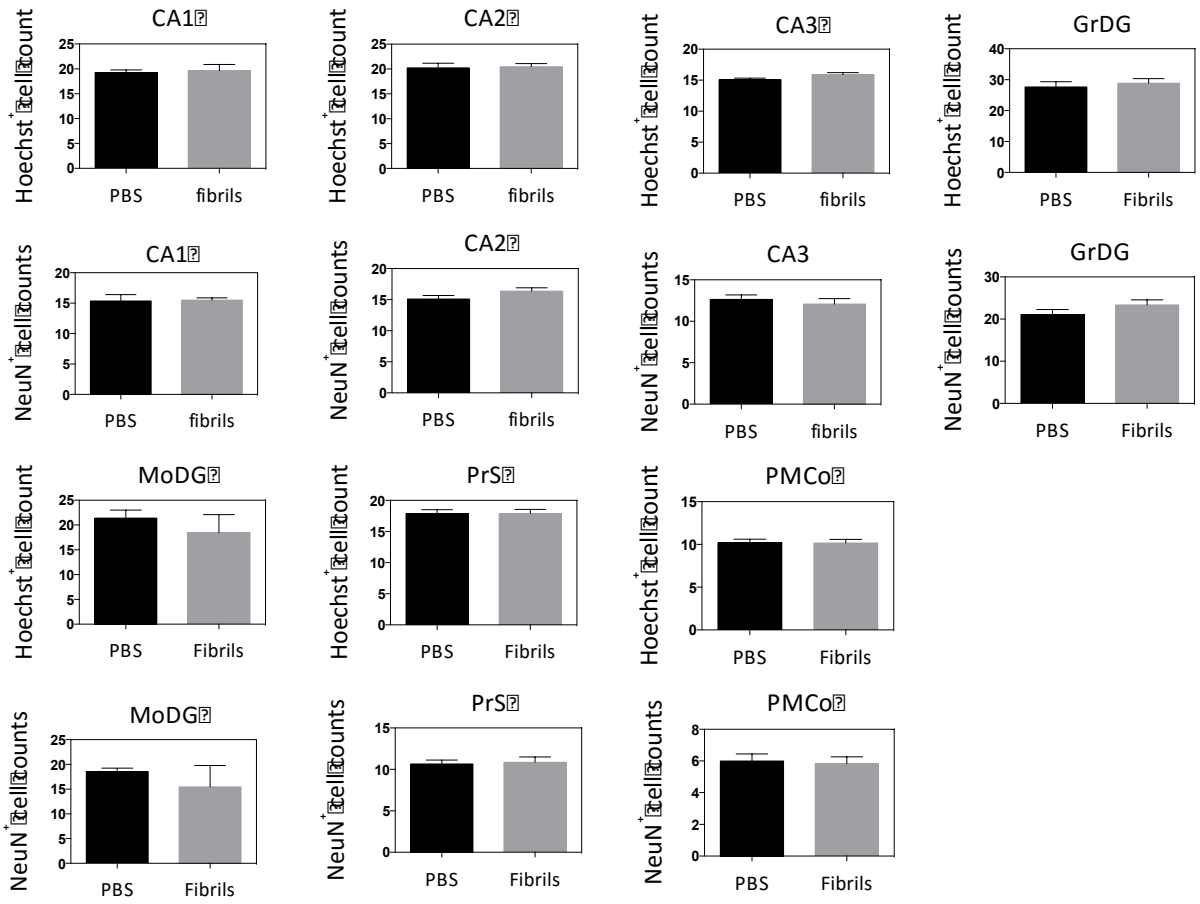

Fig. 28. Alpha-synuclein infusions had no effect on Hoechst$^+$ and NeuN$^+$ cell numbers. Two month-old CD1 mice were bilaterally infused with alpha-synuclein fibrils (5 μg) or PBS into CA2/3 of hippocampus. Three months later, sagittal brain sections were collected and labeled with NeuN antibodies and Hoechst. NeuN$^+$ and Hoechst+ cells were counted manually by a blinded observer. Alpha-synuclein infusions had no effect on the number of Hoechst$^+$ and NeuN$^+$ cells in any of the examined structures. (n = 8-10 mice/group). GrDG: granule cell layer of the dentate gyrus; MoDG: molecular layer of the dentate gyrus; PMCo: posteromedial cortical amygdala; PrS: presubiculum.

Alpha-synucleinopathy is correlated with behavioral deficits

Approximately 80% of Parkinson's disease patients develop dementia (Aarsland et al., 2003). Alpha-synucleinopathy in the anterior cingulate gyrus, superior frontal gyrus, temporal and entorhinal cortices, the amygdaloid complex, and hippocampal CA2 are significantly associated with dementia in Parkinson's disease (Ince et al., 1991). Disruptions in memory are also associated with tissue atrophy in CA1, CA3, and the subiculum in Parkinson's disease (Beyer et al., 2013). The amygdala is known to be significantly atrophied in Parkinson's disease and in dementia with Lewy bodies (Cordato et al., 2000). Although one study failed to observe any correlation between CA2 Lewy pathology and the severity or duration of dementia (Harding and Halliday, 2001), others have reported that Lewy neurite density in CA2 is correlated with cognitive deficits (Cordato et al., 2000, Kalaitzakis et al., 2009). As mentioned above, there is no neuron loss in CA1, CA2/CA3, the dentate gyrus, or subiculum in Parkinson's disease (Ince et al., 1991, Joelving et al., 2006). However, there is selective neuron loss in lower presubiculum pyramidal neurons of the hippocampal formation in dementia with Lewy bodies (Harding et al., 2002). We presented data above showing no overt cell loss in any subregion of the hippocampal formation. However, we have also shown robust Lewy-like pathology in the hippocampal formation, which may be linked to the development of cognitive deficits. Thus, we performed the novel object and novel place recognition tests on bilaterally-infused animals.

Olfactory dysfunction is common non-motor symptom in patients with Parkinson disease and has been associated with deposition of Lewy-like inclusions in olfactory structures (Bohnen et al., 2008). Smell impairments in Parkinson's disease are also correlated with loss of dopaminergic

innervation of the hippocampus, amygdala, and dorsal and ventral striatum (Bohnen et al., 2008). Clinical reports suggest that hyposmia in Parkinson's disease is associated with hippocampal pathology (Bohnen et al., 2008). This may reflect the dense neuroanatomical projections of CA1 to olfactory structures (Swanson and Cowan, 1977, van Groen and Wyss, 1990, Brunjes et al., 2005). Moreover, following an emotional event, the amygdala and hippocampus act synergistically in the process of long-term memory consolidation (Richter-Levin and Akirav, 2000, Richter-Levin, 2004). Therefore, Lewy pathology in the hippocampal formation and amygdala may lay the foundation for both the memory and olfactory deficits in patients with Parkinson's disease. The CA1 and CA3 subregions are both implicated in spatial learning and there is evidence that dorsal CA1 is involved in the processing of object recognition (Sauvage et al., 2013). In addition, aging and alpha-synucleinopathy both lead to impaired synaptic plasticity in the dentate gyrus (Gureviciene et al., 2009). Thus, we infused preformed alpha-synuclein fibrils into hippocampal CA2/CA3 in both hemispheres and performed the novel object and novel place recognition tests for learning and memory and buried peanut test for olfactory function two and three months later. Animals with bilateral infusions of alpha-synuclein fibrils did not exhibit significant functional deficits at two or three months post-infusion compared to PBS-infused animals (Fig. 29).

The measurements of Lewy-like inclusion counts in hippocampal subregions and the amygdala suggested a high degree of variability in inclusion counts across animals, likely due to 1) slight differences in the placement of the infusate in a palisade-like structure such as the hippocampus or 2) inter-animal variability in vulnerability. Thus, we investigated if there is a correlation between Lewy-like inclusion counts and behavioral deficits. We discovered a significant

correlation between pSer129^{+} inclusions counts in the dentate gyrus, the region with the densest pathology in following CA2/3 injection of fibrils, and behavioral deficits in mice treated with alpha-synuclein fibrils (Fig. 30). In the present study, the dentate gyrus developed the densest Lewy-pathology, likely via the axons of the mossy fibers that arise in the dentate fascia and terminate at the site of injection, CA2/3 (Acsady et al., 1998, Paxinos, 2015). In Parkinson's disease, CA2 develops greater inclusion numbers than the dentate gyrus (Parkkinen et al., 2008). However, the pathology in CA2 is not the densest in our model. One potential explanation for this observation is that labeling in CA2 would involve anterograde uptake into the somata, which may be less likely than uptake at the level of the synapse, as suggested by our previous work (Mason et al., 2016). In other words, there may be greater uptake of fibrils by axon terminals of mossy fibers projecting from the dentate gyrus to the site of infusion, compared to direct anterograde update of fibrils by CA2 perikarya.

In this study, we also discovered that the Lewy-like pathology in molecular layer of dentate gyrus is positively correlated with the latency to find a buried peanut test, suggesting olfactory dysfunction at 2 months (Fig. 30). Similarly, alpha-synucleinopathy in the granule cell layer and molecular layer of the dentate gyrus was negatively correlated with novel object recognition at 2 months and spatial memory at 3 months, respectively (Fig. 30). In short, our data suggests that alpha-synucleinopathy in the dentate gyrus is statistically correlated with behavioral deficits in the absence of frank neurodegeneration at these sites. Some of the effects may be evident only at 2 months and not at 3 months because the animals have grown accustomed to the testing paradigm (*i.e.* testing fatigue) or some of the pathology is cleared up with the passage of time post-infusion. This hypothesis could be readily tested with a temporal kinetic analysis of Lewy-

like pathology over the course of 1, 2, 3, and 6 months post-infusion in future studies. Furthermore, by infusing human alpha-synuclein into the mouse brain, we could determine if the fibrils are cleared over time by using a human-specific alpha-synuclein antibody. Despite these limitations, our study is the first to exhibit significant correlation between $pSer129^{+}$ inclusions in the dentate gyrus and functional deficits following bilateral infusion of fibrils. However, these observations are correlative, as we do not have evidence that the Lewy pathology is actually causing functional deficits. If the fibrils were eliciting functional deficits, we would have expected significant effects in Figure 29. It remains possible that inter-animal differences in vulnerability to Lewy pathology (rather than differences in Lewy pathology *per se*) may underlie differences in behavioral performances in the memory and olfactory tests. For example, one might speculate that animals that are genetically predisposed to be more physically fit may be less vulnerable to Lewy-like pathology and may also be superior performers on cognitive and olfactory tasks. For example, studies in mice have shown both intra- and inter-strain differences in running speed (Billat et al., 2005). This could explain the correlation between Lewy-like pathology and the behavioral tests in the absence of significant effects of the fibrils in Figure 29. This discussion reflects the important differences between associations that are merely correlative and those that are established as causal links. If our results can be translated to humans, the data we have collected suggest that other pathologies besides the presence of Lewy structures *per se* may underlie dementia in the human condition. Alternatively, the presence of Lewy structures in the neocortex may exert a greater influence on cognitive symptoms than Lewy pathology in the allocortical hippocampus. Yet another possibility is that degeneration of presubicular neurons is a prerequisite for the emergence of dementia symptoms, a feature of dementia with Lewy bodies

that we failed to recapitulate (Harding et al., 2002). Neurodegeneration may have become evident in our model had our animals lived longer, as suggested by some previous fibril studies (Luk et al., 2012a, Paumier et al., 2015).

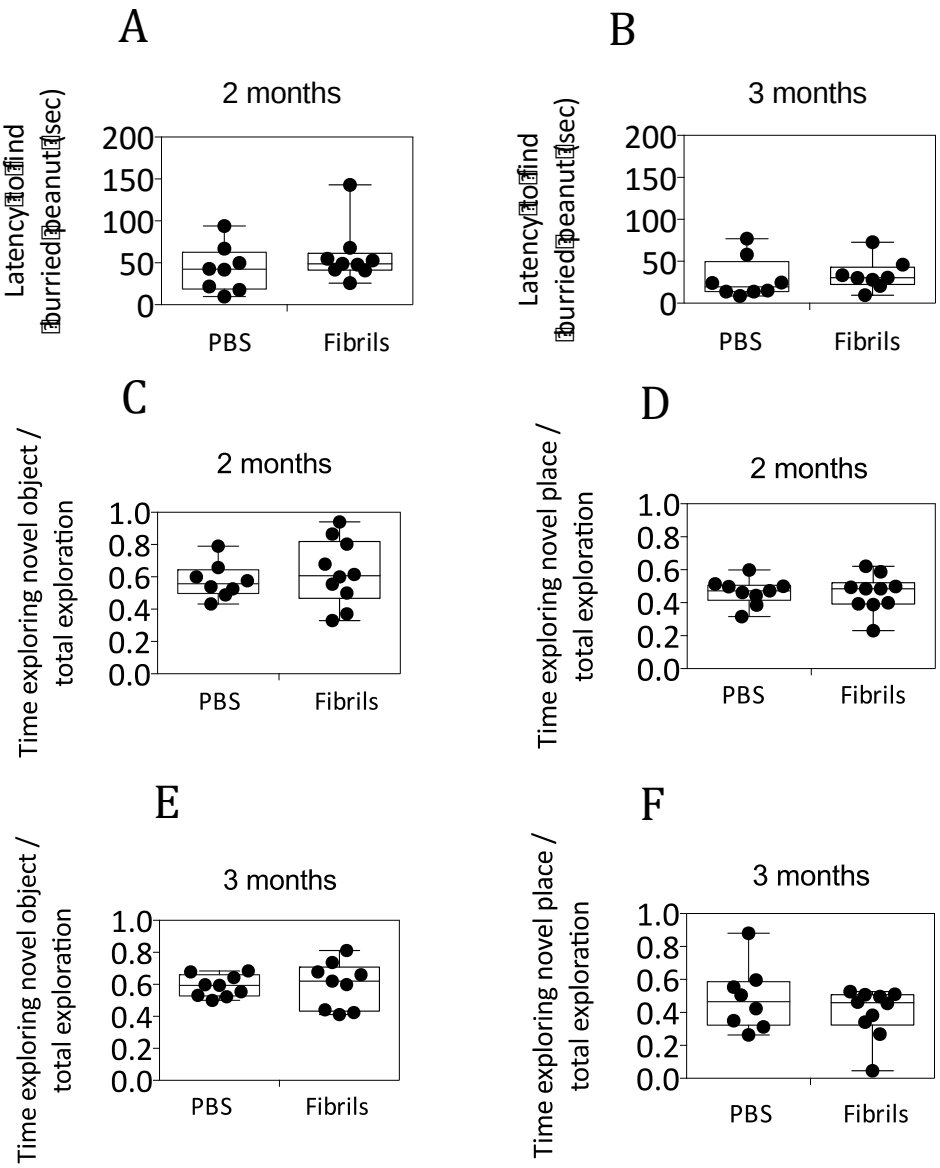

Fig. 29. Animals with bilateral infusions of alpha-synuclein fibrils did not exhibit any functional deficits at two or three months post-infusion. Two month-old CD1 mice were bilaterally infused with alpha-synuclein fibrils (5 μg) into CA2/3 of hippocampus. (A-B) Olfactory function was assessed using the buried peanut test at 2 and 3 months post-infusion. (C-F) Memory function was also measured using novel object/place recognition tests at the same timepoints. Bilateral infusions of alpha-synuclein fibrils did not elicit any functional deficits at two or three months post-infusion compared to the PBS group (n = 8-10 mice/group).

	pSer129^{+} inclusion counts						
Behavioral tests	CA1	CA2	CA3	GrDG	MoDG	PMCo	PrS
Latency to find buried peanut (sec) at 2 months	r = 0.2713 p = 0.5157	r = 0.1644 p = 0.6973	r = 0.2356 p = 0.5744	r = 0.03041 p = 0.9375	r = 0.9710 p = 0.0059**	r = 0.0042 p = 0.9921	r = 0.3093 p = 0.4996
Latency to find buried peanut (sec) at 3 months	r = 0.5920 p = 0.1614	r = 0.4976 p = 0.2558	r = 0.5396 p = 0.2113	r = 0.3916 p = 0.4426	r = 0.4420 p = 0.4561	r = 0.5203 p = 0.2313	r = 0.3456 p = 0.5022
Novel object exploration/total exploration at 2 months	r = 0.4187 p = 0.3019	r = 0.5720 p = 0.1385	r = 0.3107 p = 0.4538	r = 0.8162 p = 0.0251*	r = 0.5528 p = 0.3339	r = 0.3658 p = 0.3728	r = 0.3743 p = 0.4082
Novel place exploration/total exploration at 2 months	r = 0.4428 p = 0.2718	r = 0.3640 p = 0.3754	r = 0.3536 p = 0.3902	r = 0.0155 p = 0.9736	r = 0.2014 p = 0.7454	r = 0.1986 p = 0.6373	r = 0.3851 p = 0.3937
Novel object exploration/total exploration (sec) at 3 months	r = 0.4628 p = 0.2957	r = 0.3688 p = 0.4156	r = 0.2697 p = 0.5587	r = 0.1681 p = 0.7503	r = 0.6115 p = 0.2731	r = 0.4454 p = 0.3165	r = 0.5994 p = 0.2086
Novel place exploration/total exploration (sec) at 3 months	r = 0.3923 p = 0.3364	r = 0.3756 p = 0.3592	r = 0.4631 p = 0.2479	r = 0.1895 p = 0.6840	r = 0.8981 p = 0.0384*	r = 0.2348 p = 0.5756	r = 0.1948 p = 0.6755

Fig. 30. Alpha-synucleinopathy in the dentate gyrus is correlated with behavioral deficits. Two month-old CD1 mice were bilaterally infused with alpha-synuclein fibrils (5 µg) into CA2/3 of hippocampus. pSer129^{+} inclusion counts in the dentate gyrus were correlated with olfactory impairments at 2 months, and novel and place object recognition deficits at 2 and 3 months following fibril treatments. *p ≤ 0.05, **p ≤ 0.01, ***p ≤ 0.001 vs PBS, Pearson correlation coefficients-two tailed, (n = 8-10 mice/group). GrDG: granule cell layer of the dentate gyrus; MoDG: molecular layer of the dentate gyrus; PMCo: posteromedial cortical amygdala; PrS: presubiculum.

Discussion

In our previous study, we used FluoroGold tract-tracing combined with fibril infusions to show that alpha-synucleinopathy is transmitted in the retrograde direction from olfactory structures into areas that send first-order projections into the OB/AON (Mason et al., 2016). In the present study, alpha-synuclein fibrils were infused into CA2/3 of the hippocampus in the quest for a model of dementia with Lewy bodies or Parkinson's disease dementia. We examined the brains for Lewy-like pathology three months after unilateral fibril infusions. Perinuclear inclusions appeared in the pyramidal cell layer of Ammon's horn as well the granule cell layer of the dentate gyrus following CA2/CA3 injections. Neuritic and perinuclear inclusions extended into the subiculum and presubiculum. Extra-hippocampal pathology was evident in the superficial layers of the entorhinal cortex, the lateral septum, the nucleus accumbens, and in many amygdaloid subnuclei. As discussed earlier, all of these regions have been shown to project into the hippocampal formation (Segal, 1977, Swanson and Cowan, 1977, Swanson, 1982, Vertes, 1992, Conde et al., 1995, Yoshida and Oka, 1995, Gasbarri et al., 1997, Risold and Swanson, 1997, Acsady et al., 1998, Naber and Witter, 1998, McKenna and Vertes, 2001, O'Mara et al., 2001, Paxinos, 2015), supporting our previous work that the areas developing Lewy pathology share neuroanatomical connections with the site of infusion and are not merely distributed close to the infusion site (Mason et al., 2016). However, not all afferents exhibited Lewy pathology, such as the medial septum and diagonal band of Broca, which send dense projections into the hippocampus (Yoshida and Oka, 1995, Paxinos, 2015). These findings suggest that some neurons are less vulnerable to alpha-synucleinopathy, a conclusion that is entirely consistent with the clinical work on Lewy body disorders (Braak et al., 2003a).

The development of dense perinuclear and neuritic inclusions following fibril infusions was confirmed with two independent (monoclonal and polyclonal) pSer129 antibodies and preadsorption control experiments confirmed a loss of pSer129 staining. The Thioflavin stain labeled cells at the infusion site and some, but not all inclusions contained ubiquitin. Three-dimensional confocal analyses revealed that most perinuclear pSer129^{+} inclusions were formed within cells expressing the neuronal nuclear marker NeuN, although this subject has been a matter of some controversy (Sacino et al., 2013). It would be surprising if Lewy-like pathology were not in neuronal cells, as alpha-synuclein is a neuronal protein. We collected evidence of commissural spread of alpha-synucleinopathy through neuroanatomical circuits, as we only observed contralateral hippocampal labeling in hippocampal subregions known to project to the opposite hemisphere. Our study is the first to reveal that there is a robust correlation between pSer129^{+} inclusions in the dentate gyrus and cognitive and olfactory deficits following bilateral infusion of fibrils. The behavioral deficits were not correlated with cell numbers (not shown) as there was no overt neurodegeneration, but could have arisen due to inter-individual differences in synaptic function and protein quality control systems. Animals with greater autophagic and proteasomal clearance may have superior synaptic function and also clear misfolded proteins better. Alternatively, one possibility is that the Lewy-like inclusions observed in the present study were not mature enough at three months and had not seeded sufficient pathology to elicit substantial behavioral deficits. Future studies with longer survival timepoints are warranted, as Luk, Paumier and colleagues have shown that fibril infusions in the striatum only lead to robust degeneration at 6 months post-infusion (Luk et al., 2012a, Paumier et al., 2015).

Labeling with the pSer129 antibody is known to be subject to cross-reaction with neurofilament-

L (Sacino et al., 2014b). Therefore, we have used several controls to confirm our pSer129^{+} staining. Two independent (monoclonal and polyclonal) pSer129 antibodies revealed the same labeling patterns (Figure 22) and preadsorption control experiments confirmed a loss of pSer129 staining (Figure 21). Although we cannot rule out all cross-reactivity with certitude (Sacino et al., 2014a), the high-intensity labeling of inclusions is quite distinct from background, as evident from the stitched montages (Figures 19 and 27) and the blinded quantification shows that PBS animals do not exhibit pSer129^{+} structures (Figure 27).

One limitation of the present study is that we cannot completely rule out potential diffusion and non-specific uptake of fibrils throughout the interstitial space of the brain following fibril injections in CA2/3. However, the caudoputamen and thalamus are almost free from pSer129 label despite being close to the ventricles and to the epicenter of the infusion. In this context, it is worth mentioning the alpha-synuclein protein is found at high levels in the cerebrospinal fluid, where it may serve as a biomarker for the diagnosis of Parkinson's disease (Gao et al., 2015).

Conclusions

In the present study, multiple models of Parkinson's disease that mimic oxidative or proteotoxic stress were developed in order to test the efficacy of neuroprotective molecules. This was accomplished because no one model can mimic the range of pathologies of a complex disorder such as Parkinson's disease. Importantly, if a neuroprotectant can ameliorate multiple types of injury, it is far more likely to succeed in the clinic. The models established here include the following: 1) proteasome inhibitor infusions into the mouse hippocampus to inhibit the degradation of misfolded proteins and elicit cell death within 7 days, 2) 6-OHDA infusions into the mouse striatum to elicit oxidative stress and kill dopaminergic neurons within 7-10 days, and 3) alpha-synuclein fibril infusions into the mouse and rat hippocampus and/or striatum to seed the misfolding of endogenous alpha-synuclein and elicit the formation of Lewy bodies and Lewy neurites. We have reproduced the robustness and reliability of the 6-OHDA model of Parkinson's disease, and verified true dopaminergic neurodegeneration, as opposed to mere loss of dopaminergic phenotype. We validated the use of retrograde tracer FluoroGold as a more sensitive tool than measurements of either TH cell numbers or TH levels. We also gathered data suggesting that FluoroGold exerts some mild toxicity, as evident in nigral area measurements, but that it did not significantly affect the toxicity of 6-OHDA in either the striatum or the nigra. We validated the use of the 16-bit, high sensitivity Odyssey imager as an initial screening tool to measure loss of the nigrostriatal pathway in an economical manner. Next, we tested two therapies, the antioxidant N-acetyl-L-cysteine (NAC) and neurosteroid dehyroepiandrosterone sulfate (DHEAS), in one of these animal models of Parkinson's disease. We gathered support for the hypothesis that NAC protects dopaminergic terminals against 6-OHDA at short timeframes,

as shown by Munoz and colleagues (Munoz et al., 2004). However, we extended previous work by showing that the protective effects of NAC in our 6-OHDA model wane by three weeks post-infusion. These results demonstrate the importance of sacrificing animals at multiple timepoints when assessing the efficacy of neuroprotectants, particularly when modeling long-term conditions such as neurodegenerative disorders of the brain. Clinical trials of NAC have been relatively successful, including in Parkinson's disease patients, but have shown that NAC improves dopamine transporter binding by only 10% (Monti et al., 2016). Our findings that NAC can be slightly toxic offer one explanation for the small size of the effects in the Monti *et al.* study, and should serve as a warning to clinical investigators who intend to deliver NAC at similar doses for long timeframes. Another explanation for the discrepancy between our results and that of the study by Monti et al is that we used higher doses of NAC. However, our dose of NAC was based on a large body of previous work, including many clinical studies (Munoz et al., 2004, Chakraborti et al., 2008, Bachle et al., 2011, Smaga et al., 2012, Comparsi et al., 2014, Gunay et al., 2014, Jaccob, 2015, Prakash et al., 2015, Soleimani Asl et al., 2015, Truini et al., 2015).

In the present study, we observed that neither alpha-synuclein infusions nor DHEAS injections led to significant effects on novel object or place recognition, due to technical limitations such as improper sonication parameters and application of low doses of fibrils. During the same timeframe, the Leak lab discovered that 1h waterbath sonication of the fibrils renders the alpha-synuclein model much more aggressive and robust. Therefore, we infused PBS or synuclein fibrils in CA2/CA3 of the hippocampus and sacrificed mice three months later. These mice developed robust Lewy-like pathology in the hippocampus and at some, but not all the sites that

send first-order efferent projections to the hippocampus, such as the amygdala, entorhinal cortex, and lateral septum (Yoshida and Oka, 1995, Acsady et al., 1998, Pikkarainen et al., 1999, Baks-Te Bulte et al., 2005, Paxinos, 2015). Notably, our results strongly support the selective vulnerability to alpha-synucleinopathy that is evident in all human Lewy body disorders, as the projection from the medial septum/diagonal band was spared in our material. In Parkinson's disease, the basal forebrain does develop Lewy pathology (Hall et al., 2013, Hall et al., 2014), but our findings suggest that alpha-synuclein inclusions may not develop specifically in those medial septal neurons that project directly into the hippocampal formation.

We conducted olfactory and memory tests 2 and 3 months before sacrifice and discovered correlations between alpha-synuclein inclusion counts and olfactory and cognitive impairments. However, these observations are strictly correlational and thus far we do not have strong evidence that the Lewy pathology *per se* is the cause of poor cognitive function. Instead, we speculate that inter-animal differences in the underlying vulnerability to alpha-synucleinopathy due to varying levels of physical fitness/protein quality control may make some animals more likely to succumb to the misfolding and phosphorylation of alpha-synuclein. Further studies with longer survival timeframes are needed to address this limitation of the fibril model, as discussed further below.

The dentate gyrus may have developed the highest inclusion numbers in the present study because it sends the densest afferents—the massive mossy fiber pathway—to the site of infusion, CA2/CA3 (Acsady et al., 1998, Paxinos, 2015). In Parkinson's disease, CA2 develops greater inclusion numbers than the dentate gyrus, but may not have developed the most robust Lewy

pathology in the present study because of lack of anterograde uptake of fibrils into the somata. The CA2/CA3 study also showed transmission of alpha-synucleinopathy into superficial layer II of the entorhinal cortex, suggesting that the massive perforant pathway was seized by the Lewy pathology. As in our previous work, we did not collect evidence of robust transmission of pathology in the anterograde direction, although some transmission of Lewy-like pathology to the accumbens was observed, which receives afferent projections from the hippocampus (Floresco et al., 2001). Furthermore, the pathology in the accumbens was found in fibers and not in somata, which is also consistent with anterograde transmission. In contrast, much of the pathology in the entorhinal cortex was perinuclear, suggestive of retrograde labeling.

Future directions of the present work include studies in aged animals and animals sacrificed at longer survival periods, to facilitate additional seeding of alpha-synuclein molecules, increase the potential for presubicular degeneration and the emergence of robust behavioral deficits. Additional time until sacrifice would also increase the potential for transynaptic transport of alpha-synucleinopathy. Alternatively, the results of the present study might suggest that Lewy pathology in CA2 in humans is not causally linked to cognitive deficits and that the deficits are only correlated with CA2 alpha-synucleinopathy due to the parallel influence of a third variable on the evolution of Lewy pathology and memory function.

In conclusion, we have developed animal models of the oxidative and proteinopathic stressors that are evident in postmortem tissue from Parkinson's patients. Each model has unique strengths and limitations that may limit their predictive validity, similar to all other rodent disease models. For this reason, we developed multiple models for the preclinical testing of new or established

therapies. Future therapies that are efficacious in both the 6-OHDA and the fibril model may have greater potential for eventual success in the clinic.

References

Aarsland D (2016) Cognitive impairment in Parkinson's disease and dementia with Lewy bodies. Parkinsonism Relat Disord 22 Suppl 1:S144-148.

Aarsland D, Andersen K, Larsen JP, Lolk A, Kragh-Sorensen P (2003) Prevalence and characteristics of dementia in Parkinson disease: an 8-year prospective study. Arch Neurol 60:387-392.

Acsady L, Kamondi A, Sik A, Freund T, Buzsaki G (1998) GABAergic cells are the major postsynaptic targets of mossy fibers in the rat hippocampus. J Neurosci 18:3386-3403.

Adair JC, Knoefel JE, Morgan N (2001) Controlled trial of N-acetylcysteine for patients with probable Alzheimer's disease. Neurology 57:1515-1517.

Aisen PS, Cummings J, Schneider LS (2012) Symptomatic and nonamyloid/tau based pharmacologic treatment for Alzheimer disease. Cold Spring Harb Perspect Med 2:a006395.

Akwa Y, Ladurelle N, Covey DF, Baulieu EE (2001) The synthetic enantiomer of pregnenolone sulfate is very active on memory in rats and mice, even more so than its physiological neurosteroid counterpart: distinct mechanisms? Proc Natl Acad Sci U S A 98:14033-14037.

Alam ZI, Daniel SE, Lees AJ, Marsden DC, Jenner P, Halliwell B (1997) A generalised increase in protein carbonyls in the brain in Parkinson's but not incidental Lewy body disease. J Neurochem 69:1326-1329.

Albert MS (1996) Cognitive and neurobiologic markers of early Alzheimer disease. Proc Natl Acad Sci U S A 93:13547-13551.

Alexander GE (2004) Biology of Parkinson's disease: pathogenesis and pathophysiology of a multisystem neurodegenerative disorder. Dialogues Clin Neurosci 6:259-280.

Aluf Y, Vaya J, Khatib S, Loboda Y, Kizhner S, Finberg JP (2010) Specific oxidative stress profile associated with partial striatal dopaminergic depletion by 6-hydroxydopamine as assessed by a novel multifunctional marker molecule. Free Radic Res 44:635-644.

Amaral DG, Dolorfo C, Alvarez-Royo P (1991) Organization of CA1 projections to the subiculum: a PHA-L analysis in the rat. Hippocampus 1:415-435.

Anastasia A, Torre L, de Erausquin GA, Masco DH (2009) Enriched environment protects the nigrostriatal dopaminergic system and induces astroglial reaction in the 6-OHDA rat model of Parkinson's disease. J Neurochem 109:755-765.

Anderson JP, Walker DE, Goldstein JM, de Laat R, Banducci K, Caccavello RJ, Barbour R, Huang J, Kling K, Lee M, Diep L, Keim PS, Shen X, Chataway T, Schlossmacher MG, Seubert P, Schenk D, Sinha S, Gai WP, Chilcote TJ (2006) Phosphorylation of Ser-129 is the dominant pathological modification of alpha-synuclein in familial and sporadic Lewy body disease. J Biol Chem 281:29739-29752.

Angot E, Steiner JA, Hansen C, Li JY, Brundin P (2010) Are synucleinopathies prion-like disorders? Lancet Neurol 9:1128-1138.

Appel-Cresswell S, Vilarino-Guell C, Encarnacion M, Sherman H, Yu I, Shah B, Weir D, Thompson C, Szu-Tu C, Trinh J, Aasly JO, Rajput A, Rajput AH, Jon Stoessl A, Farrer MJ (2013) Alpha-synuclein p.H50Q, a novel pathogenic mutation for Parkinson's disease. Mov Disord 28:811-813.

Arriagada PV, Growdon JH, Hedley-Whyte ET, Hyman BT (1992) Neurofibrillary tangles but not senile plaques parallel duration and severity of Alzheimer's disease. Neurology 42:631-639.

Ataei S, Hadjibabaie M, Moslehi A, Taghizadeh-Ghehi M, Ashouri A, Amini E, Gholami K, Hayatshahi A, Vaezi M, Ghavamzadeh A (2015) A double-blind, randomized, controlled trial on N-acetylcysteine for the prevention of acute kidney injury in patients undergoing allogeneic hematopoietic stem cell transplantation. Hematol Oncol 33:67-74.

Athanassiadou A, Voutsinas G, Psiouri L, Leroy E, Polymeropoulos MH, Ilias A, Maniatis GM, Papapetropoulos T (1999) Genetic analysis of families with Parkinson disease that carry the Ala53Thr mutation in the gene encoding alpha-synuclein. Am J Hum Genet 65:555-558.

Auluck PK, Chan HY, Trojanowski JQ, Lee VM, Bonini NM (2002) Chaperone suppression of alpha-synuclein toxicity in a Drosophila model for Parkinson's disease. Science 295:865-868.

Aymerich MS, Barroso-Chinea P, Perez-Manso M, Munoz-Patino AM, Moreno-Igoa M, Gonzalez-Hernandez T, Lanciego JL (2006) Consequences of unilateral nigrostriatal denervation on the thalamostriatal pathway in rats. Eur J Neurosci 23:2099-2108.

Baba M, Nakajo S, Tu PH, Tomita T, Nakaya K, Lee VM, Trojanowski JQ, Iwatsubo T (1998) Aggregation of alpha-synuclein in Lewy bodies of sporadic Parkinson's disease and dementia with Lewy bodies. Am J Pathol 152:879-884.

Babalola PA, Fitz NF, Gibbs RB, Flaherty PT, Li PK, Johnson DA (2012) The effect of the steroid sulfatase inhibitor (p-O-sulfamoyl)-tetradecanoyl tyramine (DU-14) on learning and memory in rats with selective lesion of septal-hippocampal cholinergic tract. Neurobiol Learn Mem 98:303-310.

Bachle AC, Morsdorf P, Rezaeian F, Ong MF, Harder Y, Menger MD (2011) N-acetylcysteine attenuates leukocytic inflammation and microvascular perfusion failure in critically ischemic random pattern flaps. Microvasc Res 82:28-34.

Bagga V, Dunnett SB, Fricker RA (2015) The 6-OHDA mouse model of Parkinson's disease - Terminal striatal lesions provide a superior measure of neuronal loss and replacement than median forebrain bundle lesions. Behav Brain Res 288:107-117.

Baks-Te Bulte L, Wouterlood FG, Vinkenoog M, Witter MP (2005) Entorhinal projections terminate onto principal neurons and interneurons in the subiculum: a quantitative electron microscopical analysis in the rat. Neuroscience 136:729-739.

Baruchin A, Weisberg EP, Miner LL, Ennis D, Nisenbaum LK, Naylor E, Stricker EM, Zigmond MJ, Kaplan BB (1990) Effects of cold exposure on rat adrenal tyrosine hydroxylase: an analysis of RNA, protein, enzyme activity, and cofactor levels. J Neurochem 54:1769-1775.

Baulieu EE (1997) Neurosteroids: a role in aging? New functions in the central and peripheral nervous systems. Aging (Milano) 9:12.

Bellucci A, Mercuri NB, Venneri A, Faustini G, Longhena F, Pizzi M, Missale C, Spano P (2016) Review: Parkinson's disease: from synaptic loss to connectome dysfunction. Neuropathol Appl Neurobiol 42:77-94.

Berk M, Copolov D, Dean O, Lu K, Jeavons S, Schapkaitz I, Anderson-Hunt M, Judd F, Katz F, Katz P, Ording-Jespersen S, Little J, Conus P, Cuenod M, Do KQ, Bush AI (2008a) N-acetyl cysteine as a glutathione precursor for schizophrenia--a double-blind, randomized, placebo-controlled trial. Biol Psychiatry 64:361-368.

Berk M, Copolov DL, Dean O, Lu K, Jeavons S, Schapkaitz I, Anderson-Hunt M, Bush AI (2008b) N-acetyl cysteine for depressive symptoms in bipolar disorder--a double-blind randomized placebo-controlled trial. Biol Psychiatry 64:468-475.

Berman AE, Chan WY, Brennan AM, Reyes RC, Adler BL, Suh SW, Kauppinen TM, Edling Y, Swanson RA (2011) N-acetylcysteine prevents loss of dopaminergic neurons in the EAAC1-/- mouse. Ann Neurol 69:509-520.

Bernis ME, Babila JT, Breid S, Wusten KA, Wullner U, Tamguney G (2015) Prion-like propagation of human brain-derived alpha-synuclein in transgenic mice expressing human wild-type alpha-synuclein. Acta Neuropathol Commun 3:75.

Betarbet R, Sherer TB, MacKenzie G, Garcia-Osuna M, Panov AV, Greenamyre JT (2000) Chronic systemic pesticide exposure reproduces features of Parkinson's disease. Nature neuroscience 3:1301-1306.

Beyer MK, Bronnick KS, Hwang KS, Bergsland N, Tysnes OB, Larsen JP, Thompson PM, Somme JH, Apostolova LG (2013) Verbal memory is associated with structural hippocampal changes in newly diagnosed Parkinson's disease. J Neurol Neurosurg Psychiatry 84:23-28.

Bezard E, Gross CE, Fournier MC, Dovero S, Bloch B, Jaber M (1999) Absence of MPTP-induced neuronal death in mice lacking the dopamine transporter. Experimental neurology 155:268-273.

Billat VL, Mouisel E, Roblot N, Melki J (2005) Inter- and intrastrain variation in mouse critical running speed. J Appl Physiol (1985) 98:1258-1263.

Blesa J, Phani S, Jackson-Lewis V, Przedborski S (2012) Classic and new animal models of Parkinson's disease. J Biomed Biotechnol 2012:845618.

Blesa J, Trigo-Damas I, Quiroga-Varela A, Jackson-Lewis VR (2015) Oxidative stress and Parkinson's disease. Front Neuroanat 9:91.

Bliss TV, Collingridge GL (1993) A synaptic model of memory: long-term potentiation in the hippocampus. Nature 361:31-39.

Bohnen NI, Gedela S, Herath P, Constantine GM, Moore RY (2008) Selective hyposmia in Parkinson disease: association with hippocampal dopamine activity. Neurosci Lett 447:12-16.

Bove J, Zhou C, Jackson-Lewis V, Taylor J, Chu Y, Rideout HJ, Wu DC, Kordower JH, Petrucelli L, Przedborski S (2006) Proteasome inhibition and Parkinson's disease modeling. Annals of neurology 60:260-264.

Braak H, Braak E (1996) Development of Alzheimer-related neurofibrillary changes in the neocortex inversely recapitulates cortical myelogenesis. Acta Neuropathol 92:197-201.

Braak H, Del Tredici K, Rub U, de Vos RA, Jansen Steur EN, Braak E (2003a) Staging of brain pathology related to sporadic Parkinson's disease. Neurobiol Aging 24:197-211.

Braak H, Rub U, Gai WP, Del Tredici K (2003b) Idiopathic Parkinson's disease: possible routes by which vulnerable neuronal types may be subject to neuroinvasion by an unknown pathogen. J Neural Transm (Vienna) 110:517-536.

Braak H, Rüb U, Schultz C, Del Tredici K (2006) Vulnerability of cortical neurons to Alzheimer's and Parkinson's diseases. J Alzheimers Dis 9:35-44.

Braendgaard H, Gundersen HJ (1986) The impact of recent stereological advances on quantitative studies of the nervous system. J Neurosci Methods 18:39-78.

Brooks AI, Chadwick CA, Gelbard HA, Cory-Slechta DA, Federoff HJ (1999) Paraquat elicited neurobehavioral syndrome caused by dopaminergic neuron loss. Brain research 823:1-10.

Brunjes PC, Illig KR, Meyer EA (2005) A field guide to the anterior olfactory nucleus (cortex). Brain Res Brain Res Rev 50:305-335.
Bukhatwa S, Iravani MM, Zeng BY, Cooper JD, Rose S, Jenner P (2009) An immunohistochemical and stereological analysis of PSI-induced nigral neuronal degeneration in the rat. J Neurochem 109:52-59.
Calabrese EJ, Baldwin LA (2002) Defining hormesis. Hum Exp Toxicol 21:91-97.
Cannon JR, Greenamyre JT (2009) NeuN is not a reliable marker of dopamine neurons in rat substantia nigra. Neurosci Lett 464:14-17.
Castello PR, Drechsel DA, Patel M (2007) Mitochondria are a major source of paraquat-induced reactive oxygen species production in the brain. J Biol Chem 282:14186-14193.
Caviness JN, Lue L, Adler CH, Walker DG (2011) Parkinson's disease dementia and potential therapeutic strategies. CNS Neurosci Ther 17:32-44.
Cenquizca LA, Swanson LW (2007) Spatial organization of direct hippocampal field CA1 axonal projections to the rest of the cerebral cortex. Brain Res Rev 56:1-26.
Chakraborti A, Gulati K, Ray A (2008) Age related differences in stress-induced neurobehavioral responses in rats: modulation by antioxidants and nitrergic agents. Behav Brain Res 194:86-91.
Chang MS, Sved AF, Zigmond MJ, Austin MC (2000) Increased transcription of the tyrosine hydroxylase gene in individual locus coeruleus neurons following footshock stress. Neuroscience 101:131-139.
Choi JM, Woo MS, Ma HI, Kang SY, Sung YH, Yong SW, Chung SJ, Kim JS, Shin HW, Lyoo CH, Lee PH, Baik JS, Kim SJ, Park MY, Sohn YH, Kim JH, Kim JW, Lee MS, Lee MC, Kim DH, Kim YJ (2008) Analysis of PARK genes in a Korean cohort of early-onset Parkinson disease. Neurogenetics 9:263-269.
Choi-Lundberg DL, Lin Q, Schallert T, Crippens D, Davidson BL, Chang YN, Chiang YL, Qian J, Bardwaj L, Bohn MC (1998) Behavioral and cellular protection of rat dopaminergic neurons by an adenoviral vector encoding glial cell line-derived neurotrophic factor. Exp Neurol 154:261-275.
Churchyard A, Lees AJ (1997) The relationship between dementia and direct involvement of the hippocampus and amygdala in Parkinson's disease. Neurology 49:1570-1576.
Clark J, Clore EL, Zheng K, Adame A, Masliah E, Simon DK (2010) Oral N-acetyl-cysteine attenuates loss of dopaminergic terminals in alpha-synuclein overexpressing mice. PLoS One 5:e12333.
Cohen AD, Zigmond MJ, Smith AD (2011) Effects of intrastriatal GDNF on the response of dopamine neurons to 6-hydroxydopamine: time course of protection and neurorestoration. Brain Res 1370:80-88.
Colin E, Zala D, Liot G, Rangone H, Borrell-Pages M, Li XJ, Saudou F, Humbert S (2008) Huntingtin phosphorylation acts as a molecular switch for anterograde/retrograde transport in neurons. EMBO J 27:2124-2134.
Comparsi B, Meinerz DF, Dalla Corte CL, Prestes AS, Stefanello ST, Santos DB, De Souza D, Farina M, Dafre AL, Posser T, Franco JL, Rocha JB (2014) N-Acetylcysteine does not protect behavioral and biochemical toxicological effect after acute exposure of diphenyl ditelluride. Toxicol Mech Methods 24:529-535.
Conde F, Maire-Lepoivre E, Audinat E, Crepel F (1995) Afferent connections of the medial frontal cortex of the rat. II. Cortical and subcortical afferents. J Comp Neurol 352:567-593.

Cordato NJ, Halliday GM, Harding AJ, Hely MA, Morris JG (2000) Regional brain atrophy in progressive supranuclear palsy and Lewy body disease. Ann Neurol 47:718-728.
Cuervo AM, Bergamini E, Brunk UT, Droge W, Ffrench M, Terman A (2005) Autophagy and aging: the importance of maintaining "clean" cells. Autophagy 1:131-140.
Cuervo AM, Stefanis L, Fredenburg R, Lansbury PT, Sulzer D (2004) Impaired degradation of mutant alpha-synuclein by chaperone-mediated autophagy. Science 305:1292-1295.
Czlonkowska A, Kurkowska-Jastrzebska I, Czlonkowski A, Peter D, Stefano GB (2002) Immune processes in the pathogenesis of Parkinson's disease - a potential role for microglia and nitric oxide. Medical science monitor : international medical journal of experimental and clinical research 8:RA165-177.
Damier P, Hirsch EC, Agid Y, Graybiel AM (1999) The substantia nigra of the human brain. I. Nigrosomes and the nigral matrix, a compartmental organization based on calbindin D(28K) immunohistochemistry. Brain 122 (Pt 8):1421-1436.
DaRocha-Souto B, Scotton TC, Coma M, Serrano-Pozo A, Hashimoto T, Sereno L, Rodriguez M, Sanchez B, Hyman BT, Gomez-Isla T (2011) Brain oligomeric beta-amyloid but not total amyloid plaque burden correlates with neuronal loss and astrocyte inflammatory response in amyloid precursor protein/tau transgenic mice. J Neuropathol Exp Neurol 70:360-376.
Das KC, Lewis-Molock Y, White CW (1995) Activation of NF-kappa B and elevation of MnSOD gene expression by thiol reducing agents in lung adenocarcinoma (A549) cells. Am J Physiol 269:L588-602.
Dehay B, Bourdenx M, Gorry P, Przedborski S, Vila M, Hunot S, Singleton A, Olanow CW, Merchant KM, Bezard E, Petsko GA, Meissner WG (2015) Targeting alpha-synuclein for treatment of Parkinson's disease: mechanistic and therapeutic considerations. Lancet Neurol 14:855-866.
Del Ser T, Hachinski V, Merskey H, Munoz DG (2001) Clinical and pathologic features of two groups of patients with dementia with Lewy bodies: effect of coexisting Alzheimer-type lesion load. Alzheimer Dis Assoc Disord 15:31-44.
Deumens R, Blokland A, Prickaerts J (2002) Modeling Parkinson's disease in rats: an evaluation of 6-OHDA lesions of the nigrostriatal pathway. Experimental neurology 175:303-317.
Dias IH, Chapple IL, Milward M, Grant MM, Hill E, Brown J, Griffiths HR (2013) Sulforaphane restores cellular glutathione levels and reduces chronic periodontitis neutrophil hyperactivity in vitro. PLoS One 8:e66407.
Dickinson DA, Forman HJ (2002) Cellular glutathione and thiols metabolism. Biochem Pharmacol 64:1019-1026.
Dickson DW (2012) Parkinson's disease and parkinsonism: neuropathology. Cold Spring Harb Perspect Med 2.
Dickson DW, Ruan D, Crystal H, Mark MH, Davies P, Kress Y, Yen SH (1991) Hippocampal degeneration differentiates diffuse Lewy body disease (DLBD) from Alzheimer's disease: light and electron microscopic immunocytochemistry of CA2-3 neurites specific to DLBD. Neurology 41:1402-1409.
Dickson DW, Schmidt ML, Lee VM, Zhao ML, Yen SH, Trojanowski JQ (1994) Immunoreactivity profile of hippocampal CA2/3 neurites in diffuse Lewy body disease. Acta Neuropathol 87:269-276.

Dinkova-Kostova AT (2012) The Role of Sulfhydryl Reactivity of Small Molecules for the Activation of the KEAP1/NRF2 Pathway and the Heat Shock Response. Scientifica (Cairo) 2012:606104.
Dinkova-Kostova AT, Fahey JW, Talalay P (2004) Chemical structures of inducers of nicotinamide quinone oxidoreductase 1 (NQO1). Methods Enzymol 382:423-448.
Djaldetti R, Ziv I, Melamed E (2006) The mystery of motor asymmetry in Parkinson's disease. Lancet Neurol 5:796-802.
Double KL, Reyes S, Werry EL, Halliday GM (2010) Selective cell death in neurodegeneration: why are some neurons spared in vulnerable regions? Prog Neurobiol 92:316-329.
Dringen R (2000) Metabolism and functions of glutathione in brain. Prog Neurobiol 62:649-671.
Duda JE, Lee VM, Trojanowski JQ (2000) Neuropathology of synuclein aggregates. J Neurosci Res 61:121-127.
Dutta G, Zhang P, Liu B (2008) The lipopolysaccharide Parkinson's disease animal model: mechanistic studies and drug discovery. Fundamental & clinical pharmacology 22:453-464.
Ebert AD, Hann HJ, Bohn MC (2008) Progressive degeneration of dopamine neurons in 6-hydroxydopamine rat model of Parkinson's disease does not involve activation of caspase-9 and caspase-3. J Neurosci Res 86:317-325.
Ebrahimi-Fakhari D, Cantuti-Castelvetri I, Fan Z, Rockenstein E, Masliah E, Hyman BT, McLean PJ, Unni VK (2011a) Distinct roles in vivo for the ubiquitin-proteasome system and the autophagy-lysosomal pathway in the degradation of alpha-synuclein. J Neurosci 31:14508-14520.
Ebrahimi-Fakhari D, Wahlster L, McLean PJ (2011b) Molecular chaperones in Parkinson's disease--present and future. J Parkinsons Dis 1:299-320.
Eshraghi A, Talasaz AH, Salamzadeh J, Salarifar M, Pourhosseini H, Nozari Y, Bahremand M, Jalali A, Boroumand MA (2016) Evaluating the Effect of Intracoronary N-Acetylcysteine on Platelet Activation Markers After Primary Percutaneous Coronary Intervention in Patients With ST-Elevation Myocardial Infarction. Am J Ther 23:e44-51.
Finch DM, Babb TL (1981) Demonstration of caudally directed hippocampal efferents in the rat by intracellular injection of horseradish peroxidase. Brain Res 214:405-410.
Finch DM, Nowlin NL, Babb TL (1983) Demonstration of axonal projections of neurons in the rat hippocampus and subiculum by intracellular injection of HRP. Brain Res 271:201-216.
Fisher M, Feuerstein G, Howells DW, Hurn PD, Kent TA, Savitz SI, Lo EH, Group S (2009) Update of the stroke therapy academic industry roundtable preclinical recommendations. Stroke 40:2244-2250.
Fishman-Jacob T, Reznichenko L, Youdim MB, Mandel SA (2009) A sporadic Parkinson disease model via silencing of the ubiquitin-proteasome/E3 ligase component SKP1A. J Biol Chem 284:32835-32845.
Fleming SM, Chesselet MF (2006) Behavioral phenotypes and pharmacology in genetic mouse models of Parkinsonism. Behav Pharmacol 17:383-391.
Flood JF, Smith GE, Roberts E (1988) Dehydroepiandrosterone and its sulfate enhance memory retention in mice. Brain Res 447:269-278.
Floresco SB, Todd CL, Grace AA (2001) Glutamatergic afferents from the hippocampus to the nucleus accumbens regulate activity of ventral tegmental area dopamine neurons. J Neurosci 21:4915-4922.

Foltynie T, Brayne CE, Robbins TW, Barker RA (2004) The cognitive ability of an incident cohort of Parkinson's patients in the UK. The CamPaIGN study. Brain 127:550-560.
Fornai F, Lenzi P, Gesi M, Ferrucci M, Lazzeri G, Busceti CL, Ruffoli R, Soldani P, Ruggieri S, Alessandri MG, Paparelli A (2003) Fine structure and biochemical mechanisms underlying nigrostriatal inclusions and cell death after proteasome inhibition. J Neurosci 23:8955-8966.
Fornai F, Lenzi P, Gesi M, Ferrucci M, Lazzeri G, Capobianco L, de Blasi A, Battaglia G, Nicoletti F, Ruggieri S, Paparelli A (2004) Similarities between methamphetamine toxicity and proteasome inhibition. Ann N Y Acad Sci 1025:162-170.
Fornai F, Schluter OM, Lenzi P, Gesi M, Ruffoli R, Ferrucci M, Lazzeri G, Busceti CL, Pontarelli F, Battaglia G, Pellegrini A, Nicoletti F, Ruggieri S, Paparelli A, Sudhof TC (2005) Parkinson-like syndrome induced by continuous MPTP infusion: convergent roles of the ubiquitin-proteasome system and alpha-synuclein. Proceedings of the National Academy of Sciences of the United States of America 102:3413-3418.
Francisco E. Olucha-Bordonau LF-M, Marcos Otero-Gardia, Enrique Lanuza, Ferando Martinez-Garcia (2015) Amygdala: Structure and Function. In: the rat nervous system (Paxinos, G., ed).
Fujiwara H, Hasegawa M, Dohmae N, Kawashima A, Masliah E, Goldberg MS, Shen J, Takio K, Iwatsubo T (2002) alpha-Synuclein is phosphorylated in synucleinopathy lesions. Nat Cell Biol 4:160-164.
Fyhn M, Molden S, Witter MP, Moser EI, Moser MB (2004) Spatial representation in the entorhinal cortex. Science 305:1258-1264.
Gallea JI, Celej MS (2014) Structural insights into amyloid oligomers of the Parkinson disease-related protein alpha-synuclein. J Biol Chem 289:26733-26742.
Gao L, Tang H, Nie K, Wang L, Zhao J, Gan R, Huang J, Zhu R, Feng S, Duan Z, Zhang Y, Wang L (2015) Cerebrospinal fluid alpha-synuclein as a biomarker for Parkinson's disease diagnosis: a systematic review and meta-analysis. Int J Neurosci 125:645-654.
Garrett WT, McBride RL, Williams JK, Jr., Feringa ER (1991) Fluoro-Gold's toxicity makes it inferior to True Blue for long-term studies of dorsal root ganglion neurons and motoneurons. Neurosci Lett 128:137-139.
Gasbarri A, Sulli A, Packard MG (1997) The dopaminergic mesencephalic projections to the hippocampal formation in the rat. Prog Neuropsychopharmacol Biol Psychiatry 21:1-22.
Glabe CG, Kayed R (2006) Common structure and toxic function of amyloid oligomers implies a common mechanism of pathogenesis. Neurology 66:S74-78.
Goedert M, Clavaguera F, Tolnay M (2010) The propagation of prion-like protein inclusions in neurodegenerative diseases. Trends Neurosci 33:317-325.
Gomez-Isla T, Hollister R, West H, Mui S, Growdon JH, Petersen RC, Parisi JE, Hyman BT (1997) Neuronal loss correlates with but exceeds neurofibrillary tangles in Alzheimer's disease. Ann Neurol 41:17-24.
Gomez-Isla T, Price JL, McKeel DW, Jr., Morris JC, Growdon JH, Hyman BT (1996) Profound loss of layer II entorhinal cortex neurons occurs in very mild Alzheimer's disease. J Neurosci 16:4491-4500.
Gorell JM, Johnson CC, Rybicki BA, Peterson EL, Richardson RJ (1998) The risk of Parkinson's disease with exposure to pesticides, farming, well water, and rural living. Neurology 50:1346-1350.

Griffith OW (1999) Biologic and pharmacologic regulation of mammalian glutathione synthesis. Free Radic Biol Med 27:922-935.
Guardia-Laguarta C, Area-Gomez E, Rub C, Liu Y, Magrane J, Becker D, Voos W, Schon EA, Przedborski S (2014) alpha-Synuclein is localized to mitochondria-associated ER membranes. J Neurosci 34:249-259.
Gunay Y, Altaner S, Ekmen N (2014) The Role of e-NOS in Chronic Cholestasis-Induced Liver and Renal Injury in Rats: The Effect of N-Acetyl Cysteine. Gastroenterol Res Pract 2014:564949.
Gureviciene I, Gurevicius K, Tanila H (2009) Aging and alpha-synuclein affect synaptic plasticity in the dentate gyrus. J Neural Transm (Vienna) 116:13-22.
Hall H, Jewett M, Landeck N, Nilsson N, Schagerlof U, Leanza G, Kirik D (2013) Characterization of cognitive deficits in rats overexpressing human alpha-synuclein in the ventral tegmental area and medial septum using recombinant adeno-associated viral vectors. PLoS One 8:e64844.
Hall H, Reyes S, Landeck N, Bye C, Leanza G, Double K, Thompson L, Halliday G, Kirik D (2014) Hippocampal Lewy pathology and cholinergic dysfunction are associated with dementia in Parkinson's disease. Brain 137:2493-2508.
Halliwell B (1992) Reactive oxygen species and the central nervous system. J Neurochem 59:1609-1623.
Hansen C, Angot E, Bergstrom AL, Steiner JA, Pieri L, Paul G, Outeiro TF, Melki R, Kallunki P, Fog K, Li JY, Brundin P (2011) alpha-Synuclein propagates from mouse brain to grafted dopaminergic neurons and seeds aggregation in cultured human cells. J Clin Invest 121:715-725.
Hanslick JL, Lau K, Noguchi KK, Olney JW, Zorumski CF, Mennerick S, Farber NB (2009) Dimethyl sulfoxide (DMSO) produces widespread apoptosis in the developing central nervous system. Neurobiol Dis 34:1-10.
Hara T, Nakamura K, Matsui M, Yamamoto A, Nakahara Y, Suzuki-Migishima R, Yokoyama M, Mishima K, Saito I, Okano H, Mizushima N (2006) Suppression of basal autophagy in neural cells causes neurodegenerative disease in mice. Nature 441:885-889.
Harding AJ, Halliday GM (2001) Cortical Lewy body pathology in the diagnosis of dementia. Acta Neuropathol 102:355-363.
Harding AJ, Lakay B, Halliday GM (2002) Selective hippocampal neuron loss in dementia with Lewy bodies. Ann Neurol 51:125-128.
He Y, Lee T, Leong SK (2000) 6-Hydroxydopamine induced apoptosis of dopaminergic cells in the rat substantia nigra. Brain research 858:163-166.
Heikkila RE, Manzino L, Cabbat FS, Duvoisin RC (1985) Studies on the oxidation of the dopaminergic neurotoxin 1-methyl-4-phenyl-1,2,5,6-tetrahydropyridine by monoamine oxidase B. Journal of neurochemistry 45:1049-1054.
Hely MA, Reid WG, Adena MA, Halliday GM, Morris JG (2008) The Sydney multicenter study of Parkinson's disease: the inevitability of dementia at 20 years. Mov Disord 23:837-844.
Hertzman C, Wiens M, Bowering D, Snow B, Calne D (1990) Parkinson's disease: a case-control study of occupational and environmental risk factors. Am J Ind Med 17:349-355.
Hisahara S, Shimohama S (2010) Toxin-induced and genetic animal models of Parkinson's disease. Parkinsons Dis 2011:951709.
Hobson P, Meara J (2004) Risk and incidence of dementia in a cohort of older subjects with Parkinson's disease in the United Kingdom. Mov Disord 19:1043-1049.

Hoffer ME, Balaban C, Slade MD, Tsao JW, Hoffer B (2013) Amelioration of acute sequelae of blast induced mild traumatic brain injury by N-acetyl cysteine: a double-blind, placebo controlled study. PLoS One 8:e54163.
Hoglinger GU, Carrard G, Michel PP, Medja F, Lombes A, Ruberg M, Friguet B, Hirsch EC (2003) Dysfunction of mitochondrial complex I and the proteasome: interactions between two biochemical deficits in a cellular model of Parkinson's disease. Journal of neurochemistry 86:1297-1307.
Hoglinger GU, Lannuzel A, Khondiker ME, Michel PP, Duyckaerts C, Feger J, Champy P, Prigent A, Medja F, Lombes A, Oertel WH, Ruberg M, Hirsch EC (2005) The mitochondrial complex I inhibitor rotenone triggers a cerebral tauopathy. Journal of neurochemistry 95:930-939.
Holmay MJ, Terpstra M, Coles LD, Mishra U, Ahlskog M, Oz G, Cloyd JC, Tuite PJ (2013) N-Acetylcysteine boosts brain and blood glutathione in Gaucher and Parkinson diseases. Clin Neuropharmacol 36:103-106.
Hyde DM, Tyler NK, Plopper CG (2007) Morphometry of the respiratory tract: avoiding the sampling, size, orientation, and reference traps. Toxicol Pathol 35:41-48.
Ii K, Ito H, Tanaka K, Hirano A (1997) Immunocytochemical co-localization of the proteasome in ubiquitinated structures in neurodegenerative diseases and the elderly. J Neuropathol Exp Neurol 56:125-131.
Imai Y, Soda M, Takahashi R (2000) Parkin suppresses unfolded protein stress-induced cell death through its E3 ubiquitin-protein ligase activity. J Biol Chem 275:35661-35664.
Ince P, Irving D, MacArthur F, Perry RH (1991) Quantitative neuropathological study of Alzheimer-type pathology in the hippocampus: comparison of senile dementia of Alzheimer type, senile dementia of Lewy body type, Parkinson's disease and non-demented elderly control patients. J Neurol Sci 106:142-152.
Ittner LM, Ke YD, Delerue F, Bi M, Gladbach A, van Eersel J, Wolfing H, Chieng BC, Christie MJ, Napier IA, Eckert A, Staufenbiel M, Hardeman E, Gotz J (2010) Dendritic function of tau mediates amyloid-beta toxicity in Alzheimer's disease mouse models. Cell 142:387-397.
Jaccob AA (2015) Protective effect of N-acetylcysteine against ethanol-induced gastric ulcer: A pharmacological assessment in mice. J Intercult Ethnopharmacol 4:90-95.
Jenner P (2003) Oxidative stress in Parkinson's disease. Ann Neurol 53 Suppl 3:S26-36; discussion S36-28.
Jiang Y, Rumble JL, Gleixner AM, Unnithan AS, Pulugulla SH, Posimo JM, Choi HJ, Crum TS, Pant DB, Leak RK (2013) N-Acetyl cysteine blunts proteotoxicity in a heat shock protein-dependent manner. Neuroscience 255:19-32.
Joelving FC, Billeskov R, Christensen JR, West M, Pakkenberg B (2006) Hippocampal neuron and glial cell numbers in Parkinson's disease--a stereological study. Hippocampus 16:826-833.
Johnson DA, Rhodes ME, Boni RL, Li PK (1997) Chronic steroid sulfatase inhibition by (p-O-sulfamoyl)-N-tetradecanoyl tyramine increases dehydroepiandrosterone sulfate in whole brain. Life Sci 61:PL 355-359.
Johnson DA, Wu T, Li P, Maher TJ (2000) The effect of steroid sulfatase inhibition on learning and spatial memory. Brain Res 865:286-290.

Josephs KA, Whitwell JL, Ahmed Z, Shiung MM, Weigand SD, Knopman DS, Boeve BF, Parisi JE, Petersen RC, Dickson DW, Jack CR, Jr. (2008) Beta-amyloid burden is not associated with rates of brain atrophy. Ann Neurol 63:204-212.
Jucker M, Walker LC (2013) Self-propagation of pathogenic protein aggregates in neurodegenerative diseases. Nature 501:45-51.
Kalaitzakis ME, Christian LM, Moran LB, Graeber MB, Pearce RK, Gentleman SM (2009) Dementia and visual hallucinations associated with limbic pathology in Parkinson's disease. Parkinsonism Relat Disord 15:196-204.
Kalaitzakis ME, Pearce RK (2009) The morbid anatomy of dementia in Parkinson's disease. Acta Neuropathol 118:587-598.
Katz M, Won SJ, Park Y, Orr A, Jones DP, Swanson RA, Glass GA (2015) Cerebrospinal fluid concentrations of N-acetylcysteine after oral administration in Parkinson's disease. Parkinsonism Relat Disord 21:500-503.
Kendig EL, Le HH, Belcher SM (2010) Defining hormesis: evaluation of a complex concentration response phenomenon. Int J Toxicol 29:235-246.
Ki CS, Stavrou EF, Davanos N, Lee WY, Chung EJ, Kim JY, Athanassiadou A (2007) The Ala53Thr mutation in the alpha-synuclein gene in a Korean family with Parkinson disease. Clin Genet 71:471-473.
Kiffin R, Bandyopadhyay U, Cuervo AM (2006) Oxidative stress and autophagy. Antioxid Redox Signal 8:152-162.
Komatsu M, Waguri S, Chiba T, Murata S, Iwata J, Tanida I, Ueno T, Koike M, Uchiyama Y, Kominami E, Tanaka K (2006) Loss of autophagy in the central nervous system causes neurodegeneration in mice. Nature 441:880-884.
Kowal SL, Dall TM, Chakrabarti R, Storm MV, Jain A (2013) The current and projected economic burden of Parkinson's disease in the United States. Mov Disord 28:311-318.
Kozlowski DA, Connor B, Tillerson JL, Schallert T, Bohn MC (2000) Delivery of a GDNF gene into the substantia nigra after a progressive 6-OHDA lesion maintains functional nigrostriatal connections. Exp Neurol 166:1-15.
Kruger R, Kuhn W, Muller T, Woitalla D, Graeber M, Kosel S, Przuntek H, Epplen JT, Schols L, Riess O (1998) Ala30Pro mutation in the gene encoding alpha-synuclein in Parkinson's disease. Nat Genet 18:106-108.
Kumer SC, Vrana KE (1996) Intricate regulation of tyrosine hydroxylase activity and gene expression. J Neurochem 67:443-462.
Kuzuhara S, Mori H, Izumiyama N, Yoshimura M, Ihara Y (1988) Lewy bodies are ubiquitinated. A light and electron microscopic immunocytochemical study. Acta Neuropathol 75:345-353.
Kwak MK, Wakabayashi N, Itoh K, Motohashi H, Yamamoto M, Kensler TW (2003) Modulation of gene expression by cancer chemopreventive dithiolethiones through the Keap1-Nrf2 pathway. Identification of novel gene clusters for cell survival. J Biol Chem 278:8135-8145.
Laurie C, Reynolds A, Coskun O, Bowman E, Gendelman HE, Mosley RL (2007) CD4+ T cells from Copolymer-1 immunized mice protect dopaminergic neurons in the 1-methyl-4-phenyl-1,2,3,6-tetrahydropyridine model of Parkinson's disease. Journal of neuroimmunology 183:60-68.

Lazzarini M, Martin S, Mitkovski M, Vozari RR, Stuhmer W, Bel ED (2013) Doxycycline restrains glia and confers neuroprotection in a 6-OHDA Parkinson model. Glia 61:1084-1100.

Leblhuber F, Neubauer C, Peichl M, Reisecker F, Steinparz FX, Windhager E, Dienstl E (1993) Age and sex differences of dehydroepiandrosterone sulfate (DHEAS) and cortisol (CRT) plasma levels in normal controls and Alzheimer's disease (AD). Psychopharmacology (Berl) 111:23-26.

Lehmkuhl AM, Dirr ER, Fleming SM (2014) Olfactory assays for mouse models of neurodegenerative disease. J Vis Exp e51804.

Lennox G, Lowe J, Morrell K, Landon M, Mayer RJ (1989) Anti-ubiquitin immunocytochemistry is more sensitive than conventional techniques in the detection of diffuse Lewy body disease. J Neurol Neurosurg Psychiatry 52:67-71.

Leroy E, Boyer R, Auburger G, Leube B, Ulm G, Mezey E, Harta G, Brownstein MJ, Jonnalagada S, Chernova T, Dehejia A, Lavedan C, Gasser T, Steinbach PJ, Wilkinson KD, Polymeropoulos MH (1998) The ubiquitin pathway in Parkinson's disease. Nature 395:451-452.

Lesage S, Anheim M, Letournel F, Bousset L, Honore A, Rozas N, Pieri L, Madiona K, Durr A, Melki R, Verny C, Brice A, French Parkinson's Disease Genetics Study G (2013) G51D alpha-synuclein mutation causes a novel parkinsonian-pyramidal syndrome. Ann Neurol 73:459-471.

Li N, Ragheb K, Lawler G, Sturgis J, Rajwa B, Melendez JA, Robinson JP (2003) Mitochondrial complex I inhibitor rotenone induces apoptosis through enhancing mitochondrial reactive oxygen species production. J Biol Chem 278:8516-8525.

Li PK, Rhodes ME, Burke AM, Johnson DA (1997) Memory enhancement mediated by the steroid sulfatase inhibitor (p-O-sulfamoyl)-N-tetradecanoyl tyramine. Life Sci 60:PL45-51.

Liang Y, Li S, Wen C, Zhang Y, Guo Q, Wang H, Su B (2008) Intrastriatal injection of colchicine induces striatonigral degeneration in mice. J Neurochem 106:1815-1827.

Lim Y, Kehm VM, Lee EB, Soper JH, Li C, Trojanowski JQ, Lee VM (2011) alpha-Syn suppression reverses synaptic and memory defects in a mouse model of dementia with Lewy bodies. J Neurosci 31:10076-10087.

Lindersson E, Beedholm R, Hojrup P, Moos T, Gai W, Hendil KB, Jensen PH (2004) Proteasomal inhibition by alpha-synuclein filaments and oligomers. J Biol Chem 279:12924-12934.

Liou HH, Chen RC, Tsai YF, Chen WP, Chang YC, Tsai MC (1996) Effects of paraquat on the substantia nigra of the wistar rats: neurochemical, histological, and behavioral studies. Toxicol Appl Pharmacol 137:34-41.

Liu M, Bing G (2011) Lipopolysaccharide animal models for Parkinson's disease. Parkinson's disease 2011:327089.

Lowe J, McDermott H, Landon M, Mayer RJ, Wilkinson KD (1990) Ubiquitin carboxyl-terminal hydrolase (PGP 9.5) is selectively present in ubiquitinated inclusion bodies characteristic of human neurodegenerative diseases. J Pathol 161:153-160.

Lue LF, Schmitz CT, Snyder NL, Chen K, Walker DG, Davis KJ, Belden C, Caviness JN, Driver-Dunckley E, Adler CH, Sabbagh MN, Shill HA (2016) Converging mediators from immune and trophic pathways to identify Parkinson disease dementia. Neurol Neuroimmunol Neuroinflamm 3:e193.

Luk KC, Kehm V, Carroll J, Zhang B, O'Brien P, Trojanowski JQ, Lee VM (2012a) Pathological alpha-synuclein transmission initiates Parkinson-like neurodegeneration in nontransgenic mice. Science 338:949-953.
Luk KC, Kehm VM, Zhang B, O'Brien P, Trojanowski JQ, Lee VM (2012b) Intracerebral inoculation of pathological alpha-synuclein initiates a rapidly progressive neurodegenerative alpha-synucleinopathy in mice. J Exp Med 209:975-986.
Luk KC, Song C, O'Brien P, Stieber A, Branch JR, Brunden KR, Trojanowski JQ, Lee VM (2009) Exogenous alpha-synuclein fibrils seed the formation of Lewy body-like intracellular inclusions in cultured cells. Proc Natl Acad Sci U S A 106:20051-20056.
Lushchak VI (2012) Glutathione homeostasis and functions: potential targets for medical interventions. J Amino Acids 2012:736837.
Malek N, Swallow D, Grosset KA, Anichtchik O, Spillantini M, Grosset DG (2014) Alpha-synuclein in peripheral tissues and body fluids as a biomarker for Parkinson's disease - a systematic review. Acta neurologica Scandinavica 130:59-72.
Mandel RJ, Spratt SK, Snyder RO, Leff SE (1997) Midbrain injection of recombinant adeno-associated virus encoding rat glial cell line-derived neurotrophic factor protects nigral neurons in a progressive 6-hydroxydopamine-induced degeneration model of Parkinson's disease in rats. Proc Natl Acad Sci U S A 94:14083-14088.
Mao X, Barger SW (1998) Neuroprotection by dehydroepiandrosterone-sulfate: role of an NFkappaB-like factor. Neuroreport 9:759-763.
Maroteaux L, Campanelli JT, Scheller RH (1988) Synuclein: a neuron-specific protein localized to the nucleus and presynaptic nerve terminal. J Neurosci 8:2804-2815.
Martinez-Vicente M, Talloczy Z, Kaushik S, Massey AC, Mazzulli J, Mosharov EV, Hodara R, Fredenburg R, Wu DC, Follenzi A, Dauer W, Przedborski S, Ischiropoulos H, Lansbury PT, Sulzer D, Cuervo AM (2008) Dopamine-modified alpha-synuclein blocks chaperone-mediated autophagy. J Clin Invest 118:777-788.
Mason DM, Nouraei N, Pant DB, Miner KM, Hutchison DF, Luk KC, Stolz JF, Leak RK (2016) Transmission of alpha-synucleinopathy from olfactory structures deep into the temporal lobe. Mol Neurodegener 11:49.
Mathis C, Paul SM, Crawley JN (1994) The neurosteroid pregnenolone sulfate blocks NMDA antagonist-induced deficits in a passive avoidance memory task. Psychopharmacology (Berl) 116:201-206.
Mattila PM, Rinne JO, Helenius H, Roytta M (1999) Neuritic degeneration in the hippocampus and amygdala in Parkinson's disease in relation to Alzheimer pathology. Acta Neuropathol 98:157-164.
Maurice T, Su TP, Privat A (1998) Sigma1 (sigma 1) receptor agonists and neurosteroids attenuate B25-35-amyloid peptide-induced amnesia in mice through a common mechanism. Neuroscience 83:413-428.
McCormack AL, Atienza JG, Johnston LC, Andersen JK, Vu S, Di Monte DA (2005) Role of oxidative stress in paraquat-induced dopaminergic cell degeneration. Journal of neurochemistry 93:1030-1037.
McCormack AL, Thiruchelvam M, Manning-Bog AB, Thiffault C, Langston JW, Cory-Slechta DA, Di Monte DA (2002) Environmental risk factors and Parkinson's disease: selective degeneration of nigral dopaminergic neurons caused by the herbicide paraquat. Neurobiol Dis 10:119-127.

McKenna JT, Vertes RP (2001) Collateral projections from the median raphe nucleus to the medial septum and hippocampus. Brain Res Bull 54:619-630.
McNaught KS, Belizaire R, Jenner P, Olanow CW, Isacson O (2002a) Selective loss of 20S proteasome alpha-subunits in the substantia nigra pars compacta in Parkinson's disease. Neurosci Lett 326:155-158.
McNaught KS, Bjorklund LM, Belizaire R, Isacson O, Jenner P, Olanow CW (2002b) Proteasome inhibition causes nigral degeneration with inclusion bodies in rats. Neuroreport 13:1437-1441.
McNaught KS, Jenner P (2001) Proteasomal function is impaired in substantia nigra in Parkinson's disease. Neurosci Lett 297:191-194.
McNaught KS, Mytilineou C, Jnobaptiste R, Yabut J, Shashidharan P, Jennert P, Olanow CW (2002c) Impairment of the ubiquitin-proteasome system causes dopaminergic cell death and inclusion body formation in ventral mesencephalic cultures. J Neurochem 81:301-306.
McNaught KS, Olanow CW (2006) Proteasome inhibitor-induced model of Parkinson's disease. Annals of neurology 60:243-247.
McNaught KS, Perl DP, Brownell AL, Olanow CW (2004) Systemic exposure to proteasome inhibitors causes a progressive model of Parkinson's disease. Ann Neurol 56:149-162.
McNaught KS, Shashidharan P, Perl DP, Jenner P, Olanow CW (2002d) Aggresome-related biogenesis of Lewy bodies. Eur J Neurosci 16:2136-2148.
Metzler-Baddeley C (2007) A review of cognitive impairments in dementia with Lewy bodies relative to Alzheimer's disease and Parkinson's disease with dementia. Cortex 43:583-600.
Meyer M, Schreck R, Baeuerle PA (1993) H2O2 and antioxidants have opposite effects on activation of NF-kappa B and AP-1 in intact cells: AP-1 as secondary antioxidant-responsive factor. EMBO J 12:2005-2015.
Meziane H, Mathis C, Paul SM, Ungerer A (1996) The neurosteroid pregnenolone sulfate reduces learning deficits induced by scopolamine and has promnestic effects in mice performing an appetitive learning task. Psychopharmacology (Berl) 126:323-330.
Migues PV, Johnston AN, Rose SP (2002) Dehydroepiandosterone and its sulphate enhance memory retention in day-old chicks. Neuroscience 109:243-251.
Mizuno Y, Sone N, Saitoh T (1987) Effects of 1-methyl-4-phenyl-1,2,3,6-tetrahydropyridine and 1-methyl-4-phenylpyridinium ion on activities of the enzymes in the electron transport system in mouse brain. Journal of Neurochemistry 48:1787-1793.
Monti DA, Zabrecky G, Kremens D, Liang TW, Wintering NA, Cai J, Wei X, Bazzan AJ, Zhong L, Bowen B, Intenzo CM, Iacovitti L, Newberg AB (2016) N-Acetyl Cysteine May Support Dopamine Neurons in Parkinson's Disease: Preliminary Clinical and Cell Line Data. PLoS One 11:e0157602.
Morimoto RI (2008) Proteotoxic stress and inducible chaperone networks in neurodegenerative disease and aging. Genes Dev 22:1427-1438.
Moslehi A, Taghizadeh-Ghehi M, Gholami K, Hadjibabaie M, Jahangard-Rafsanjani Z, Sarayani A, Javadi M, Esfandbod M, Ghavamzadeh A (2014) N-acetyl cysteine for prevention of oral mucositis in hematopoietic SCT: a double-blind, randomized, placebo-controlled trial. Bone Marrow Transplant 49:818-823.

Mosley RL, Benner EJ, Kadiu I, Thomas M, Boska MD, Hasan K, Laurie C, Gendelman HE (2006) Neuroinflammation, Oxidative Stress and the Pathogenesis of Parkinson's Disease. Clinical neuroscience research 6:261-281.
Mrak RE, Griffin WS (2007) Dementia with Lewy bodies: Definition, diagnosis, and pathogenic relationship to Alzheimer's disease. Neuropsychiatr Dis Treat 3:619-625.
Muller JM, Cahill MA, Rupec RA, Baeuerle PA, Nordheim A (1997) Antioxidants as well as oxidants activate c-fos via Ras-dependent activation of extracellular-signal-regulated kinase 2 and Elk-1. Eur J Biochem 244:45-52.
Munoz AM, Rey P, Soto-Otero R, Guerra MJ, Labandeira-Garcia JL (2004) Systemic administration of N-acetylcysteine protects dopaminergic neurons against 6-hydroxydopamine-induced degeneration. J Neurosci Res 76:551-562.
Murialdo G, Nobili F, Rollero A, Gianelli MV, Copello F, Rodriguez G, Polleri A (2000) Hippocampal perfusion and pituitary-adrenal axis in Alzheimer's disease. Neuropsychobiology 42:51-57.
Muslimovic D, Post B, Speelman JD, Schmand B (2005) Cognitive profile of patients with newly diagnosed Parkinson disease. Neurology 65:1239-1245.
Naber PA, Witter MP (1998) Subicular efferents are organized mostly as parallel projections: a double-labeling, retrograde-tracing study in the rat. J Comp Neurol 393:284-297.
Nagano-Saito A, Washimi Y, Arahata Y, Kachi T, Lerch JP, Evans AC, Dagher A, Ito K (2005) Cerebral atrophy and its relation to cognitive impairment in Parkinson disease. Neurology 64:224-229.
Nasman B, Olsson T, Backstrom T, Eriksson S, Grankvist K, Viitanen M, Bucht G (1991) Serum dehydroepiandrosterone sulfate in Alzheimer's disease and in multi-infarct dementia. Biol Psychiatry 30:684-690.
Natalie L.M. Cappaert NMVS, Menno P. Witter (2015) Hippocampal Formation. In: The rat nervous system (Paxinos, G., ed).
Nathan JA, Kim HT, Ting L, Gygi SP, Goldberg AL (2013) Why do cellular proteins linked to K63-polyubiquitin chains not associate with proteasomes? EMBO J 32:552-565.
Naumann T, Hartig W, Frotscher M (2000) Retrograde tracing with Fluoro-Gold: different methods of tracer detection at the ultrastructural level and neurodegenerative changes of back-filled neurons in long-term studies. J Neurosci Methods 103:11-21.
Nicklas WJ, Saporito M, Basma A, Geller HM, Heikkila RE (1992) Mitochondrial mechanisms of neurotoxicity. Annals of the New York Academy of Sciences 648:28-36.
Nicklas WJ, Youngster SK, Kindt MV, Heikkila RE (1987) MPTP, MPP+ and mitochondrial function. Life sciences 40:721-729.
O'Mara SM, Commins S, Anderson M, Gigg J (2001) The subiculum: a review of form, physiology and function. Prog Neurobiol 64:129-155.
Olsson B, Johansson M, Gabrielsson J, Bolme P (1988) Pharmacokinetics and bioavailability of reduced and oxidized N-acetylcysteine. Eur J Clin Pharmacol 34:77-82.
Osterberg VR, Spinelli KJ, Weston LJ, Luk KC, Woltjer RL, Unni VK (2015) Progressive aggregation of alpha-synuclein and selective degeneration of lewy inclusion-bearing neurons in a mouse model of parkinsonism. Cell Rep 10:1252-1260.
Pagani E, Rocca MA, Gallo A, Rovaris M, Martinelli V, Comi G, Filippi M (2005) Regional brain atrophy evolves differently in patients with multiple sclerosis according to clinical phenotype. AJNR Am J Neuroradiol 26:341-346.

Palma JA, Kaufmann H (2014) Autonomic disorders predicting Parkinson's disease. Parkinsonism Relat Disord 20 Suppl 1:S94-98.
Pan J, Xiao Q, Sheng CY, Hong Z, Yang HQ, Wang G, Ding JQ, Chen SD (2009) Blockade of the translocation and activation of c-Jun N-terminal kinase 3 (JNK3) attenuates dopaminergic neuronal damage in mouse model of Parkinson's disease. Neurochem Int 54:418-425.
Papapetropoulos S, Adi N, Ellul J, Argyriou AA, Chroni E (2007) A prospective study of familial versus sporadic Parkinson's disease. Neurodegener Dis 4:424-427.
Parkkinen L, Pirttila T, Alafuzoff I (2008) Applicability of current staging/categorization of alpha-synuclein pathology and their clinical relevance. Acta Neuropathol 115:399-407.
Paul SM, Purdy RH (1992) Neuroactive steroids. FASEB J 6:2311-2322.
Pauley KA, Sandritter TL, Lowry JA, Algren DA (2015) Evaluation of an Alternative Intravenous N-Acetylcysteine Regimen in Pediatric Patients. J Pediatr Pharmacol Ther 20:178-185.
Paumier KL, Luk KC, Manfredsson FP, Kanaan NM, Lipton JW, Collier TJ, Steece-Collier K, Kemp CJ, Celano S, Schulz E, Sandoval IM, Fleming S, Dirr E, Polinski NK, Trojanowski JQ, Lee VM, Sortwell CE (2015) Intrastriatal injection of pre-formed mouse alpha-synuclein fibrils into rats triggers alpha-synuclein pathology and bilateral nigrostriatal degeneration. Neurobiol Dis 82:185-199.
Paumier KL, Sukoff Rizzo SJ, Berger Z, Chen Y, Gonzales C, Kaftan E, Li L, Lotarski S, Monaghan M, Shen W, Stolyar P, Vasilyev D, Zaleska M, W DH, Dunlop J (2013) Behavioral characterization of A53T mice reveals early and late stage deficits related to Parkinson's disease. PLoS One 8:e70274.
Paxinos G (2015) The rat nervous system. Amsterdam ; Boston: Elsevier Academic Press.
Perry TL, Yong VW, Clavier RM, Jones K, Wright JM, Foulks JG, Wall RA (1985) Partial protection from the dopaminergic neurotoxin N-methyl-4-phenyl-1,2,3,6-tetrahydropyridine by four different antioxidants in the mouse. Neurosci Lett 60:109-114.
Petrucelli L, O'Farrell C, Lockhart PJ, Baptista M, Kehoe K, Vink L, Choi P, Wolozin B, Farrer M, Hardy J, Cookson MR (2002) Parkin protects against the toxicity associated with mutant alpha-synuclein: proteasome dysfunction selectively affects catecholaminergic neurons. Neuron 36:1007-1019.
Pikkarainen M, Ronkko S, Savander V, Insausti R, Pitkanen A (1999) Projections from the lateral, basal, and accessory basal nuclei of the amygdala to the hippocampal formation in rat. J Comp Neurol 403:229-260.
Pocernich CB, Butterfield DA (2012) Elevation of glutathione as a therapeutic strategy in Alzheimer disease. Biochim Biophys Acta 1822:625-630.
Pollanen MS, Dickson DW, Bergeron C (1993) Pathology and biology of the Lewy body. J Neuropathol Exp Neurol 52:183-191.
Polymeropoulos MH, Lavedan C, Leroy E, Ide SE, Dehejia A, Dutra A, Pike B, Root H, Rubenstein J, Boyer R, Stenroos ES, Chandrasekharappa S, Athanassiadou A, Papapetropoulos T, Johnson WG, Lazzarini AM, Duvoisin RC, Di Iorio G, Golbe LI, Nussbaum RL (1997) Mutation in the alpha-synuclein gene identified in families with Parkinson's disease. Science 276:2045-2047.
Porter CC, Totaro JA, Burcin A (1965) The relationship between radioactivity and norepinephrine concentrations in the brains and hearts of mice following administration

of labeled methyldopa or 6-hydroxydopamine. The Journal of pharmacology and experimental therapeutics 150:17-22.
Porter CC, Totaro JA, Stone CA (1963) Effect of 6-hydroxydopamine and some other compounds on the concentration of norepinephrine in the hearts of mice. The Journal of pharmacology and experimental therapeutics 140:308-316.
Powers SK, Jackson MJ (2008) Exercise-induced oxidative stress: cellular mechanisms and impact on muscle force production. Physiol Rev 88:1243-1276.
Prakash A, Kalra JK, Kumar A (2015) Neuroprotective effect of N-acetyl cysteine against streptozotocin-induced memory dysfunction and oxidative damage in rats. J Basic Clin Physiol Pharmacol 26:13-23.
Pringsheim T, Jette N, Frolkis A, Steeves TD (2014) The prevalence of Parkinson's disease: a systematic review and meta-analysis. Mov Disord 29:1583-1590.
Puschmann A, Ross OA, Vilarino-Guell C, Lincoln SJ, Kachergus JM, Cobb SA, Lindquist SG, Nielsen JE, Wszolek ZK, Farrer M, Widner H, van Westen D, Hagerstrom D, Markopoulou K, Chase BA, Nilsson K, Reimer J, Nilsson C (2009) A Swedish family with de novo alpha-synuclein A53T mutation: evidence for early cortical dysfunction. Parkinsonism Relat Disord 15:627-632.
Qin L, Wu X, Block ML, Liu Y, Breese GR, Hong JS, Knapp DJ, Crews FT (2007) Systemic LPS causes chronic neuroinflammation and progressive neurodegeneration. Glia 55:453-462.
Recasens A, Dehay B (2014) Alpha-synuclein spreading in Parkinson's disease. Front Neuroanat 8:159.
Reeg S, Jung T, Castro JP, Davies KJ, Henze A, Grune T (2016) The Molecular Chaperone Hsp70 Promotes the Proteolytic Removal of Oxidatively Damaged Proteins by the Proteasome. Free Radic Biol Med.
Ren ZY, Liu MM, Xue YX, Ding ZB, Xue LF, Zhai SD, Lu L (2013) A critical role for protein degradation in the nucleus accumbens core in cocaine reward memory. Neuropsychopharmacology 38:778-790.
Rhodes ME, Li PK, Flood JF, Johnson DA (1996) Enhancement of hippocampal acetylcholine release by the neurosteroid dehydroepiandrosterone sulfate: an in vivo microdialysis study. Brain Res 733:284-286.
Richter-Levin G (2004) The amygdala, the hippocampus, and emotional modulation of memory. Neuroscientist 10:31-39.
Richter-Levin G, Akirav I (2000) Amygdala-hippocampus dynamic interaction in relation to memory. Mol Neurobiol 22:11-20.
Rideout HJ, Lang-Rollin IC, Savalle M, Stefanis L (2005) Dopaminergic neurons in rat ventral midbrain cultures undergo selective apoptosis and form inclusions, but do not up-regulate iHSP70, following proteasomal inhibition. J Neurochem 93:1304-1313.
Risold PY, Swanson LW (1997) Connections of the rat lateral septal complex. Brain Res Brain Res Rev 24:115-195.
Rodriguez-Pallares J, Parga JA, Munoz A, Rey P, Guerra MJ, Labandeira-Garcia JL (2007) Mechanism of 6-hydroxydopamine neurotoxicity: the role of NADPH oxidase and microglial activation in 6-hydroxydopamine-induced degeneration of dopaminergic neurons. Journal of neurochemistry 103:145-156.

Russell A, Drozdova A, Wang W, Thomas M (2014) The impact of dementia development concurrent with Parkinson's disease: a new perspective. CNS & neurological disorders drug targets 13:1160-1168.
Ryan BJ, Hoek S, Fon EA, Wade-Martins R (2015) Mitochondrial dysfunction and mitophagy in Parkinson's: from familial to sporadic disease. Trends Biochem Sci 40:200-210.
Sachs C, Jonsson G (1975a) Effects of 6-hydroxydopamine on central noradrenaline neurons during ontogeny. Brain research 99:277-291.
Sachs C, Jonsson G (1975b) Mechanisms of action of 6-hydroxydopamine. Biochemical pharmacology 24:1-8.
Sacino AN, Brooks M, McGarvey NH, McKinney AB, Thomas MA, Levites Y, Ran Y, Golde TE, Giasson BI (2013) Induction of CNS alpha-synuclein pathology by fibrillar and non-amyloidogenic recombinant alpha-synuclein. Acta Neuropathol Commun 1:38.
Sacino AN, Brooks M, McKinney AB, Thomas MA, Shaw G, Golde TE, Giasson BI (2014a) Brain injection of alpha-synuclein induces multiple proteinopathies, gliosis, and a neuronal injury marker. J Neurosci 34:12368-12378.
Sacino AN, Brooks M, Thomas MA, McKinney AB, McGarvey NH, Rutherford NJ, Ceballos-Diaz C, Robertson J, Golde TE, Giasson BI (2014b) Amyloidogenic alpha-synuclein seeds do not invariably induce rapid, widespread pathology in mice. Acta Neuropathol 127:645-665.
Saper CB (2005) An open letter to our readers on the use of antibodies. J Comp Neurol 493:477-478.
Sato H, Kato T, Arawaka S (2013) The role of Ser129 phosphorylation of alpha-synuclein in neurodegeneration of Parkinson's disease: a review of in vivo models. Rev Neurosci 24:115-123.
Sauer H, Oertel WH (1994) Progressive degeneration of nigrostriatal dopamine neurons following intrastriatal terminal lesions with 6-hydroxydopamine: a combined retrograde tracing and immunocytochemical study in the rat. Neuroscience 59:401-415.
Sauvage MM, Nakamura NH, Beer Z (2013) Mapping memory function in the medial temporal lobe with the immediate-early gene Arc. Behav Brain Res 254:22-33.
Saxena S, Caroni P (2011) Selective neuronal vulnerability in neurodegenerative diseases: from stressor thresholds to degeneration. Neuron 71:35-48.
Schlossmacher MG, Frosch MP, Gai WP, Medina M, Sharma N, Forno L, Ochiishi T, Shimura H, Sharon R, Hattori N, Langston JW, Mizuno Y, Hyman BT, Selkoe DJ, Kosik KS (2002) Parkin localizes to the Lewy bodies of Parkinson disease and dementia with Lewy bodies. Am J Pathol 160:1655-1667.
Schmued LC, Fallon JH (1986) Fluoro-Gold: a new fluorescent retrograde axonal tracer with numerous unique properties. Brain Res 377:147-154.
Schumacher M, Weill-Engerer S, Liere P, Robert F, Franklin RJ, Garcia-Segura LM, Lambert JJ, Mayo W, Melcangi RC, Parducz A, Suter U, Carelli C, Baulieu EE, Akwa Y (2003) Steroid hormones and neurosteroids in normal and pathological aging of the nervous system. Prog Neurobiol 71:3-29.
Segal M (1977) Afferents to the entorhinal cortex of the rat studied by the method of retrograde transport of horseradish peroxidase. Exp Neurol 57:750-765.
Semchuk KM, Love EJ, Lee RG (1993) Parkinson's disease: a test of the multifactorial etiologic hypothesis. Neurology 43:1173-1180.

Sharma A, Kaur P, Kumar V, Gill KD (2007) Attenuation of 1-methyl-4-phenyl-1, 2,3,6-tetrahydropyridine induced nigrostriatal toxicity in mice by N-acetyl cysteine. Cell Mol Biol (Noisy-le-grand) 53:48-55.

Sherer TB, Kim JH, Betarbet R, Greenamyre JT (2003) Subcutaneous rotenone exposure causes highly selective dopaminergic degeneration and alpha-synuclein aggregation. Experimental neurology 179:9-16.

Shimizu K, Matsubara K, Ohtaki K, Fujimaru S, Saito O, Shiono H (2003) Paraquat induces long-lasting dopamine overflow through the excitotoxic pathway in the striatum of freely moving rats. Brain Res 976:243-252.

Shimura H, Hattori N, Kubo S, Mizuno Y, Asakawa S, Minoshima S, Shimizu N, Iwai K, Chiba T, Tanaka K, Suzuki T (2000) Familial Parkinson disease gene product, parkin, is a ubiquitin-protein ligase. Nat Genet 25:302-305.

Smaga I, Pomierny B, Krzyzanowska W, Pomierny-Chamiolo L, Miszkiel J, Niedzielska E, Ogorka A, Filip M (2012) N-acetylcysteine possesses antidepressant-like activity through reduction of oxidative stress: behavioral and biochemical analyses in rats. Prog Neuropsychopharmacol Biol Psychiatry 39:280-287.

Smith MP, Fletcher-Turner A, Yurek DM, Cass WA (2006) Calcitriol protection against dopamine loss induced by intracerebroventricular administration of 6-hydroxydopamine. Neurochemical research 31:533-539.

Soleimani Asl S, Saifi B, Sakhaie A, Zargooshnia S, Mehdizadeh M (2015) Attenuation of ecstasy-induced neurotoxicity by N-acetylcysteine. Metab Brain Dis 30:171-181.

Solerte SB, Fioravanti M, Schifino N, Cuzzoni G, Fontana I, Vignati G, Govoni S, Ferrari E (1999) Dehydroepiandrosterone sulfate decreases the interleukin-2-mediated overactivity of the natural killer cell compartment in senile dementia of the Alzheimer type. Dement Geriatr Cogn Disord 10:21-27.

Spillantini MG, Crowther RA, Jakes R, Cairns NJ, Lantos PL, Goedert M (1998a) Filamentous alpha-synuclein inclusions link multiple system atrophy with Parkinson's disease and dementia with Lewy bodies. Neuroscience letters 251:205-208.

Spillantini MG, Crowther RA, Jakes R, Hasegawa M, Goedert M (1998b) alpha-Synuclein in filamentous inclusions of Lewy bodies from Parkinson's disease and dementia with lewy bodies. Proc Natl Acad Sci U S A 95:6469-6473.

Spira PJ, Sharpe DM, Halliday G, Cavanagh J, Nicholson GA (2001) Clinical and pathological features of a Parkinsonian syndrome in a family with an Ala53Thr alpha-synuclein mutation. Ann Neurol 49:313-319.

Stefanis L (2012) alpha-Synuclein in Parkinson's disease. Cold Spring Harb Perspect Med 2:a009399.

Sun F, Anantharam V, Zhang D, Latchoumycandane C, Kanthasamy A, Kanthasamy AG (2006) Proteasome inhibitor MG-132 induces dopaminergic degeneration in cell culture and animal models. Neurotoxicology 27:807-815.

Sun L, Gu L, Wang S, Yuan J, Yang H, Zhu J, Zhang H (2012) N-acetylcysteine protects against apoptosis through modulation of group I metabotropic glutamate receptor activity. PLoS One 7:e32503.

Swanson LW (1982) The projections of the ventral tegmental area and adjacent regions: a combined fluorescent retrograde tracer and immunofluorescence study in the rat. Brain Res Bull 9:321-353.

Swanson LW, Cowan WM (1977) An autoradiographic study of the organization of the efferent connections of the hippocampal formation in the rat. J Comp Neurol 172:49-84.
Swanson LW, Sawchenko PE, Cowan WM (1980) Evidence that the commissural, associational and septal projections of the regio inferior of the hippocampus arise from the same neurons. Brain Res 197:207-212.
Tank AW, Xu L, Chen X, Radcliffe P, Sterling CR (2008) Post-transcriptional regulation of tyrosine hydroxylase expression in adrenal medulla and brain. Ann N Y Acad Sci 1148:238-248.
Tanner CM, Kamel F, Ross GW, Hoppin JA, Goldman SM, Korell M, Marras C, Bhudhikanok GS, Kasten M, Chade AR, Comyns K, Richards MB, Meng C, Priestley B, Fernandez HH, Cambi F, Umbach DM, Blair A, Sandler DP, Langston JW (2011) Rotenone, paraquat, and Parkinson's disease. Environmental health perspectives 119:866-872.
Tekin I, Roskoski R, Jr., Carkaci-Salli N, Vrana KE (2014) Complex molecular regulation of tyrosine hydroxylase. J Neural Transm (Vienna) 121:1451-1481.
Terman A, Brunk UT (2004) Lipofuscin. Int J Biochem Cell Biol 36:1400-1404.
Thiruchelvam M, McCormack A, Richfield EK, Baggs RB, Tank AW, Di Monte DA, Cory-Slechta DA (2003) Age-related irreversible progressive nigrostriatal dopaminergic neurotoxicity in the paraquat and maneb model of the Parkinson's disease phenotype. Eur J Neurosci 18:589-600.
Tieu K (2011) A guide to neurotoxic animal models of Parkinson's disease. Cold Spring Harb Perspect Med 1:a009316.
Truini A, Piroso S, Pasquale E, Notartomaso S, Di Stefano G, Lattanzi R, Battaglia G, Nicoletti F, Cruccu G (2015) N-acetyl-cysteine, a drug that enhances the endogenous activation of group-II metabotropic glutamate receptors, inhibits nociceptive transmission in humans. Mol Pain 11:14.
Uttara B, Singh AV, Zamboni P, Mahajan RT (2009) Oxidative stress and neurodegenerative diseases: a review of upstream and downstream antioxidant therapeutic options. Curr Neuropharmacol 7:65-74.
van Groen T, Wyss JM (1990) Extrinsic projections from area CA1 of the rat hippocampus: olfactory, cortical, subcortical, and bilateral hippocampal formation projections. J Comp Neurol 302:515-528.
Vertes RP (1992) PHA-L analysis of projections from the supramammillary nucleus in the rat. J Comp Neurol 326:595-622.
Vjestica A, Zhang D, Liu J, Oliferenko S (2013) Hsp70-Hsp40 chaperone complex functions in controlling polarized growth by repressing Hsf1-driven heat stress-associated transcription. PLoS Genet 9:e1003886.
Volpicelli-Daley LA, Luk KC, Lee VM (2014) Addition of exogenous alpha-synuclein preformed fibrils to primary neuronal cultures to seed recruitment of endogenous alpha-synuclein to Lewy body and Lewy neurite-like aggregates. Nat Protoc 9:2135-2146.
Volpicelli-Daley LA, Luk KC, Patel TP, Tanik SA, Riddle DM, Stieber A, Meaney DF, Trojanowski JQ, Lee VM (2011) Exogenous α-synuclein fibrils induce Lewy body pathology leading to synaptic dysfunction and neuron death. Neuron 72:57-71.
Wakabayashi K, Tanji K, Mori F, Takahashi H (2007) The Lewy body in Parkinson's disease: molecules implicated in the formation and degradation of alpha-synuclein aggregates. Neuropathology 27:494-506.

Weintraub S, Wicklund AH, Salmon DP (2012) The neuropsychological profile of Alzheimer disease. Cold Spring Harb Perspect Med 2:a006171.
Wessendorf MW (1991) Fluoro-Gold: composition, and mechanism of uptake. Brain Res 553:135-148.
Whitwell JL, Josephs KA, Murray ME, Kantarci K, Przybelski SA, Weigand SD, Vemuri P, Senjem ML, Parisi JE, Knopman DS, Boeve BF, Petersen RC, Dickson DW, Jack CR, Jr. (2008) MRI correlates of neurofibrillary tangle pathology at autopsy: a voxel-based morphometry study. Neurology 71:743-749.
Winslow AR, Chen CW, Corrochano S, Acevedo-Arozena A, Gordon DE, Peden AA, Lichtenberg M, Menzies FM, Ravikumar B, Imarisio S, Brown S, O'Kane CJ, Rubinsztein DC (2010) alpha-Synuclein impairs macroautophagy: implications for Parkinson's disease. J Cell Biol 190:1023-1037.
Wojtal K, Trojnar MK, Czuczwar SJ (2006) Endogenous neuroprotective factors: neurosteroids. Pharmacol Rep 58:335-340.
Wooten GF, Currie LJ, Bovbjerg VE, Lee JK, Patrie J (2004) Are men at greater risk for Parkinson's disease than women? J Neurol Neurosurg Psychiatry 75:637-639.
Xie W, Li X, Li C, Zhu W, Jankovic J, Le W (2010) Proteasome inhibition modeling nigral neuron degeneration in Parkinson's disease. J Neurochem 115:188-199.
Xu J, Gong DD, Man CF, Fan Y (2014) Parkinson's disease and risk of mortality: meta-analysis and systematic review. Acta Neurol Scand 129:71-79.
Yamada M, Oligino T, Mata M, Goss JR, Glorioso JC, Fink DJ (1999) Herpes simplex virus vector-mediated expression of Bcl-2 prevents 6-hydroxydopamine-induced degeneration of neurons in the substantia nigra in vivo. Proc Natl Acad Sci U S A 96:4078-4083.
Yan CY, Greene LA (1998) Prevention of PC12 cell death by N-acetylcysteine requires activation of the Ras pathway. J Neurosci 18:4042-4049.
Yoritaka A, Hattori N, Uchida K, Tanaka M, Stadtman ER, Mizuno Y (1996) Immunohistochemical detection of 4-hydroxynonenal protein adducts in Parkinson disease. Proc Natl Acad Sci U S A 93:2696-2701.
Yoshida K, Oka H (1995) Topographical projections from the medial septum-diagonal band complex to the hippocampus: a retrograde tracing study with multiple fluorescent dyes in rats. Neurosci Res 21:199-209.
Zaeri S, Emamghoreishi M (2015) Acute and Chronic Effects of N-acetylcysteine on Pentylenetetrazole-induced Seizure and Neuromuscular Coordination in Mice. Iran J Med Sci 40:118-124.
Zappone CA, Sloviter RS (2001) Commissurally projecting inhibitory interneurons of the rat hippocampal dentate gyrus: a colocalization study of neuronal markers and the retrograde tracer Fluoro-gold. J Comp Neurol 441:324-344.
Zarow C, Lyness SA, Mortimer JA, Chui HC (2003) Neuronal loss is greater in the locus coeruleus than nucleus basalis and substantia nigra in Alzheimer and Parkinson diseases. Archives of neurology 60:337-341.
Zarranz JJ, Alegre J, Gomez-Esteban JC, Lezcano E, Ros R, Ampuero I, Vidal L, Hoenicka J, Rodriguez O, Atares B, Llorens V, Gomez Tortosa E, del Ser T, Munoz DG, de Yebenes JG (2004) The new mutation, E46K, of alpha-synuclein causes Parkinson and Lewy body dementia. Ann Neurol 55:164-173.

Zhang F, Lau SS, Monks TJ (2011) The cytoprotective effect of N-acetyl-L-cysteine against ROS-induced cytotoxicity is independent of its ability to enhance glutathione synthesis. Toxicol Sci 120:87-97.
Zhang YH, Liu SS, Liu HL, Liu ZZ (2010) Evaluation of the combined toxicity of 15 pesticides by uniform design. Pest management science 66:879-887.
Zorzi E, Bonvini P (2011) Inducible hsp70 in the regulation of cancer cell survival: analysis of chaperone induction, expression and activity. Cancers (Basel) 3:3921-3956.

Appendix

Table 3: Primary antibodies

Primary Antibody	Source	Company	Catalog #	Lot #	Dilution
Anti-tyrosine hydroxylase	Sheep	Millipore	AB1542	2554850	1:1000
Anti-fluorescent gold	Rabbit	Millipore	AB153-1	2533847	1:3000
GFAP	Rabbit	DAKO	Z0334	20001046	1:1000
Anti-α-synuclein (pSer129) (aa 124 – 134; AYEMPS^{p}EEGYQ)	Mouse	Gift from Kelvin Luk (81A) (Waxman and Giasson, 2008)	-	-	1:5000
Anti-α-synuclein (pSer129) (aa 127-131; MPS^{p}EE)	Rabbit	Abcam	Ab59264	GR52476-25	1:300
Anti K48-linked ubiquitin	Rabbit	Millipore	05-1307	2299608	1:500
Anti-NeuN	Guinea pig	Millipore	ABN90	2031353	1:6000

Table 4: Secondary antibodies

Secondary Antibody	Source	Company	Catalog #	Lot #	Dilution
Anti-sheep @800	Donkey	Jackson Laboratories	713-655-147	106089	1:500
Anti-sheep @488	Donkey	Life Technologie	A11015	1567206	1:500
Anti-rabbit @ 700	Donkey	Jackson Laboratories	711-625-152	111285	1:500
Anti-guinea pig @ 790	Donkey	Jackson Laboratories	706-655-148	106036	1:1000
Anti-guinea pig@ 647	Donkey	Jackson ImmunoResearch	706-605-148	123960	1:700
Anti-guinea pig @ 488	Donkey	Jackson ImmunoResearch	706-545-148	108077	1:1000
Anti-mouse @680	Donkey	Jackson ImmunoResearch	715-625-151	106244	1:1000
Anti-mouse @ 555	Goat	Invitrogen	A21424	1141876	1:1000
Anti-mouse @ 488	Donkey	Life Technologies	A21202	1423052	1:800
Anti-rabbit @ 647	Donkey	Jackson ImmunoResearch	711-605-152	123104	1:1000
Anti-rabbit @ 488	Donkey	Jackson ImmunoResearch	711-545-152	120705	1:700
Anti-rabbit@ 546	Goat	Life Technologies	A11035	1579044	1:500
Anti-rabbit @ 555	Goat	Life Technologies	A21429	1562309	1:800

Table 5: Abbreviations

5N	motor trigeminal nucleus	HDB	horizontal limb of the diagonal band
7n	facial nerve	HP	hippocampus
7N	facial nucleus	ic	internal capsule
8n	vestibulocochlear nerve	IC	inferior colliculus
A30	cingulate cortex area 30	lab	longitudinal association bundle
AA	anterior amygdaloid area	LH	lateral habenula
ac	anterior commissure	lo	lateral olfactory tract
aca	anterior commissure, anterior part	LOT	nucleus of the lateral olfactory tract
Acb	nucleus accumbens	Lrt	lateral reticular nucleus
aci	anterior commissure, intrabulbar	LS	lateral septal nucleus
acp	anterior commissure, posterior part	LSd	lateral septal nucleus, dorsal part
AHi	amygdalohippocampal area	LSI	lateral septal nucleus
AMG	amygdala	LSv	lateral septal nucleus, ventral part
AOB	accessory olfactory bulb	LTDg	laterodorsal tegmental nucleus
AOD	anterior olfactory area, dorsal	LV	lateral ventricle
AOE	anterior olfactory nucleus, external	M2	secondary motor cortex
AOM	anterior olfactory nucleus, medial	MD	mediodorsal thalamic nucleus
AON	anterior olfactory nucleus	MEA	medial amygdala
AOP	anterior olfactory area, posterior	MEnt	medial entorhinal cortex
AOV	anterior olfactory area, ventral	mlf	medial longitudinal fasciculus
APir	amygdalopiriform transition area	MoDG	molecular layer of the dentate gyrus
AV	anteroventral thalamic nucleus	MS	medial septal nucleus
bic	brachium of the inferior colliculus	mt	mammillothalamic tract
BLA	basolateral nucleus of amygdala	OB	olfactory bulb
BMA	basomedial nucleus of amygdala	och	optic chiasm
CA1	cornu ammonis, field 1	opt	optic tract
CA2	cornu ammonis, field 2	PaS	parasubiculum
CA3	cornu ammonis, field 3	Pir	piriform cortex
cc	corpus callosum	PMCo	posteromedial cortical amygdala
CeA	central nucleus of amygdala	Pn	pontine nuclei
CEnt	caudomedial entorhinal cortex	Pr5	principal trigeminal nucleus
cp	cerebral peduncle	PrG	pregeniculate nu
CPu	caudoputamen	PRh	perirhinal cortex
cst	commissural stria terminalis	PrS	presubiculum
CxA	cortex-amygdala transition zone	rf	rhinal fissure
DCIC	pericentral nucleus of inferior colliculus	rms	rostral migratory stream
DEn	dorsal nucleus of the endopiriform claustrum	Rtg	rostral temporal gyrus
		S	subiculum
DG	dentate gyrus	S1	primary somatosensory cortex
DLEnt	dorsolateral entorhinal cortex	S1BF	somatosensory 1, barrel field
DS	dorsal subiculum	SC	superior colliculus
DTT	dorsal tenia tecta	Scc	splenium of corpus callosum

ec	external capsule	sm	stria medullaris
ECIC	external nucleus of inferior colliculus	SNpr	substantia nigra pars reticulata
Ect	ectorhinal cortex	sp5	spinal trigeminal tract
Ent	entorhinal cortex	Sp	spinal trigeminal nucleus
EPl	external plexiform layer, olfactory bulb	st	stria terminalis
f	fornix	SuG	superficial gray layer of the superior colliculus
FC	frontal cortex		
fi	fimbria	SVZ	subventricular zone
fmi	forceps minor of the corpus callosum	TeA	temporal cortex, association area
fmj	forceps major of the corpus callosum	Tu	olfactory tubercle
fr	fasciculus retroflexus	VDB	ventral diagonal band
gcc	genu of corpus callosum	VM	ventromedial thalamic nucleus
Gl	glomerular layer, olfactory bulb	VMH	ventromedial hypothalamic nucleus
GP	globus pallidus	VTT	ventral tenia tecta
GrDG	granular layer of dentate gyrus	VS	ventral subiculum
GrO	granule cell layer of olfactory bulb		